



In the IOCCG Report Series:

1. *Minimum Requirements for an Operational Ocean-Colour Sensor for the Open Ocean (1998)*
2. *Status and Plans for Satellite Ocean-Colour Missions: Considerations for Complementary Missions (1999)*
3. *Remote Sensing of Ocean Colour in Coastal, and Other Optically-Complex, Waters (2000)*
4. *Guide to the Creation and Use of Ocean-Colour, Level-3, Binned Data Products (2004)*
5. *Remote Sensing of Inherent Optical Properties: Fundamentals, Tests of Algorithms, and Applications (2006)*
6. *Ocean-Colour Data Merging (2007)*
7. *Why Ocean Colour? The Societal Benefits of Ocean-Colour Technology (2008)*
8. *Remote Sensing in Fisheries and Aquaculture (2009)*
9. *Partition of the Ocean into Ecological Provinces: Role of Ocean-Colour Radiometry (2009)*
10. *Atmospheric Correction for Remotely-Sensed Ocean-Colour Products (2010)*
11. *Bio-Optical Sensors on Argo Floats (2011)*
12. *Ocean-Colour Observations from a Geostationary Orbit (2012)*
13. *Mission Requirements for Future Ocean-Colour Sensors (2012)*
14. *In-flight Calibration of Satellite Ocean-Colour Sensors (2013)*
15. *Phytoplankton Functional Types from Space (2014)*
16. *Ocean Colour Remote Sensing in Polar Seas (2015)*
17. *Observation of Harmful Algal Blooms with Ocean Colour Radiometry (this volume)*

**Disclaimer:** The opinions expressed here are those of the authors; in no way do they represent the policy of agencies that support or participate in the IOCCG.

The printing of this report was sponsored and carried out by xxx, which is gratefully acknowledged.

# Reports and Monographs of the International Ocean Colour Coordinating Group

An Affiliated Program of the Scientific Committee on Oceanic Research (SCOR)  
An Associated Member of the Committee on Earth Observation Satellites (CEOS)

IOCCG Report Number 17, 2016

## Observation of Harmful Algal Blooms with Ocean Colour Radiometry

Edited by:

Stewart Bernard (CSIR, South Africa)

Report of an IOCCG working group on Harmful Algal Blooms and Ocean Colour, chaired by  
Stewart Bernard and based on contributions from (in alphabetical order):

Stewart Bernard, Mariano Bresciani, Jennifer Cannizzaro, Hongtao Duan, Claudia Giardino,  
Patricia M. Glibert, Chuanmin Hu, Tiit Kutser, Ronghua Ma, Erica Matta, Mark Matthews, Frank  
E. Muller-Karger, Stefan Simis, Inia M. Soto, Jennifer Wolny

Series Editor: Venetia Stuart

Correct citation for this publication:

*IOCCG (2016). Observation of Harmful Algal Blooms with Ocean Colour Radiometry. Bernard, S. (ed.), IOCCG Report Series, No. 17, International Ocean Colour Coordinating Group, Dartmouth, Canada.*

The International Ocean Colour Coordinating Group (IOCCG) is an international group of experts in the field of satellite ocean colour, acting as a liaison and communication channel between users, managers and agencies in the ocean colour arena.

The IOCCG is sponsored by Centre National d'Etudes Spatiales (CNES, France), Canadian Space Agency (CSA), Commonwealth Scientific and Industrial Research Organisation (CSIRO, Australia), Department of Fisheries and Oceans (Bedford Institute of Oceanography, Canada), European Space Agency (ESA), European Organisation for the Exploitation of Meteorological Satellites (EUMETSAT), National Institute for Space Research (INPE, Brazil), Indian Space Research Organisation (ISRO), Japan Aerospace Exploration Agency (JAXA), Joint Research Centre (JRC, EC), Korea Institute of Ocean Science and Technology (KIOST), National Aeronautics and Space Administration (NASA, USA), National Oceanic and Atmospheric Administration (NOAA, USA), Scientific Committee on Oceanic Research (SCOR), and Second Institute of Oceanography (SIO), China.

<http://www.ioccg.org>

Published by the International Ocean Colour Coordinating Group,  
P.O. Box 1006, Dartmouth, Nova Scotia, B2Y 4A2, Canada.

ISSN: 1098-6030

ISBN: 978-1-896246-66-6

©IOCCG 2016

*Printed by XXXXX*

# Contents

---

<b>1 Harmful Algal Blooms, their Changing Ecosystem Dynamics and Related Conceptual Models</b>	<b>1</b>
1.1 Introduction to Harmful Algal Blooms and their Effects . . . . .	1
1.2 Introduction to the Global Ecology and Oceanography of Harmful Algal Blooms (GEOHAB) Programme . . . . .	3
1.3 HABs and Global Change . . . . .	6
1.3.1 Relationships with eutrophication . . . . .	6
1.3.2 Relationships with changing climate . . . . .	9
1.4 Trophic Interactions: HABs as Prey and as Predators . . . . .	10
1.5 Conceptual models of the influence of nutrients and the physical environment on species selection . . . . .	12
1.6 Changes in HABs assessed with Ocean Colour: Case Study of the Arabian Sea and Arabian Gulf . . . . .	16
<b>2 Case Study: Blooms of the Neurotoxic Dinoflagellate <i>Karenia brevis</i> on the West Florida Shelf</b>	<b>21</b>
2.1 Background . . . . .	21
2.1.1 Organism description, impact, and distribution . . . . .	21
2.1.2 Ecological niche, nutrient and environmental preferences, and bloom mechanism . . . . .	23
2.2 Principles . . . . .	24
2.3 Data and Methods . . . . .	27
2.4 Ocean Colour Case Demonstration . . . . .	27
2.5 Discussion and Summary . . . . .	31
<b>3 Case Studies: Remote Sensing of Cyanobacteria Blooms</b>	<b>33</b>
3.1 Introduction . . . . .	33
3.1.1 Terminology, taxonomy, and functional diversity . . . . .	33
3.1.2 Pigmentation . . . . .	34
3.1.3 Buoyancy . . . . .	36
3.2 Case 1: Bloom Distribution in Lake Trasimeno . . . . .	38
3.2.1 Objective . . . . .	38
3.2.2 Study area . . . . .	39
3.2.3 Image processing . . . . .	39
3.2.4 Results . . . . .	40
3.2.5 Discussion . . . . .	41
3.3 Case 2: Lake Taihu, China . . . . .	41

ii • *Observation of Harmful Algal Blooms with Ocean Colour Radiometry*

3.3.1	Objective	41
3.3.2	Study area	42
3.3.3	Image processing	42
3.3.4	Image analysis	43
3.3.5	Factors forcing blooms	46
3.3.6	Discussion	47
3.4	Case 3: Trophic Status, Cyanobacteria and Surface Scums in Lakes	48
3.4.1	Introduction	48
3.4.2	The MPH algorithm	48
3.4.3	Detection of eukaryote and cyanobacteria dominated waters	50
3.5	Case 4: Summer Blooms in the Baltic Sea	52
3.5.1	Objective	52
3.5.2	Study area	52
3.5.3	Image analysis: Delineating blooms	52
3.5.4	Spatial resolution	54
3.5.5	Time series and matching <i>in situ</i> observations	55
3.5.6	Discussion	57

**Acronyms and Abbreviations**

# Harmful Algal Blooms, their Changing Ecosystem Dynamics and Related Conceptual Models

Patricia M. Glibert<sup>1</sup>

---

## 1.1 Introduction to Harmful Algal Blooms and their Effects

Over the past several decades, the frequency of occurrence, the duration, and geographic extent of blooms of toxic or harmful microalgae have been increasing in many parts of the world (e.g., Glibert and Burkholder 2006; Heisler et al. 2008), as has the appreciation of the serious impacts that such events can have on both ecosystems and on human health (e.g., Backer and McGillicuddy 2006; Johnson et al. 2010). The scientific community refers to “harmful algal blooms” (HABs) as those proliferations of algae that can cause fish kills, contaminate seafood with toxins, and alter ecosystems in ways that humans perceive as harmful (e.g., GEOHAB 2001). The term HAB is used generally and non-specifically, recognizing that some species can cause harmful effects even when at densities that are low and not at levels normally taken to be a “bloom”, while other species that have significant ecosystem or health effects are technically not “algae”. Some HABs are small protists that obtain their nutrition by grazing on other small algae or bacteria; either they do not photosynthesize at all, or only do so in conjunction with grazing (Glibert et al. 2005; Jeong et al. 2005; Burkholder et al. 2008; Jeong et al. 2010; Flynn et al. 2013). Other HABs are cyanobacteria (CyanoHABs), some of which have the ability to “fix” nitrogen from the atmosphere as their nitrogen source. Thus, the term “HAB” is an operational term, not a technical one. Some HABs are planktonic, while others live in or near the sediment, or attached to surfaces for some or all of their life cycle. Among those that are planktonic, some form visible surface accumulations, while other remain well distributed throughout the water column. Relating the diversity of these characteristics to their observation using remote sensing of ocean colour is a tall challenge — but at least for many types of HABs the scale of expansion of HABs has been well established using ocean colour radiometry in conjunction with other approaches.

By definition, all HABs cause harm — either ecological, economic, or human health. Not all HABs make toxins; some are harmful in other ways. In a broad sense, there are two general types of HABs: those which can contaminate seafood or wildlife largely through their toxin production, and those that cause ecological harm, largely through their sheer biomass

---

<sup>1</sup>University of Maryland, Center for Environmental Science, Horn Point Lab, Cambridge, MD 21613, USA

production, which in turn can cause anoxia or indiscriminate mortalities of marine life (Figure 1.1). The latter occurs after these cells either reach dense accumulations or when these dense accumulations begin to die and oxygen is consumed through their decomposition. Some HABs have characteristics of both: they may be both toxic and may accumulate in high biomass blooms. Among those that are toxic, there are many types of toxins with new toxins being discovered frequently (e.g., Landsberg 2002; Backer and McGillicuddy 2006). Some algal toxins kill fish directly. Others do not have direct effects on the organisms that feed on them, such as fish or filter-feeding shellfish, but the toxin can accumulate in the shellfish and then cause harm to the humans who consume them. In other cases, the toxins are released into the water column where they can get into the water supply and affect human consumers through their drinking water. Some toxins may also be aerosolized, as is the case with *Karenia brevis* in Florida, and respiratory distress can result for those in contact with these air-borne toxins. Making the task of understanding these phenomena all the more complex, not all species are toxic under all conditions, and it is not completely understood when and why different species may become toxic.

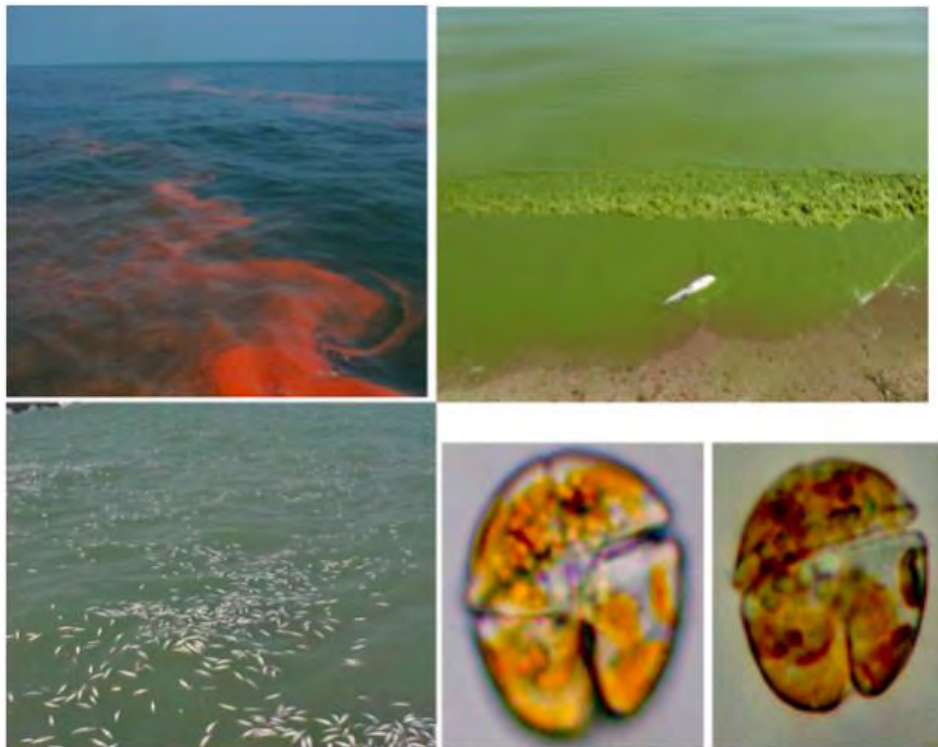


**Figure 1.1** Various images of HABs and their effect, including a “red tide” in East China Sea (upper left; photo by J. Li), a freshwater “green tide” (upper right; photo by T. Archer), a fish kill from toxic algae (lower left; photo by P. Glibert), and microscopic views of a common toxic red tide microorganism (lower right; photos by Y. Fukuyo).

In terms of algal classes that can be considered HABs, there are many, including dinoflagellates, diatoms, raphidophytes, prymnesiophytes, and cyanobacteria among others. The most

common toxic marine HABs are the dinoflagellates, and the most common toxic freshwater HABs are cyanobacteria, but increasingly toxic diatoms are also of concern, particularly in coastal waters.

## 1.2 Introduction to the Global Ecology and Oceanography of Harmful Algal Blooms (GEOHAB) Programme

Acknowledging that the HAB problem is global, but recognizing that there is still much to be understood with regard to the biological, chemical, and physical factors that regulate HAB dynamics and impacts, the SCOR/IOC Global Ecology and Oceanography of Harmful Algal Blooms (GEOHAB) programme (c.f., GEOHAB 2001) was formed with a mission to: *Foster international co-operative research on HABs in ecosystem types sharing common features, comparing the key species involved and the oceanographic processes that influence their population dynamics.* Ultimately the goal of GEOHAB was to: *Improve prediction of HABs by determining the ecological and oceanographic mechanisms underlying their population dynamics, integrating biological, chemical and physical studies supported by enhanced observation and modeling systems.*

The work of the GEOHAB Program was multifaceted, from advancing understanding of the adaptive strategies of HABs, to improved linkages between the expansion of HABs and other global changes such as eutrophication and climate change, and to improved characterization of HABs in regions, especially Asia, where HABs and their effects are particularly pervasive (GEOHAB 2010). GEOHAB was not intended as a research programme *per se*, but rather as an international forum to advance the understanding of the ecology and oceanography of HABs, and to improve the prediction of HABs through advanced approaches. GEOHAB is currently undergoing a transition to a new mission, inclusive of issues related to both freshwater and to toxin effects, and so GEOHAB is transitioning to its new identity, GlobalHAB. In the decade since the launch of GEOHAB, the dynamics of a changing world have become increasingly apparent. From climate to ocean acidification to changing anthropogenic nutrient loads and species transport around the world, the potential trajectory of change for HABs is ever more important to understand.

Through the work supported by GEOHAB as well as other studies, we have gained a better understanding of the relationships between many HAB species, particularly dinoflagellate HABs, and their environment. The biogeographical ranges of HAB organisms and how they have changed over time is of fundamental importance in resolving how species may have been introduced to new areas, and what areas may be susceptible to new introductions in the future. Certain species have a rather circumscribed distribution within fairly narrow environmental constraints. For example, species such as *Pyrodinium bahamense* are generally restricted to tropical and subtropical regions in the Pacific Ocean and the Caribbean Sea (e.g., Hallegraeff and Maclean 1989), while other species, such as *Alexandrium catenella*, are only found in temperate waters at mid- to high latitudes. Other species, such as *Prorocentrum minimum* have a more cosmopolitan distribution, from temperate to tropical waters (Glibert et al. 2008, 2012). An understanding of the environmental constraints on species distribution aids in

understanding how species biogeography may change on both short and long-term scales as (OK??) climate and other environmental conditions may change. Ocean colour approaches have helped advance our understanding of expanding species ranges.

The GEOHAB Programme has been instrumental in raising the global awareness of how many new areas, not previously impacted by HABS, are now experiencing HABS on either an event-scale basis or on a longer term scale, reflective of environmentally changed conditions. Several examples highlight the occurrence of new or increasing events and their impacts in China, a region where the expansion of HABS is readily apparent. The number of HABS has increased in all waters of China in the past three decades and most inland and coastal waters are rated in the moderately to severely polluted range (Wang et al. 2011; Ti 2013).

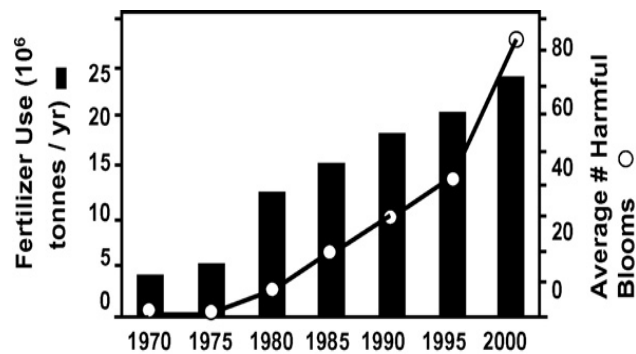


**Figure 1.2** The recent increase in HAB events off the coast of China is related to the increase in nitrogen-based fertilizer use over the past two decades. Reproduced from Heisler et al. (2008) with permission of *Harmful Algae* (Elsevier). Does IOCCG have permission to reproduce this figure as well??

Occurrences of HABS in the East China Sea were rare in the 1970s, increased to a few dozen during the 1980s, and increased to >130 in the 5 years from 1992 to 1997 (Shen and Liu 2009) but the scale of the blooms has soared in the years since (Figure 1.2); the spatial scale of the annual blooms increased from thousands of km<sup>2</sup> in 2000 to >15,000 km<sup>2</sup> by 2005, with many millions of dollars lost in high value aquaculture products due to associated fish kills (Li et al. 2009). The dinoflagellates *Prorocentrum donghaiense* and *Karenia mikimotoi* are among the common HABS now reported in East China Sea (e.g., Zhou et al. 2008; Li et al. 2009). In the Huanghai Sea region there has also been nearly a six-fold increase in HAB occurrences and a shift to proportionately more dinoflagellates compared to diatoms (Fu et al. 2012), while in the South China Sea region, there has been both an increase in number of HABS as well as a change in species composition, with an increasing dominance of species such as *Chattonella*, *Gymnodinium breve*, and *Dinophysis* (Wang et al. 2008; Glibert et al. 2014b) - is this the correct ref??. A particularly large and unusual bloom in China received international coverage in 2008 (Figure 1.3). This was a bloom of the macroalgal species *Enteromorpha prolifera* that occurred at the venue of the Olympic Games sailing competition, almost blanketing the water with filamentous scum (Hu et al. 2010). Blooms of this magnitude in this region had not previously been observed. One of the features of this species and its blooms is that it tends to float,

making detection from satellite imaging feasible. It is from such approaches that the scale of these blooms and their change over time can be estimated. A 10-year record of images of the region shows that prior to 2007, the area covered by *E. proliferata* was <math><21\text{ km}^2</math>. In 2008 the scale of the bloom was >math>1900\text{ km}^2</math>, and in 2009 it was

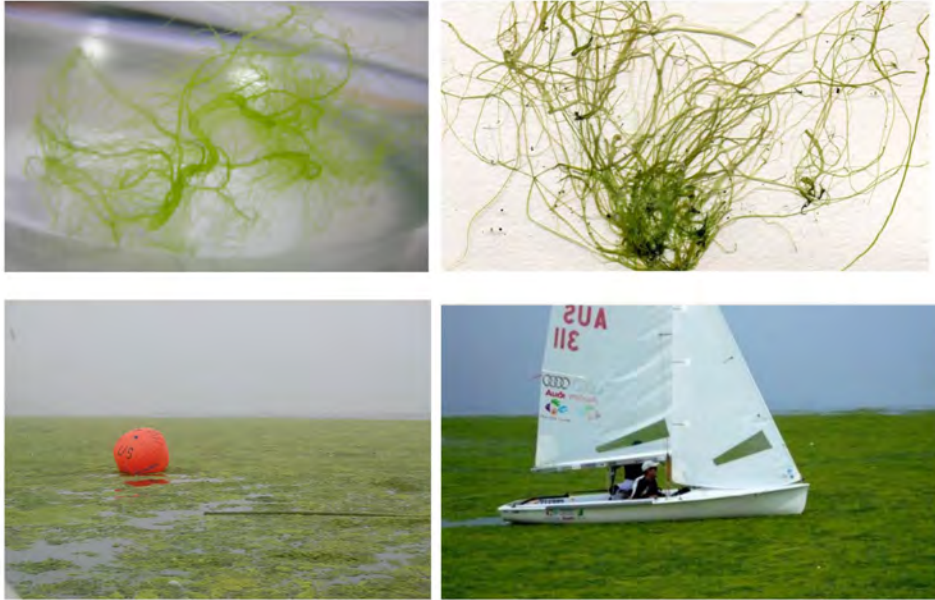


**Figure 1.3** The 2008 bloom that blanketed the venue for the Olympic Sailing Regatta in Qingdao was caused by *Enteromorpha proliferata* (left panel; photo by M.J. Zhou), causing a massive area of the region to be covered by algae (right panel; reproduced from GEOHAB (2010)).

For HAB management, the question of the extent to which shifts in biodiversity are the result of changing environmental conditions, anthropogenic introductions, or a combination of both, is important in devising strategies to ultimately limit their distribution or impact. Changes in species biogeography are becoming increasingly documented. For example, blooms of *Chrysochromulina* (now *Prymnesium*) *polylepis* and *C. leadbeateri* were rare in Scandinavian waters prior to their massive blooms in 1988–1991 (Moestrup 1994), but they have been commonly observed in the plankton since that time. The diatom *Pseudo-nitzschia australis*, while present in the plankton off the coast of California prior to the mid-1990s, has now become an annual bloom-former of increasing geographic distribution. In contrast, some blooms occur for a period of years and then appear to be of lesser intensity. Such was the case with brown tide, *Aureococcus anophagefferens*, off the coast of Long Island, United States, which bloomed intensively in the late 1980s–1990s, but, while present, has not bloomed annually with such strength in more recent years. The intensity of blooms of the latter species appears to be related to long-term patterns in environmental and weather conditions, being more common during dry years than wet years (e.g., LaRoche et al. 1997; Glibert et al. 2014a - assume LaRoche 1997 and not 1998?? Also is Glibert ref the correct one??).

## 1.3 HABs and Global Change

### 1.3.1 Relationships with eutrophication

The expansion of HABs in relation to both local and global expansion in nutrient loading is now well recognized (e.g., Anderson et al. 2002; Glibert et al. 2005; Heisler et al. 2008; Glibert et al. 2014b). While the relationship between HABs and increased nutrient availability has been recognized for decades, in recent years there has been much that has been learned regarding how specific nutrient loads have changed, and how such changes may mechanistically or physiologically promote the growth of certain species. Adaptive strategies such as mixotrophy and/or use of organic substrates in addition to inorganic nutrients may infer some advantages for HABs, particularly when nutrient loads are not in stoichiometric proportion relative to the optima for growth of these cells (Glibert and Burkholder 2011; Flynn et al. 2013; Glibert et al. 2014b). Moreover, the responses of ecosystems to nutrients have become better understood, including the types of systems that may be retentive of nutrients and the ones that may have high enough flushing rates for nutrients to be exported spatially from the point of loading (e.g., Dürr et al. 2011).

Eutrophication of both inland and coastal waters is the result of human population growth and the production of food (agriculture, animal operations and aquaculture) and energy, and is considered one of the largest pollution problems globally (e.g., Howarth et al. 2002; Howarth 2008). Population growth and increased food production result in major changes to the landscape, in turn increasing sewage discharges and runoff from farmed and populated lands. In addition to population growth, eutrophication arises from the large increase in chemical fertilizers that began in the 1950s and which are projected to continue to escalate in the coming decades (e.g., Smil 2001; Glibert et al. 2006, 2014b). For HAB growth, it is also of importance to note that the rate of change in use of nitrogen (N) fertilizers has eclipsed that of phosphorus (P) fertilizers in large part due to this large-scale capacity for anthropogenic synthesis. Global use of N fertilizer has increased nine-fold, while that of P has increased three-fold (Sutton et al. 2013; Glibert et al. 2014b). Increased N use is particularly pronounced in many parts of the developing world, including China. Fertilizer N use in China has escalated from about 0.5 MT in the early 1960s to 42 MT around 2010, with the fraction of urea increasing nearly five-fold over just the past two decades (Glibert et al. 2014b and references therein). Between 1980 and 2010, river export of N increased from  $\sim 500$  to  $>1200$  kg N km<sup>-2</sup> yr<sup>-1</sup> in the Chiangjiang River, from  $\sim 100$  to  $\sim 200$  kg N km<sup>-2</sup> yr<sup>-1</sup> in the Yellow River and from  $\sim 400$  to  $>1200$  kg N km<sup>-2</sup> yr<sup>-1</sup> in the Pearl River basins (Ti 2013). Accordingly, the number of HABs has increased in virtually all waters of China in the past three decades.

Nutrients can stimulate or enhance the impact of toxic or harmful species in several ways (Anderson et al. 2002; Glibert et al. 2011). At the simplest level, harmful phytoplankton may increase in abundance due to increased nutrient enrichment, but may stay at the relative fraction of the total phytoplankton biomass. Even though non-HAB species are stimulated proportionately, a modest increase in the abundance of a HAB species may cause it to have increased effects on the ecosystem. A more frequent response to nutrient enrichment occurs

when a species or group of species begins to dominate under the altered nutrient regime. High biomass blooms, which are easier to detect using ocean colour radiometry, occur when the HAB species is disproportionately stimulated, often to the point where the HAB becomes the dominant species. In the extreme, the HAB species may displace virtually all other algal species and the bloom becomes essentially mono-specific.

One of the results of alterations in global N and P is that many receiving waters are now not only enriched with nutrients, but nutrient loads to many aquatic environments also diverge considerably from those that have long been associated with phytoplankton growth. The ratio of dissolved inorganic N:P (DIN:DIP) — when in the proportion of 16:1 on a molar basis — is classically identified as the Redfield ratio (Redfield 1934) - please rephrase sentence??. Various surveys of the “optimal” N:P molar ratios in a broad range of phytoplankton groups have found that, while the data clustered around the Redfield ratio, there were numerous examples at both the high and low ends of the spectrum (e.g., Hecky 1988; Klausmeier et al. 2004). Note that the “optimum” N:P is the ratio of the values where the cell maintains the minimum N and P cell quotas (Klausmeier et al. 2004). Changes in this ratio have been compared to shifts in phytoplankton composition, yielding insight about the dynamics of nutrient regulation of plankton assemblages (e.g., Tilman 1977 - missing ref??. Smayda 1990; Hodgkiss and Ho 1997; Hodgkiss 2001; Heil et al. 2007).

Efforts to understand the relationships between nutrient loading and algal blooms have largely focused on total nutrient loads and altered nutrient ratios (N:P or N:Si (silica)) that result from selected nutrient addition or removal. Alterations in the composition of nutrient loads have correlated with shifts from diatom-dominated to flagellated-dominated algal assemblages in many regions. Continuing with the example of China introduced above, in the Huanghai Sea region of China, inorganic N:P ratios are now about twice Redfield proportions, and about four-fold higher than in the 1990s (Ning et al. 2009; Glibert et al. 2014b). Also, in this region there has been nearly a six-fold increase in HAB occurrences and a shift to proportionately more dinoflagellates compared to diatoms (Fu et al. 2012; Glibert et al. 2014b). Similarly, in the South China Sea region, water column inorganic N:P ratios increased from ~2 in the mid-1980s to >20 in the early 2000s (Ning et al. 2009). In addition to the increase in number of HABs, a change in species composition has also occurred with increasing dominance of species such as *Chattonella*, *Gymnodinium breve* (now *Karenia brevis*) and *Dinophysis* (Wang et al. 2008).

The form in which particular nutrients are supplied may also affect the likelihood for a specific nutrient load to promote HABs, in addition to the impact of nutrient ratios that promote certain species with a higher or lower requirement for a particular nutrient (rephrase OK?). Organic nutrients have been shown to be important in the development of blooms of various HAB species, in particular cyanobacteria and dinoflagellates (e.g., Paerl 1988; Glibert et al. 2001) and the importance of this phenomenon is being recognized in blooms around the world (e.g., Granéli et al. 1985; Berman 1997; Berg et al. 2003; Berman and Bronk 2003). It has been well demonstrated, for example, that cyanobacterial blooms in Florida Bay and on the southwest Florida shelf are positively correlated with the fraction of nitrogen taken up as urea and negatively correlated with the fraction of nitrogen taken up as nitrate (Glibert et al. 2004).

The impacts of differing anthropogenic activities with respect to HABs are not necessarily

the same. For example, nutrient delivery associated with sewage may bear little similarity in quantity or composition to that associated with inputs from agriculture, aquaculture or dredging operations, depending on what form of sewage treatment (if any) exists. In turn, nutrients from these sources may also differ in quantity and composition from those associated with natural nutrient delivery mechanisms such as groundwater flow and atmospheric deposition, recognizing that these sources as well may be influenced by human activities. The timing of nutrient delivery also affects the extent to which the associated nutrients may stimulate HABs. Long-distance transport of nutrients, and of organisms (e.g., Franks and Anderson 1992), accumulation of biomass in response to water flows, buoyancy regulation, and swimming behaviours (e.g., Kamykowski and Yamazaki 1997 - I assume this should be 1997 not 1995??) and maintenance of suitable environmental conditions (including temperature, salinity, stratification, irradiance) as well as nutrient supply, are all critical to understanding the environmental response to nutrients.

Among the high biomass bloom formers, pelagic *Prorocentrum*, especially *P. minimum*, has been well documented to be a species expanding in global distribution in concert with eutrophication (Heil et al. 2005; Glibert et al. 2008, 2012). Global maps of nutrient loads, by form and dominant source (Dumont et al. 2005; Harrison et al. 2005a,b; Seitzinger et al. 2005) illustrate that this species is most prevalent when nitrogen loads are high, where these nitrogen loads are in organic form, and where the organic nutrients are predominantly from anthropogenic origin (Glibert et al. 2008, 2012). Other studies have shown that *P. minimum* is common near sewage outfalls and near nutrient-rich shrimp ponds or other aquaculture operations (Cannon 1990; Sierra-Beltran et al. 2005). In the Baltic Sea, its expansion has also been linked to impacts from human activities (Olenina et al. 2010).

The coast of China again provides a relevant example (the expansion of HABs in this region is highlighted above). Many of these blooms are associated with pelagic *Prorocentrum* spp. in the East China Sea in the convergence area of the Yangtze (Changjiang) River plume and the Taiwan Warm Current (Lu and Gobel 2001; Zhou et al. 2003; Zhou et al. 2008; Wang and Wu 2009 - assume this should be 2009 not 2008??, Lu et al. 2005; 2006 - both refs missing). The dominant species is *P. donghaiense* and such blooms can form up to 90% of the planktonic biomass (Zhou et al. 2008; Li et al. 2009, 2010a, Lu et al. 2011 - missing ref??). Blooms form in the in the convergence area of the N-rich (but comparatively P-poor) water from the Changjiang River plume and the P-enriched Taiwan Warm Current (Tang et al. 2000; Li et al. 2009). While satellite imagery can readily detect the chlorophyll accumulation in this region when blooms are present, there is also a very large plume of sediment that is readily apparent. A “red tide” bloom index has been developed for this region, based on both false colour images of the East China Sea acquired by MODIS Terra during a bloom in 2005 (Lou et al. 2006) and SeaWiFS data (Ahn and Shannmugam 2006; Figure 1.4) which illustrates the scope of these blooms when they occur.

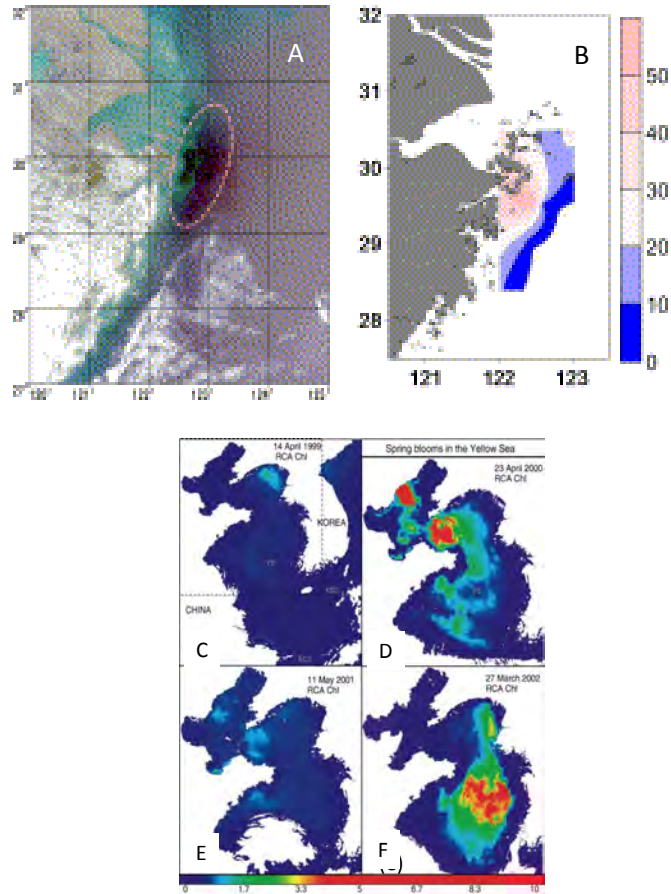


**Figure 1.4** (A) False colour image of the East China Sea on 29 May 2005 acquired by MODIS Terra showing the red tide distribution; (B) mean DIN:DIP ratio in the surface waters of the East China Sea during spring 2005 when *Prorocentrum donghaiense* was the dominant phytoplankton species. The dashed line indicates the location of the bloom. Panels C-F represent SeaWiFS images for the Yellow and Bohai Seas during spring (1999–2002) converted to a red tide index using an algorithm developed from bio-optical data from native HAB species (scale represents Red tide Chlorophyll Algorithm, RCA, index). Panel (A) reproduced from Lou et al. (2006) with permission of the International Society of Optical Engineering, panel (B) reproduced from Glibert et al. (2012) with permission of the journal *Harmful Algae* (Elsevier) and panels C-F are reproduced from Ahn and Shannmugam (2006) with permission of the publisher (Elsevier). Does IOCCG also have permission to reproduce these as well??

### 1.3.2 Relationships with changing climate

Average sea surface temperatures are expected to rise as much as 5°C over the coming century and many parts of the ocean are expected to freshen significantly due to ice melt and altered precipitation (e.g., Fu et al. 2012 and references therein). These changes will alter stratification, availability of nutrients and their forms and ratios, and will also alter pCO<sub>2</sub> and light regimes among other factors (e.g., Boyd and Doney 2003).

Massive changes in the carbon (C) cycle are also expected, and are actually occurring, with

large effects on pH. The change in C chemistry is expected not only to affect those organisms that are pH sensitive, but may also affect, and favour, those algae that depend on diffusive CO<sub>2</sub> rather than HCO<sub>3</sub><sup>-</sup> as their C source. This includes many of the HABs, such as *Amphidium carterae* and *Heterocapsa oceanica* (Dason et al. 2004), but this is certainly not the case for all HABs. High CO<sub>2</sub> may also affect toxicity of HABs through a variety of routes. The synthesis of some toxins is light dependent, as is the case with karlotoxin in *Karlodinium veneficum* and saxitoxin in *Alexandrium catenella* (Proctor et al. 1975; Adolf et al. 2009) suggesting that as photosynthesis is affected by changing pCO<sub>2</sub>, so too is toxin synthesis. Those species that produce copious amounts of reactive oxygen species (ROS), such as the raphidophytes, also produce more under light conditions (Fu et al. 2012 and references therein). In the diatom *Pseudo-nitzschia*, concentrations of the toxin domoic acid appear to increase at high CO<sub>2</sub>/low pH levels, at least as shown in some studies (e.g., Sun et al. 2011; Tatters et al. 2012), and this effect is more pronounced when cells are nutrient limited or when forms of nitrogen shift away from oxidized to reduced forms (Glibert et al. 2015 and references therein).

Temperature alone also affects metabolism in multiple ways. It affects growth rate, pigment content, enzyme reactions and photosynthesis, among other processes, but not always in the direction of increasing with higher temperatures. As an example, the uptake of NO<sub>3</sub><sup>-</sup> and its reduction actually generally decrease at higher temperatures, at least in many diatoms (e.g., Lomas and Glibert 1999; Glibert et al. 2015), suggesting that diatoms may be negatively impacted as temperatures continue to rise. Toxicity of many HABs also increases with warming, but this is not the case in all HABs (Fu et al. 2012 and references therein). The combination of elevated pCO<sub>2</sub> together with nutrient limitation and altered nutrient ratios appears to be an especially potent combination in terms of toxicity of some HABs.

## 1.4 Trophic Interactions: HABs as Prey and as Predators

High-biomass algal blooms often result in reduced transfer of energy to higher trophic levels, as many HAB species are not efficiently grazed, resulting in a decreased transfer of carbon and other nutrients to fish stocks when HAB species replace more readily consumed algal species (Irigoien et al. 2005; Mitra and Flynn 2006).

One of the important advancements in our understanding of HABs and eutrophication over the past decade or more has been the evolving recognition of the importance of mixotrophy in the nutritional ecology of many HABs, especially those that are prevalent in nutrient rich environments (Burkholder et al. 2008). Therefore, many HABs are important predators as well as prey. For decades it was thought that mixotrophy was either relatively rare, or when present was more common in those cells that thrived under nutrient impoverished conditions. Essential elements, such as N, P and C, are typically rich in microbial prey and thus mixotrophy has been thought to provide a supplement when there is an elemental imbalance in the dissolved nutrient substrates (Granéli et al. 1999 - should this be 1989??, Vadstein 2000 - missing ref??, Stibor and Sommer 2003; Stoecker et al. 2006). In eutrophic environments, although nutrients may be proportionately more available than in oligotrophic environments, it is not uncommon

for such nutrients to be out of stoichiometric balance, leading to nutrient deficiency even in a nutrient rich habitat (Burkholder et al. 2008).

A diverse array of HAB species are mixotrophic, either osmotrophic or phagotrophic or both (Glibert and Legendre 2006; Burkholder et al. 2008). There is an equally diverse array of prey that may be consumed by such HAB species. The extent to which species may be mixotrophic and the type of prey they may ingest affect the ability to remotely detect such blooms. At the extreme are those species that, while considered to be HABs, are not algae at all but rather heterotrophs and any pigment signature they may have would be of their ingested prey or of kleptochloroplasts. The latter is exemplified by *Noctiluca scintillans*, a heterotrophic dinoflagellate that forms spectacular “red tide” blooms (Harrison et al. 2011). This species is purely heterotrophic, and is of two forms, red and green, the latter a result of an endosymbiont (Harrison et al. 2011). *Noctiluca* is now recognized to be increasing in global distribution in relation to eutrophication, but its blooms are often displaced from the origin of the nutrient load as it is hypothesized that nutrients first fuel another type of bloom, either diatom or dinoflagellate, which are then grazed in succession leading to *Noctiluca* as the offshore manifestation of eutrophication (Harrison et al. 2011). The specific case of *Noctiluca* in the Arabian Gulf and Arabian Sea is developed in Section 1.6.

Another mixotrophic dinoflagellate group that forms spectacular blooms is that of *Karenia/Karlodinium*. Members of this group have been shown to graze the cyanobacterium *Synechococcus* sp., as well as cryptophytes (Jeong et al. 2005; Adolf et al. 2008; Glibert et al. 2009). In laboratory experiments, Jeong et al. (2005) estimated that 5 cells h<sup>-1</sup> of *Synechococcus* could be grazed by the mixotroph *Karenia brevis* while Glibert et al. (2009) found that from ~1 - 80 cells of *Synechococcus* h<sup>-1</sup> could be grazed by *K. brevis* with the rate varying with the predator:prey ratio. Two species of the genus *Karenia* are easily distinguished by their respective pigment signatures: *Karenia* sp. having the pigment gyroxanthin-diester, while *Synechococcus* sp. has the cyanobacterial pigment zeaxanthin (Kana et al. 1988; Johnsen et al. 2011) - how does this distinguish the two *Karenia* species?? Did you mean distinguish between *Karenia* and *Synechococcus*?? Interestingly, on the western coast of Florida, USA, during one bloom of *K. brevis* in 2005, the unique pigment signatures for *Karenia* were located in a region where *Synechococcus* was distinctly absent, suggesting either that these species thrive under very different ecological conditions, or, that *Karenia* had grazed the *Synechococcus* (Heil et al. 2007; Glibert et al. 2009, Figure 1.5).

In summary, changes in nutrients and climate have complex effects on HABs, altering water column structure, environmental conditions for growth, potential for toxicity, and overall changing niche space on a range of scales. Competition between and among HABs and non-HABs will also change (e.g., Flynn et al. 2015 - missing ref??). Those species with adaptive strategies to thrive in these altered conditions, through changes in growth rates, toxicity, or mixotrophic capabilities, will thrive. To understand these various strategies and their relationships, a number of conceptual models have been proposed linking different algal functional groups or HAB classes to their physical environment in terms of turbulence, nutrients and light. These conceptual models are briefly summarized below.

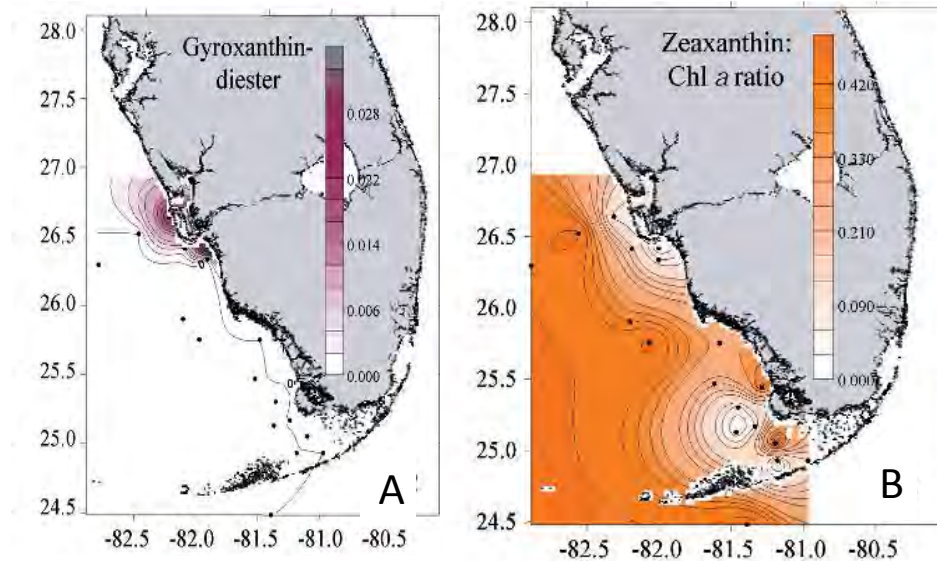


**Figure 1.5** Contour maps of the coast of western Florida, USA, illustrating (A) the abundance of the pigment gyroxanthin-diester, an indicator pigment of *Karenia brevis*, and (B) the ratio of zeaxanthin:chlorophyll-a, an indicator of cyanobacteria. Note the absence of zeaxanthin in the region where gyroxanthin-diester was most prevalent. Reproduced from Heil et al. (2007) and reproduced with permission of *Limnology and Oceanography*. Does IOCCG also have permission to reproduce these??

## 1.5 Conceptual models of the influence of nutrients and the physical environment on species selection

While there are many relationships that have been established with respect to nutrient loads, nutrient forms, various aspects of climate change and phytoplankton composition, the fundamental question is: Do systems self-assemble in fundamentally similar ways when physical parameters, including nutrient loads, are altered?

Ecological theory states that elemental stoichiometry is a fundamental constraint of food webs, and alternate stable states will develop under different nutrient regimes due to self-stabilizing feedback mechanisms. Margalef (1978) captured this fundamental principle in the now-classic “mandala” (Figure 1.6), as described by Smayda and Reynolds (2001):

Margalef’s elegant model combines the interactive effects of habitat mixing and nutrient conditions on selection of phylogenetic morphotypes and their seasonal succession, which he suggests occurs along a template of  $r$  versus  $K$  growth strategies. Margalef’s use of these two variables as the main habitat axes in his model accommodates our view that the pelagic habitat is basically hostile to phytoplankton growth, given its nutritionally-dilute nature and the various dissipative effects of turbulent mixing.

As a descriptive, rather than mechanistic model, the approach has been useful in generally conceptualizing species succession, seasonal progression, or even the gradients that may develop spatially with vertical structure and stratification.

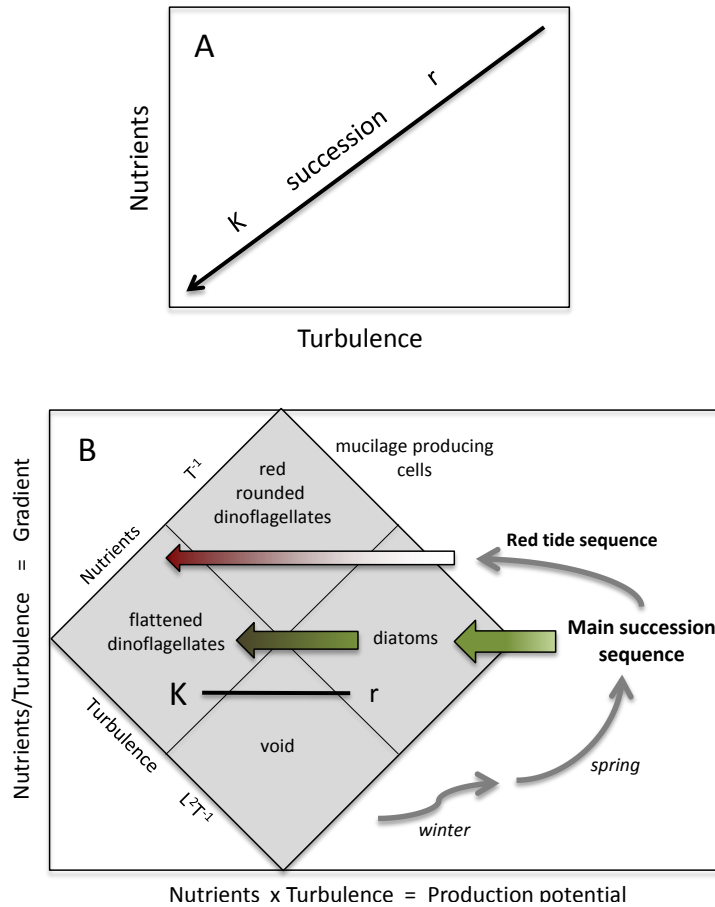


**Figure 1.6** Classic depiction of the Margalef phytoplankton mandala illustrating the relationship and sequence of diatoms and dinoflagellates in relation to nutrients and turbulence. Reproduced from Glibert (in press) under the Creative Commons license, and permission of the *Journal of Plankton Research*. Does IOCCG also have permission to reproduce these??

However, as with any simplified model, there are exceptions, difficulties in applications or reasons to believe that the simple parameters chosen may not be the important factors for species composition determination. One difficulty with the Margalef mandala is that “nutrients” are considered as a single entity and their importance only becomes significant when nutrients are “limiting”. Our evolving understanding of the role of nutrients in the development of HABs now also includes a greater appreciation for the role of nutrient ratios and their effects on food quality and on system biogeochemistry, whether nutrients are limiting or not (Sterner and Elser 2002; Glibert et al. 2011; Glibert et al. 2013). A stoichiometric perspective thus brings into question the long-held view that nutrients are only regulating when they are limiting (e.g., Reynolds 1999). Systems in which stoichiometric changes have occurred or are occurring may be uniquely poised for changes in dominant organisms. Ultimately, when more systems have been analyzed from an ecological stoichiometric viewpoint it may be possible to predict the trajectory of specific trophic responses. Of relevance to the Margalef mandala, species are

changing not only along a nutrient-light continuum, but along a stoichiometric continuum as well, and such changes may be physiologically important even when nutrients are not at limiting levels (Glibert et al. 2011; Glibert et al. 2013).

Physiological regulation of cells at saturating or super-saturating levels of nutrients can be as important in regulating food web structure as nutrients at the low end of the scale (Glibert et al. 2011). Among the many phytoplankton species, many HABs have adaptive strategies for coping with nutrient excess. Among these “strategies” are use of alternate nutritional mechanisms (such as mixotrophy), use of an alternate form of the same element (substituting organic for inorganic forms), releasing the nutrient in excess, and use of metabolism to create a favorable micro-environment (Glibert and Burkholder 2011). As noted above, toxin production, for example, by numerous harmful species has been shown to increase when the cells are not grown under nutrient-balanced conditions and when they sustain a change in N or P availability or depletion (Flynn et al. 1994; Johansson and Granéli 1999a,b; Granéli and Flynn 2006). Production of toxins rich in N might be regarded as a dissipatory mechanism, whereby cells acquire the nutrient(s) they need but release nutrients that are not needed (reviewed by Glibert et al. 2011; Glibert and Burkholder 2011). In some algal flagellates, toxin production increases under P stress (Granéli et al. 1998 - should this be 1989??, John and Flynn 2002 - missing ref??). However, the mechanism of toxin production for stoichiometric balance under N limitation appears to be less common than under P limitation, perhaps in part because many toxins are N-rich (Granéli and Flynn 2006).

Smayda and Reynolds (2001) attempted to develop a next-generation conceptual model of species succession based on environmental conditions, especially nutrients and light (Figure 1.7). They too, however, did not address the issue of nutrient proportion or nutrient ratios. They suggested that community assembly reflected life-form and species-specific selection, based on adaptive strategies consistent with C-S-R characteristics (C- colonists, predominant in chemically disturbed systems; S- stress tolerant and R-disturbance tolerant species that can withstand physical forces stresses). In their conceptual model they underscored that life-form properties over-ride phylogenetic properties in the development of species succession. The conceptual matrix of Smayda and Reynolds (2001) and Smayda and Reynolds (2003 - missing??) identifies the “nearshore, increasing eutrophic” space as dominated by certain armored dinoflagellates, including *Prorocentrum* spp. and by certain gymnodinioids, such as *Karenia* spp. or *Karlodinium* spp. However, these species groups generally do not co-occur, but rather more often occur temporally or spatially separated, as is the case in Chesapeake Bay where *Prorocentrum* generally occurs in spring, with *Karlodinium* generally occurring later in the year (Li et al. 2015).

Based on emerging trends in nutrients loads, and the fact that all nutrients are not necessarily trending similarly, a new mandala has been proposed that incorporates much greater understanding of algal nutritional physiology (Glibert in press, Figure 1.8). Similar to the Margalef mandala, the importance of differences in turbulence and nutrients are captured and diatoms and dinoflagellates again separate along the different axes. However, in contrast to Margalef, the nutrient axes herein are differentiated in two ways, by N:P and by N form. In Margalef’s diagram, the nutrient axis reflected a total nutrient load to the system and made no

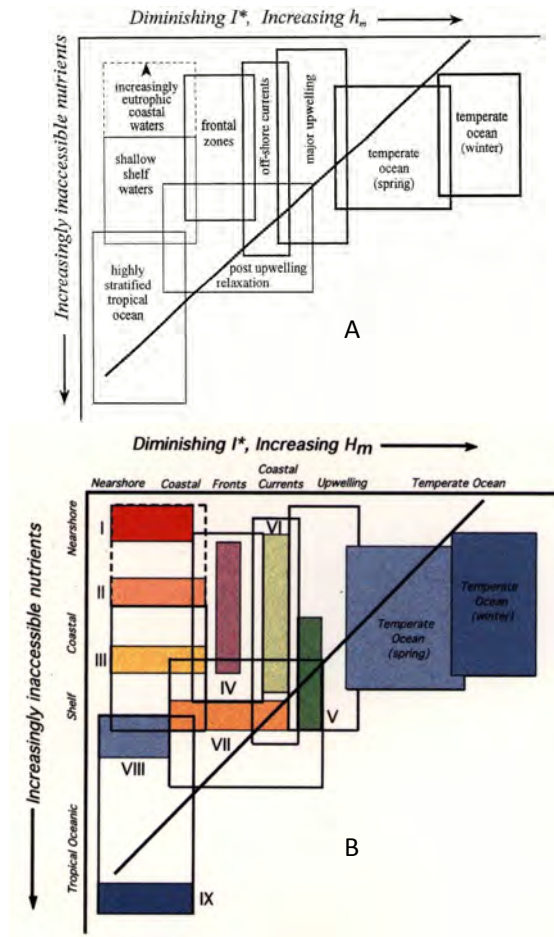


**Figure 1.7** Two illustrations of the dominant dinoflagellate (OK??) groups in relation to nutrients and light along an onshore-offshore continuum characterizing pelagic habitats. Panel A highlights the regional oceanographic regimes and panel B the associated AB types. Type I = gymnodinioids; Type II = peridinioids and prorocentroids; Type III = ceratians; Type IV = frontal zone species; Type V = upwelling relaxation taxa; Type VI = coastal current entrained taxa; Type VII = dinophysoids; Type VIII = tropical oceanic flora; Type IX = tropical shade flora. Reproduced from Smayda and Reynolds (2001) with permission of the *Journal of Plankton Research*. Does IOCCG also have permission to reproduce these??

distinction between nutrient forms (N or P) or forms of specific nutrients (e.g.,  $\text{NH}_4^+$  vs  $\text{NO}_3^-$ , organic vs. inorganic). The Margalef conceptualization was drawn primarily with systems such as upwelling in mind, where consistent injections of nutrients from deeper waters to surface were thought to be the primary nutrient source fuelling blooms, with N mainly being in the oxidized form ( $\text{NO}_3^-$ ). The new mandala therefore makes the distinction between N forms and N:P ratios, and this distinction is made in this new mandala for two important reasons. First, as noted above, N loads are generally increasing globally at a rate faster than those of P, as a consequence of our ever-expanding use of N-based fertilizers and their leakage to the environment, and the greater emphasis on P control (e.g., Galloway et al. 2002; Elser et al. 2009;

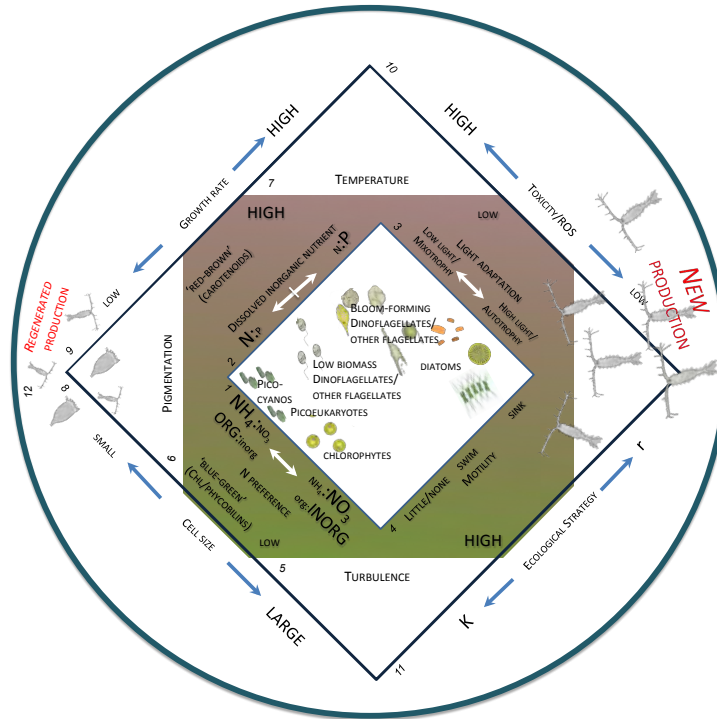


**Figure 1.8** Conceptual mandala of the relationships between nutrients and various other phytoplankton traits and environmental characteristics. Reproduced from Glibert (in press) under the Creative Commons license, and permission of the *Journal of Plankton Research*. Does IOCCG also have permission to reproduce these??

Glibert et al. 2013; Glibert et al. 2014a - or b??). Together these trends are leading, as described above, to increasing N:P ratios in many aquatic environments, both marine and freshwater. The effects of N vs. P loads have decidedly different effects on phytoplankton community assembly (e.g., Schindler et al. 2008; Paerl 2009; Hillebrand et al. 2013). Second, it is now well established that not all N forms are taken up and metabolized similarly by all phytoplankton (e.g., Glibert in press). The revised mandala also incorporates a scale that recognizes the importance of mixotrophy. Key among the notions captured in this new mandala is the relationships between and among traits. While the mandala serves to highlight the differences and trade-offs between traits, it can also be seen that, in general, some traits or associated environmental conditions tend to track each other (Glibert in press).

## 1.6 Changes in HABs assessed with Ocean Colour: Case Study of the Arabian Sea and Arabian Gulf

As described above, east Asia in general and China in particular represents a prime example of the expansion in HABs and eutrophication in relation to the expanding use of synthetic fertilizers and changes in human population. Another region where HABs have expanded is that of the Arabian Gulf and Arabian Sea, but in this case not only has nutrient loading

increased, but so too has climate variability??, leading to massive shifts in blooms species. Understanding the massive changes that have taken place in this region would not have been possible without ocean colour radiometry. This is especially true for this region of the world due to the rise in piracy and the extreme difficulty in mounting shipboard operations in the region (e.g., Goes and Gomes in press).

In the past decade, beginning about the year 2000, the northern Arabian Sea has witnessed a shift from a winter phytoplankton assemblage that had long been composed mostly of diatoms to a contemporary phytoplankton community that consists predominantly?? of the large, green, heterotrophic dinoflagellate, *Nocticula scintillans* (Gomes et al. 2014 and references therein, Goes and Gomes in press). This HAB relies on its endosymbiont *Pedinomonas noctilucae* to fix C; it also ingests a variety of prey. These blooms were not observed during the Joint Global Ocean Flux Study (JGOFS) cruises of the 1990s (Gomes et al. 2008) but have expanded considerably, consistent with climate changes and atmospheric warming (Goes et al. 2005) as well as nutrient loading (Harrison et al. 2011). Blooms of *N. scintillans* are now recognized to be an offshore manifestation of eutrophication, at least in some areas; increasing nutrients promote an increase in phytoplankton that, in turn, are the nutrient supply for this heterotrophic dinoflagellate (Harrison et al. 2011). The scale of eutrophication is massive, with the population of Mumbai doubling in just the past decade — and little advancement in sewage treatment in parallel. But, compounding this effect are large-scale changes in oceanography of the region. On the one hand, stronger summer monsoonal winds are now occurring than in past decades, bringing more nutrient-rich deep water to the surface as well. As a consequence, these blooms are now >300% more intense than in the late 1990s. Receding snow cover from the Himalayas is resulting in stronger winds across the Indian subcontinent, and this helps to intensify (intensify??) the upwelling of nutrients off the coast of Somalia, Yemen and Oman (Goes et al. 2005). On the other hand, the northern Arabian Sea appears to be experiencing weakening convective mixing, and thus a potential decline in nutrients to the surface to this area (Goes and Gomes in press).

Superimposed on this long-term trend was an unusual occurrence of a massive bloom of *Cochlodinium polykrikoides* in the Gulf of Oman in 2008 - 2009 (Al-Azri et al. 2014, and references therein). It is likely that the development of the bloom of *C. polykrikoides* in the coastal waters of Oman was facilitated by a uniquely strong mesoscale feature forced by the reversal of monsoonal periods, resulting in aggregation of cells and nutrients towards the coastal regions. The occurrence and persistence of high densities of *C. polykrikoides* was significantly influenced by an especially elevated nutrient load and warmer than normal temperatures. The progression of this regional event likely began with stronger than normal upwelling from the southwest monsoon along the Iranian coast and northern Omani coast in the Strait of Hormuz (Figure 1.9). This was likely followed by discharge of warm coastal plume water from the Arabian Gulf, and together with nutrient discharge, the *C. polykrikoides* cells were able to grow rapidly and accumulate along the Omani coast. These blooms intensified, but were also carried in an anticyclonic direction back to the Iranian shore following wind reversal in late October/November and the onset of the northeast monsoon. There, they were transported into the Arabian Gulf through the Strait of Hormuz where they affected the

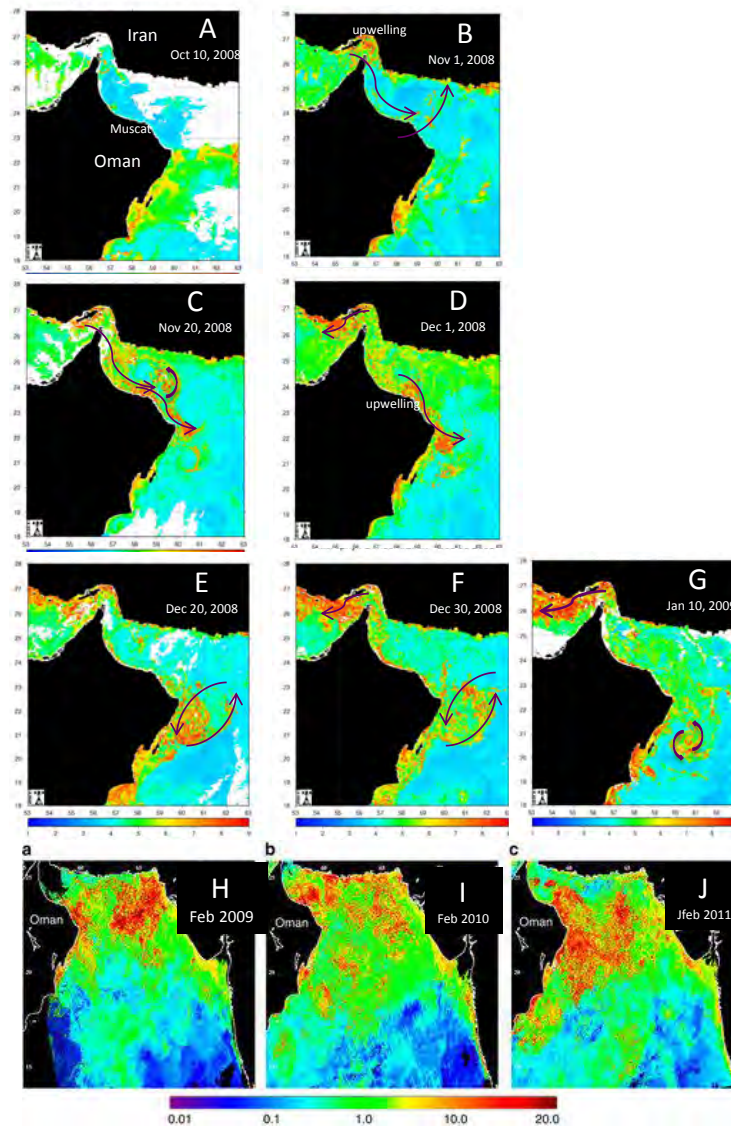


**Figure 1.9** Satellite images of the Gulf of Oman and NE Arabian Sea showing (panels A-G) the development and expansion of the *Cochlodinium polykrikoides* bloom from late fall 2008 into 2009 and (panels H-J) the expansion of blooms of *Noctiluca* in the northern Arabian Sea in the subsequent winters from 2009–2011. Panels A-G from Al-Azri et al. (2014) and reproduced with permission of *Estuaries and Coasts*; Panels H-J are from Gomes et al. (2014) and reproduced with permission of *Nature Communications*. Does IOCCG also have permission to reproduce these as well??

coast of Iran for several months into 2009 (Al-Azri et al. 2014). Export of chlorophyll-a to the Arabian Sea also apparently occurred by January 2009, as seen from the satellite images. These images also illustrate the spatial extent of these blooms compared to those observed in 2009, 2010 and 2011 (Figure 1.9). In the years since 2009 and the *C. polykrikoides* bloom, the trend for increasingly intensive outbreaks of *Noctiluca* blooms has continued, and the bloom

in February 2015 was particularly intense (Goes and Gomes in press). Interestingly, *Noctiluca* has also recently been reported to have expanded its range to the Southern Ocean from coastal Australia, a potential effect of increased warm core eddies from Tasmania to the pole (McLeod et al. 2012). As noted by Harrison et al. (2011),

Plankton dynamics have changed and are changing due to climate change and increasing eutrophication. *Noctiluca* may be a coastal or offshore manifestation of eutrophication in some areas, since an increase in nutrients provides an increase in phytoplankton, its main food supply as a grazer.

In summary, there are many factors contributing to the large global changes now occurring in HABS. Most importantly, changes (OK??) in nutrient loading, increased eutrophication and global climate change are the most important. Climate change is affecting circulation, stratification, temperature, as well as CO<sub>2</sub> and pH. Some of the most impacted regions of the globe are East Asia, especially the coast of China, and the Arabian Gulf and Sea regions. Ocean colour radiometry, together with many direct observational tools, experimental measurements as well as modelling, has contributed to advance our understanding of these important changes.



## Chapter 2

# Case Study: Blooms of the Neurotoxic Dinoflagellate *Karenia brevis* on the West Florida Shelf

Inia M. Soto<sup>1</sup>, Chuanmin Hu<sup>1</sup>, Jennifer Cannizzaro<sup>1</sup>, Jennifer Wolny<sup>1,2</sup> and Frank E. Muller-Karger<sup>1</sup>

---

## 2.1 Background

### 2.1.1 Organism description, impact, and distribution

*Karenia brevis*, previously known as *Gymnodinium breve* (Davis 1948) and *Ptychodiscus brevis* (Steidinger 1979), is an ichthyotoxic unarmored dinoflagellate that causes massive harmful algal blooms (HABs). It is commonly referred to as “Florida red tide” in the Gulf of Mexico (GoM). *K. brevis* is a eukaryotic, 18–45  $\mu\text{m}$  wide, single-celled organism, with two flagella for motility and propulsion, a distinctive apical carina, a straight apical groove, and a nucleus positioned in the lower left quadrant of the cell (Table 2.1, Figure 2.1a; Steidinger et al. 2008).

*K. brevis* produces brevetoxins, which are responsible for massive fish kills, marine animal mortality, neurotoxic shellfish poisoning (NSP), and respiratory illness in humans and marine mammals. NSP can cause severe illness in humans, which can necessitate emergency room visits and intensive care for the first few hours after intoxication; however, no fatalities have been reported (Watkins et al. 2008; Landsberg et al. 2009; Fleming et al. 2011). Reports of NSP after consumption of contaminated shellfish are rare, but the possibility of misdiagnosis is high (Watkins et al. 2008). *K. brevis* cells can break open easily with the wave action and release brevetoxins into marine aerosols. Contaminated aerosols have been measured up to six kilometers away from the coast (Kirkpatrick et al. 2010). These aerosols can cause respiratory irritation, bronchial constriction, coughing, burning sensation and itching (Kirkpatrick et al. 2004, 2011). These respiratory symptoms can be exacerbated in asthmatic patients or those with other chronic respiratory ailments (Singer 1998; Fleming et al. 2005, 2007, 2009; Kirkpatrick et al. 2011).

Brevetoxins can kill fish even at low concentrations (Baden and Mende 1982). Hence, fish kills are often an early warning sign of Florida red tides. During intense blooms, fish kills of up to 100 tons per day have been reported (Alcock 2007). Brevetoxins can bioaccumulate in fish and seagrass, which then serve as vectors for toxins in the food chain (Flewelling

---

<sup>1</sup>College of Marine Science, University of South Florida, 140 7<sup>th</sup> Ave., S., St. Petersburg, FL 33701, USA

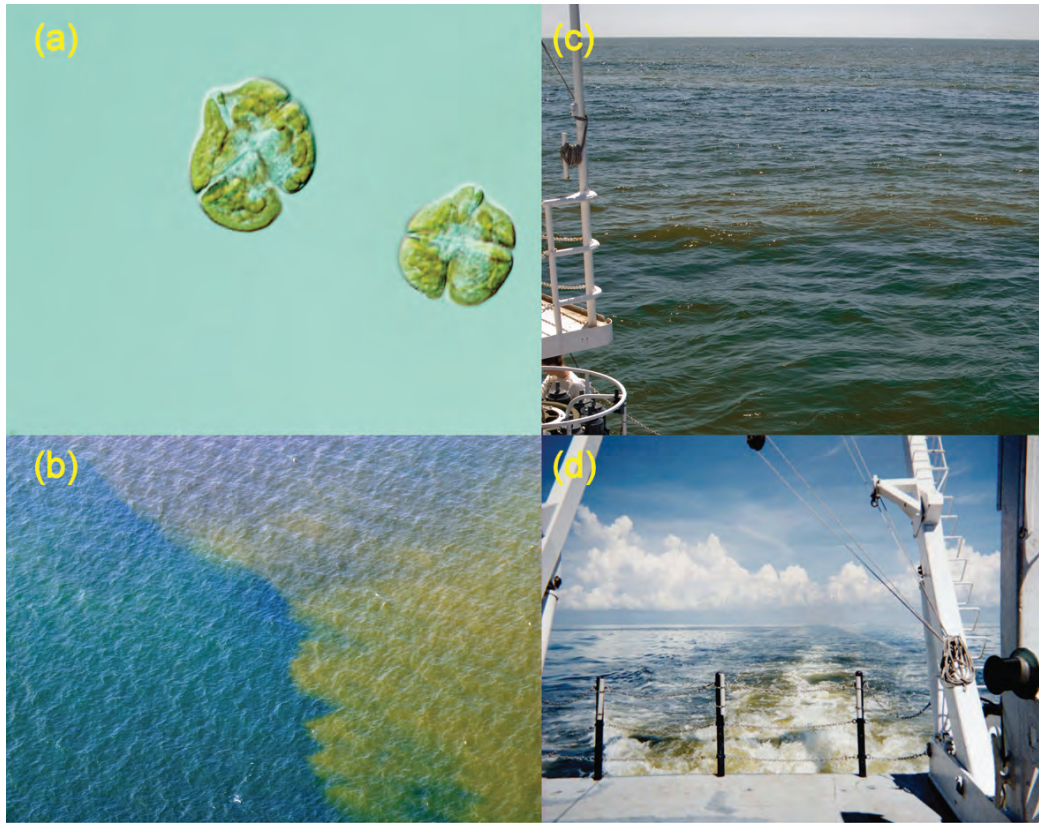
<sup>2</sup>Florida Fish and Wildlife Conservation Commission, 100 8<sup>th</sup> Ave SE, St. Petersburg, FL 33701

Table 2.1 Description of *Karenia brevis*.

Eco-physiological characterization of <i>Karenia brevis</i>	
Cell Features	Eukaryotic, 18–45 $\mu\text{m}$ wide, distinctive apical carina and straight apical groove, nucleus in the left lower quadrant, and 10–20 chloroplasts (Fig. 1a; Steidinger et al. 2008).
Temperature	Range: 9–33°C, Optimal: 20–28°C
Salinity	Range: 17–40, Optimal: 31–37
Pigments	Main pigments are chlorophyll, $\beta$ -carotene, fucoxanthin and its derivatives, and gyroxanthin-diester (Millie et al. 1995; Bjørnland et al. 2003; Pederson et al. 2004).
Nutrient preferences	Organic and inorganic phosphorus and nitrogen: nitrates, nitrite, ammonia, urea and amino acids, humic substances (Vargo 2009). Trace metals, chelators and vitamins are a requirement (Steidinger 2009). Ingestion (i.e., phagotrophy) of the cyanobacteria <i>Synechococcus</i> (Glibert et al. 2009).
Motility	Two flagella for motility and propulsion (Steidinger et al. 1998).
Ultrastructure	Unarmored dinoflagellate, no ultrastructure (Steidinger et al. 1998).
Inherent Optical Properties	Distinctive fourth derivative of the absorption spectra (Millie et al. 1997; Kirkpatrick et al. 2000). <i>K. brevis</i> blooms exhibit significant lower $b_{bp}$ (550) coefficients compared to diatom dominated waters (Cannizzaro et al. 2004; Schofield et al. 2006; Cannizzaro et al. 2008, 2009). Significant decrease in the absorption slope at 443 nm and step detrital absorption slope (Cannizzaro et al. 2008).
Apparent Optical Properties	Remote sensing reflectance ( $R_{rs}$ ) values are 3–4 times lower in high chlorophyll (1–10 $\text{mg m}^{-3}$ ) with <i>K. brevis</i> concentrations over $10^4$ $\text{cell l}^{-1}$ . $R_{rs}$ decreases with increment in concentration (Cannizzaro et al. 2008).

et al. 2005; Landsberg et al. 2009). Mass mortality of dolphins and manatees have been attributed to brevetoxin exposure either by consumption and/or inhalation (Geraci 1989; O’Shea et al. 1991; Bossart et al. 1998; Steidinger et al. 1998; Van Dolah et al. 2003; Flewelling et al. 2005; Fleming et al. 2011). The effects of *K. brevis* blooms also extend into the economy of the region. Tourists avoid beaches, water activities (e.g., diving, boating, and fishing), and businesses within close proximity to impacted beaches. Hoagland and Scatasta (2006) estimated average annual economic loss in the United States due to HABs at \$82 million, while the St. Petersburg/Clearwater Visitor and Area Convention Bureau documented a loss of \$240 million for the Tampa Bay region during the 2005 red tide event alone (Moore 2006; Alcock 2007).

*Karenia* species are globally distributed and have been reported in the Gulf of Mexico (Davis 1948), English Channel (Kurekin et al. 2014), North Sea (Kurekin et al. 2014), New Zealand (Chang 1999; Faust and Gullede 2002; Chang and Ryan 2004; Haywood et al. 2004; Rhodes et al. 2004; Davidson et al. 2009), Kuwait, (Heil et al. 2001; Glibert et al. 2002), Hong Kong (Yang et al. 2001; Yeung et al. 2005), East China Sea (Okaichi 2004), Scotland (Davidson et al. 2009), South Africa (Botes et al. 2003), western Mediterranean (Feki et al. 2013; Reñé et al. 2015), Seto-Inland Sea, Japan (Siswanto et al. 2013), and Tasmania and Australia (de Salas et al. 2004). A more complete distribution table of *Karenia* species can be found in Brand et al. (2012). *Karenia* species are commonly found at background concentrations ( $<1,000$   $\text{cells l}^{-1}$ ) in the GoM and have also been reported in Jamaica (Steidinger 2009) and Trinidad



**Figure 2.1** (a) *K. brevis* cell magnified 400× with light microscopy, (b – d) *K. brevis* blooms on the West Florida Shelf. Photos are courtesy of Florida Fish and Wildlife Conservation Commission.

(Lackey 1956). Blooms of *Karenia* species have been reported in coastal waters along Florida and Texas (see references in Magaña et al. 2003 and Steidinger 2009), Alabama, Louisiana and Mississippi (Dickey et al. 1999; Maier Brown et al. 2006); and in the following Mexican Gulf states: Tamaulipas (Cortés-Altamirano et al. 1995), Veracruz (Aké-Castillo et al. 2012), Tabasco (Mier et al. 2006), Campeche (Soto et al. 2012; Soto 2013), and Yucatan (Merino-Virgilio et al. 2012). Also, *Karenia* blooms have been observed in the South and Mid Atlantic Bights, as it is transported out of the GoM by means of the Gulf Stream (Tester et al. 1991; Walsh et al. 2009; Wolny et al. 2015).

### 2.1.2 Ecological niche, nutrient and environmental preferences, and bloom mechanism

*K. brevis* is considered to be neritic and typically occurs in continental shelf and coastal waters (Finucane 1964). Several studies indicate that *K. brevis* is well-adapted to low-nutrient environments such as the oligotrophic waters of the West Florida Shelf (WFS). This is attributed to low half-saturation constants ( $K_s$ ) for nitrate and ammonia (0.06–1.07  $\mu\text{M}$ ) and phosphorus (0.18  $\mu\text{M}$ ) (Vargo and Howard-Shamblott 1990; Steidinger et al. 1998; Bronk et al. 2004; Vargo

2009). *K. brevis* can utilize a variety of nutrient sources (both organic and inorganic), even simultaneously (Vargo and Shanley 1985). Phosphorus is not a limiting nutrient for *K. brevis* (Dragovich and Kelly 1966; Wilson 1966; Wilson et al. 1975). Instead, nitrogen typically limits growth with estimated concentrations necessary to maintain a bloom of  $10^6$  cells  $l^{-1}$  ranging from 3–8.6  $\mu\text{m}$  (Odum et al. 1955; Shanley and Vargo 1993). *K. brevis* can utilize organic nitrogen from amino acids (Baden and Mende 1979) and urea (Shimizu and Wrensford 1993; Shimizu et al. 1995; Bronk et al. 2004; Sinclair et al. 2009). On the WFS, blooms of *K. brevis* are often preceded by blooms of the nitrogen-fixing cyanobacteria *Trichodesmium*. It has been suggested that *K. brevis* can utilize *Trichodesmium*-generated dissolved nitrogen (Mulholland et al. 2004, 2006) in addition to humic substances (Ingle and Martin 1971; Martin et al. 1971; Vargo 2009).

Inorganic sources of nitrogen in the form of nitrate-nitrite and ammonium are also used; however, cell yields for certain inorganic sources have yet to be quantified (Steidinger 2009; Vargo 2009). Richardson et al. (2006) found that growth rates were indifferent of the nitrogen source. Similar to other harmful algal species, *K. brevis* is mixotrophic, which means that it can alternate between autotrophy and heterotrophy (Burkholder et al. 2008). Studies by Jeong et al. (2005) and Glibert et al. (2009) have shown that ingestion (i.e., phagotrophy) of the cyanobacteria *Synechococcus* can increase the growth rate of *K. brevis*.

Blooms of *K. brevis* have been identified since 1946 (Davis 1948), however reports of dead fish and changes in water colour date back to the 1600s (Magaña et al. 2003). On the WFS, blooms of *K. brevis* occur almost every year during late-summer and fall, but some blooms have lasted more than a year, such as in 1946–47 and 2005–06 (Steidinger 2009). It has been suggested that blooms initiate in nutrient-poor waters of the WFS between 18–74 km offshore (Steidinger 1975; Steidinger and Haddad 1981). Wind and currents are hypothesized to transport blooms inshore, where they are supported by additional nutrient sources (Steidinger et al. 1998). Several hypotheses have been suggested to explain the source of nutrients necessary for triggering blooms. These include upwelling of nutrient-rich waters along the continental shelf and oceanic fronts (e.g., Steidinger and Haddad 1981), iron-rich Saharan dust that may promote blooms of the nitrogen-fixing cyanobacteria *Trichodesmium* (Lenes et al. 2001; Walsh and Steidinger 2001), intrusions of the Mississippi River plume (Stumpf et al. 2008), and submarine groundwater discharge (Hu et al. 2006). Walsh et al. (2006) and Vargo et al. (2008) suggested that estuarine flux from Tampa Bay, Charlotte Harbor, and the Caloosahatchee River can supply nitrogen and phosphorus to meet the requirements for populations  $<10^5$  cells  $l^{-1}$ , but that additional nutrient sources (e.g., remineralization of dead fish and zooplankton excretion) are necessary to sustain large and prolonged *K. brevis* blooms.

## 2.2 Principles

*K. brevis* blooms often modify the colour of the water, commonly appearing various shades of brown to red (Figure 2.1b-d). Such changes are partially attributed to the specific absorption and backscattering properties associated with the *K. brevis* cells (Cannizzaro et al. 2004, 2008).

Water colour can also vary, though, depending on the spectral quantity and quality of incoming light, observation angle, depth of the bloom, and concentrations/types of non-algal particulate and dissolved coloured materials (e.g., suspended sediments and coloured dissolved organic matter, CDOM) that accompany blooms (Dierssen et al. 2006).

Natural populations of *K. brevis* contain approximately 8.5 pg of chlorophyll-a per cell (Evens et al. 2001), which amounts to  $\sim 0.5\text{--}1.0\text{ mg m}^{-3}$  of chlorophyll-a for a moderate bloom ( $5 \times 10^4$  to  $10^5$  cells  $\text{l}^{-1}$ ). Based on field observations, this was determined to be the minimum level for detecting blooms from space using satellite ocean colour data (Tester et al. 1998). Bloom detection on the WFS, based on satellite-derived chlorophyll-a concentrations (CHL), is possible because *K. brevis* blooms in this region are generally mono-specific, highly concentrated ( $10^4$  to  $10^7$  cells  $\text{l}^{-1}$ ), cover large areas, usually concentrate near the surface, and often last for weeks or months at time.

High concentrations of chlorophyll, though, are not unique to *K. brevis*, but can also be found in blooms of other phytoplankton types (e.g., diatoms) that occur in GoM waters. Differentiating *K. brevis* blooms from other blooms requires unique optical characteristics of either absorption or backscattering spectra of *K. brevis*. A derivative analysis of the absorption spectra has been shown to differentiate *K. brevis* blooms through a similarity index when compared with known *K. brevis* absorption spectra (Millie et al. 1997; Kirkpatrick et al. 2000; Hails et al. 2009). Application of this approach to satellite ocean colour data, though, requires hyperspectral reflectance data which is currently unavailable for the majority of current and planned ocean colour missions (Craig et al. 2006). *K. brevis* blooms also exhibit low backscattering per unit chlorophyll (Cannizzaro et al. 2004; Schofield et al. 2006; Cannizzaro et al. 2008, 2009), which may also be used to differentiate different bloom types. Therefore, in principle, *K. brevis* blooms can be detected in two steps: the first is to identify a bloom from ocean colour imagery based on high pigment concentrations, followed by analyzing spectral characteristics to differentiate bloom types. When *a priori* knowledge of the bloom type is available (e.g., from either field measurements or regional oceanography), step 1 alone is sufficient for detecting *K. brevis* blooms.

The use of satellite ocean colour imagery for *K. brevis* bloom detection has a long history. In 1978, a major *K. brevis* bloom was first detected as a high chlorophyll feature using imagery obtained from the Coastal Zone Color Scanner (1978–1986) aboard the Nimbus-7 spacecraft (Steidinger and Haddad 1981). Since then, several *K. brevis* detection methods have been developed utilizing data obtained from more modern satellite ocean colour sensors, including SeaWiFS (1997–2011), MODIS (Terra: 1999–present, Aqua: 2002–present), MERIS (2002–2012), and VIIRS (2011–present) (Tester and Stumpf 1998; Stumpf et al. 2003; Cannizzaro et al. 2004; Tomlinson et al. 2004; Hu et al. 2005; Cannizzaro et al. 2008, 2009; Amin et al. 2009; Tomlinson et al. 2009; Carvalho et al. 2010; Hu et al. 2011, 2015; Soto et al. 2015). Stumpf et al. (2003) and Tomlinson et al. (2004) demonstrated that a chlorophyll-anomaly approach effectively reduced the impact of optically significant, non-algal materials (e.g., resuspended sediments, CDOM), which often lead to overestimations in chlorophyll-a concentrations in coastal waters (Cannizzaro et al. 2013). Alternative data products, including normalized fluorescence line height (nFLH; Hu et al. 2005, 2015) and Red Band Difference (RBD; Amin et al. 2009, 2015),

help overcome this problem by utilizing red and near-infrared bands that quantify solar-stimulated chlorophyll fluorescence. Soto et al. (2015) found that the use of nFLH (or similar products such as RBD) improved the performance of all *K. brevis* detection techniques. These wavebands are less sensitive to perturbations by non-algal materials. The chlorophyll-anomaly method is used operationally by the U.S. NOAA for monitoring *K. brevis* blooms, with results distributed weekly in the form of HAB bulletins. Alternatively, the nFLH imagery has been used routinely by the Florida Fish and Wildlife Conservation Commission's Fish and Wildlife Research Institute (FWC-FWRI) for HAB assessments. However, neither of these methods is capable of differentiating between *K. brevis* blooms and blooms of non-harmful algae.

Several attempts have been made to optically distinguish *K. brevis* blooms from non-harmful blooms. Because *K. brevis* blooms tend to exhibit lower backscattering efficiencies, the slope between chlorophyll and particulate backscattering coefficients at 551 nm ( $b_{bp}(551)$ ) can be compared to a reference slope established by Morel (1988) in order to differentiate bloom types (Cannizzaro et al. 2004, 2008, 2009). Inspection of the green band against satellite-derived chlorophyll and the use of the spectral curvature in the blue-green bands have also been proposed to separate bloom types (Tomlinson et al. 2009; Carvalho et al. 2010). Soto et al. (2015) provided a thorough review and evaluation of these various techniques and found similar performance in terms of both bloom and non-bloom detection, however the best results were obtained by techniques that used nFLH or RBD, and took into consideration the low backscattering properties of *K. brevis*.

In European waters and coastal waters off New Zealand, *Karenia mikimotoi* has been identified to form HABs (Faust and Gulledege 2002; Haywood et al. 2004; Rhodes et al. 2004; Davidson et al. 2009). Similar to *K. brevis* blooms, *K. mikimotoi* blooms can also cause fish and other animal mortality through the production of hemolytic cytotoxins (Satake et al. 2005). Also similar to *K. brevis*, there are two distinct approaches to remotely detect *K. mikimotoi* blooms, based on either biomass (chlorophyll) or spectral reflectance. Miller et al. (2006) used multivariate classification of SeaWiFS data to discriminate between harmful (*K. mikimotoi* and cyanobacteria) and non-harmful algae. This approach was also applied to MERIS data (Shutler et al. 2005) and to a large *K. mikimotoi* bloom in Scottish waters in 2006 (Davidson et al. 2009). Kurekin et al. (2014) further developed the approach to study *K. mikimotoi* and the flagellate *Phaeocystis globosa* using both MERIS and MODIS data. The approach correctly identified 89% of *Phaeocystis globosa* HABs in the southern North Sea and 88% of *K. mikimotoi* blooms in the western English Channel.

For the case study presented here, we chose to combine several of these techniques, namely satellite-derived CHL, nFLH, and backscattering (Cannizzaro et al. 2008, 2009; Hu et al. 2011), to demonstrate how MODIS data was used to detect and track a *K. brevis* bloom on the WFS in 2006–2007. This approach was chosen amongst the various published techniques because of the wide availability of MODIS nFLH imagery and the operational use of these data products by FWC-FWRI (Hu et al. 2015).

## 2.3 Data and Methods

For the case study, we limited our region to the central and southern WFS (25.5–28.2°N, 81.5–83.5°W) and data for the years 2006–2007. MODIS-Aqua Level-2 data were downloaded directly from the U.S. NASA Goddard Space Flight Center (GSFC; <http://oceancolor.gsfc.nasa.gov/>). Specifically, the following products were used: Chlorophyll-a concentration estimates or CHL ( $\text{mg m}^{-3}$ ; using the OC3; O'Reilly et al. 2000), spectral remote sensing reflectance ( $R_{rs}(\lambda)$  ( $\text{sr}^{-1}$ )) at 10 wavelengths, and nFLH ( $\text{mW cm}^{-2} \mu\text{m}^{-1} \text{sr}^{-1}$ ; Letelier and Abbott 1996). Images were mapped to a cylindrical equidistant projection using the SeaWiFS Data Analysis System (SeaDAS, version 6.1). Level-2 flags (atmospheric correction failure, land, very high or saturated radiance, high sensor view zenith angle, stray-light contamination, clouds, high solar zenith angle, band navigation failure, and CHL warning) were applied to discard low-quality data.

To implement the *K. brevis* detection technique suggested in Hu et al. (2011), satellite CHL, nFLH,  $b_{bp}(551)$ , enhanced-RGB (ERGB) composite imagery, and the  $b_{bp}$  ratio were required. These data products or imagery were calculated or generated as follows:

1. CHL ( $\text{mg m}^{-3}$ ) was estimated from  $R_{rs}(\lambda)$  using the maximum band ratio algorithm (OC3; O'Reilly et al. 2000).
2. nFLH ( $\text{mW cm}^{-2} \mu\text{m}^{-1} \text{sr}^{-1}$ ) was derived using  $nL_w(\lambda)$  as the height at 678 nm above a linear baseline formed between 667 and 748 nm (Letelier and Abbott 1996).
3.  $b_{bp}$ , QAA (551) was derived from  $R_{rs}(\lambda)$  using the Quasi-Analytical Algorithm (QAA, Lee et al. 2002).
4. ERGB imagery is very similar to a true colour imagery, except that instead of using a red-green-blue band composite, a green-blue-blue composite was generated using  $nL_w(\lambda)$  at 551, 488, and 443 nm. The step-by-step process of calculating ERGB images is explained in detail in Hu et al. (2011).
5. The  $b_{bp}$  ratio was determined based on the findings of Cannizzaro et al. (2004, 2008), in which the  $b_{bp}(551)$  of *K. brevis* blooms is lower than that determined using the Morel (1988) relationship for Case 1 waters. First, we derived  $b_{bp}(551)$  using the Morel (1988) algorithm:

$$b_{(bp, \text{MOREL})} = 0.3 \times \text{CHL}^{0.62} \times (0.002 + 0.02 \times (0.5 - 0.25 \times \log_{10} \text{CHL})).$$

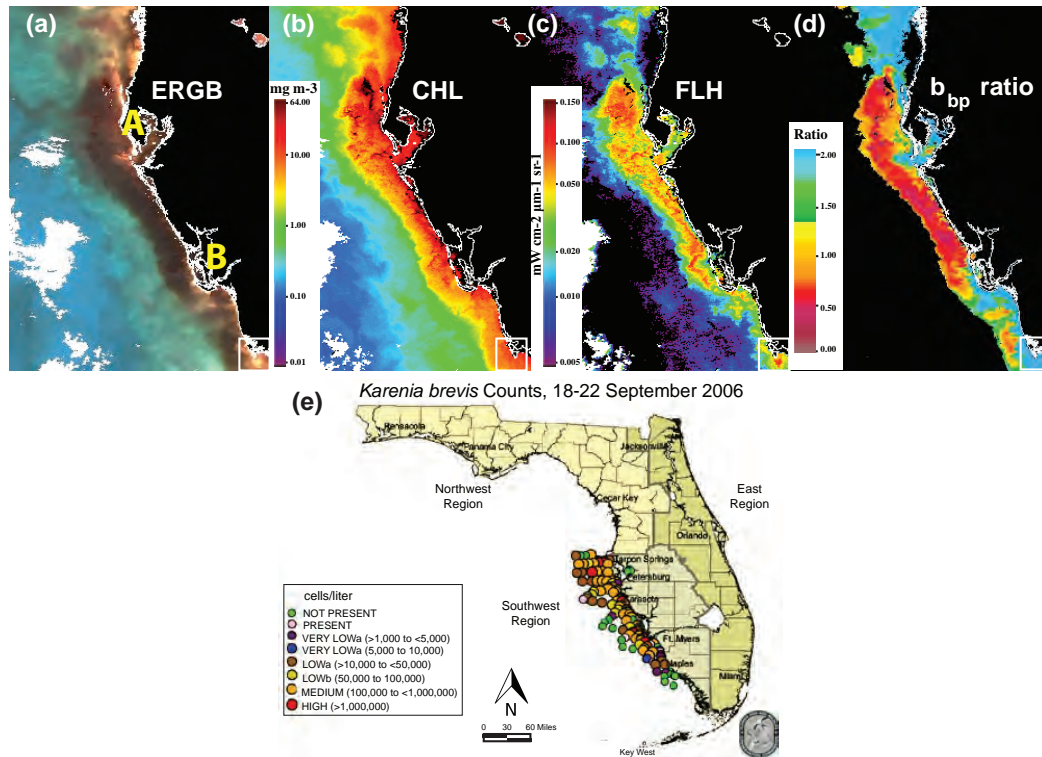
The  $b_{bp}$  ratio was then calculated as  $b_{bp, \text{QAA}}/b_{(bp, \text{MOREL})}$ .

*K. brevis* blooms were classified based on the following criteria: CHL > 1.5  $\text{mg m}^{-3}$ , nFLH > 0.01  $\text{mW cm}^{-2} \mu\text{m}^{-1} \text{sr}^{-1}$  and  $b_{bp}$  ratio < 1. Areas flagged positive as blooms were confirmed using *in situ* *K. brevis* cell count data collected by FWC-FWRI prior to patches being delineated manually using the Region of Interest tool in the image analysis software ENVI®.

## 2.4 Ocean Colour Case Demonstration

The 2006–2007 *K. brevis* bloom was first observed in early July in coastal waters near the Charlotte Harbor region. It peaked in October with expanded spatial coverage and then moved back southward, eventually entering the Florida Current with transport towards the

Mid-Atlantic Bight in February 2007. Twenty NSP cases were reported in Florida between March and December 2006, with some patients requiring hospitalization (Watkins et al. 2008). Mass mortality of dolphins was also reported in both 2005 and 2006 (Landsberg et al. 2009).



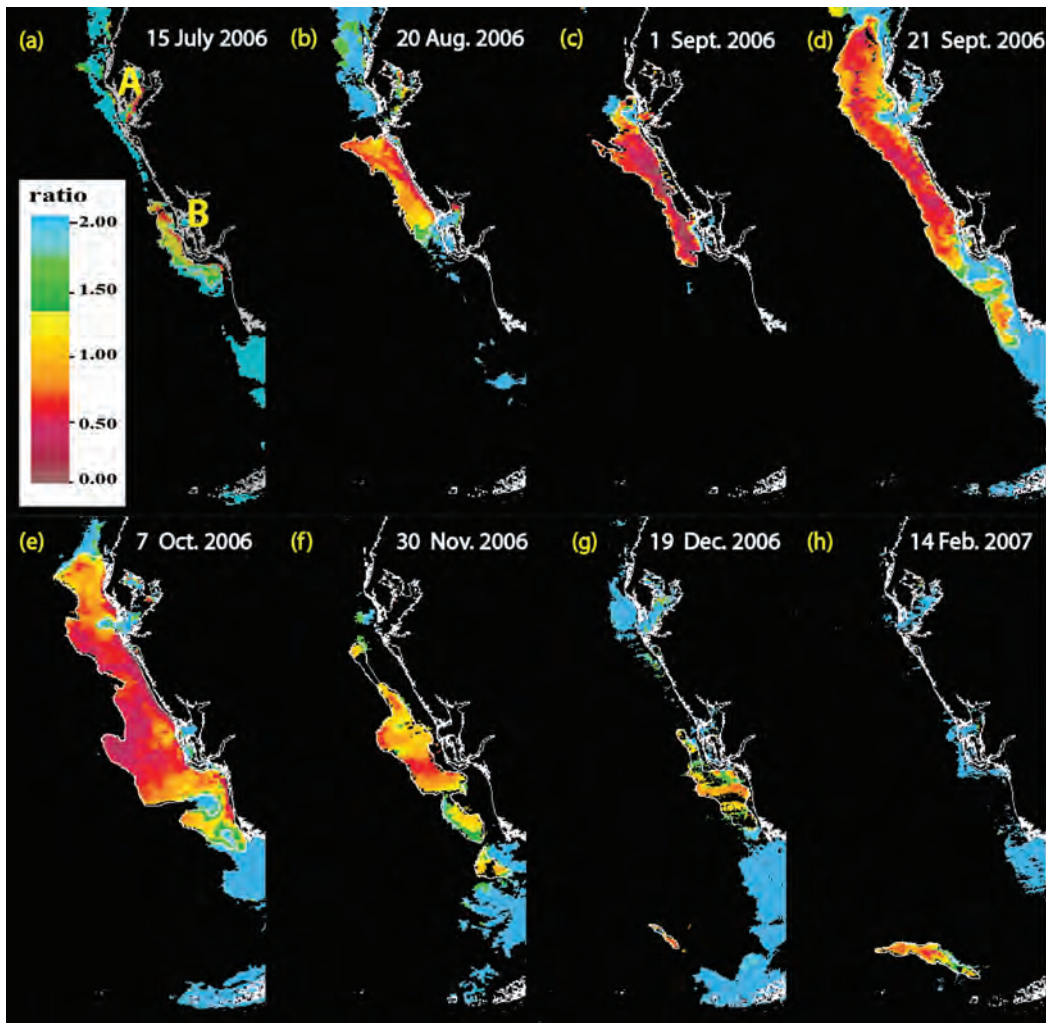
**Figure 2.2** (a-d) MODIS-Aqua images on 21 September 2006 showing a *K. brevis* bloom on the central West Florida Shelf between Tampa Bay (A, 27.75°N, 82.50°W) and Charlotte Harbor (B, 26.75°N, 82.1°W). (e) FWC-FWRI *in situ* *K. brevis* cell concentrations (cells l<sup>-1</sup>) (<https://www.flickr.com/photos/myfwc/sets/72157635398013168/>).

Figure 2.2 shows MODIS-Aqua data for 21 September 2006 and *in situ* data collected by FWC-FWRI during the week of 18-22 September 2006. In the ERGB image (Figure 2.2a), a dark reddish patch of water extending from Tarpon Springs southward to Naples was highly visible. Darkness in ERGB composite imagery denotes areas with low reflectance caused by various combinations of high CDOM and chlorophyll absorption and low backscattering. Based on the ERGB image alone, this dark patch could not be confirmed as a phytoplankton bloom. However, this type of imagery did help identify areas where blooms were unlikely to be found, including bright regions where the signal received by the satellite was at, or near, saturation due to high reflectance caused by either high sediment loads or bottom reflectance for shallow waters.

The CHL image (Figure 2.2b) indicates elevated chlorophyll along the entire west coast of Florida, while the nFLH image (Figure 2.2c) shows a distinctive pattern of high nFLH consistent with the dark patch observed in the ERGB image. Satellite CHL can be overestimated due to high CDOM absorption or sediments, and in shallow areas with high bottom contributions (Cannizzaro et al. 2013). While nFLH provides a more accurate indicator of algal biomass than

CHL in waters with elevated CDOM (Hu et al. 2005), biomass is often overestimated according to nFLH in sediment-rich areas or shallow waters with high bottom reflectance. Pairing the nFLH and ERGB image, though, allows these latter areas (e.g., shallow waters off Naples (in the south) in Figure 2.2a,c denoted by a white box) to be identified as non-bloom waters.

While areas with high nFLH that appear dark in the ERGB indicated the presence of a bloom, the specific type of bloom (*K. brevis* or other) could not be determined with this information alone. Based on the location and timing of this bloom, the likelihood that it was caused by *K. brevis* was strong, and so the  $b_{bp}$  ratio algorithm was applied. The  $b_{bp}$  ratio algorithm detected a large bloom region consistent with the dark water and high nFLH values. The *in situ* data collected by FWC confirmed that the area detected as a bloom by the  $b_{bp}$  ratio algorithm was indeed a *K. brevis* bloom and also that *K. brevis* was absent in the area to the south of Charlotte Harbor (white box, Figure 2.2).



**Figure 2.3** MODIS-Aqua images with the  $b_{bp}$  ratio showing the development and movement of the *K. brevis* bloom along the West Florida Shelf in 2006.

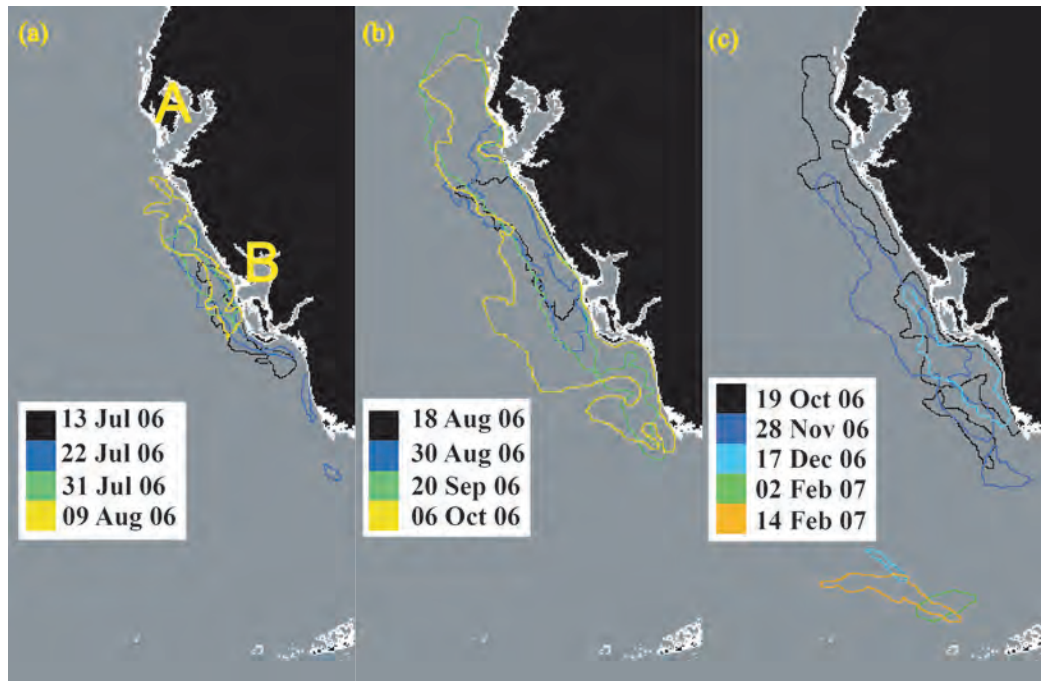


**Figure 2.4** Sequence of delineations over a map of Florida demonstrate the initiation, maintenance and dissipation of the 2006 *K. brevis* bloom.

The  $b_{bp}$  ratio algorithm was applied to daily MODIS-Aqua data collected from May 2006 to March 2007. This allowed the bloom to be tracked from the moment it reached surface concentrations detectable by the satellite to the moment it either dissipated or was transported out of the study region. In addition to the  $b_{bp}$  ratio algorithm, the nFLH, ERGB and *in situ* data were also used to validate the algorithm output. Regions flagged positive for red tide were delineated using ENVI®. Figure 2.3 shows a sequence of MODIS-Aqua  $b_{bp}$  ratio images from July 2006 to February 2007, demonstrating the northerly movement followed by southerly transport of the bloom throughout its existence.

Figure 2.4 documents the development, movement and dissipation of the 2006–2007 *K. brevis* bloom in even greater detail. Again, the bloom was first observed using satellite imagery in mid-July 2006 off the coast of Charlotte Harbor, which was consistent with *in situ* cell count data. It then expanded northward towards Tarpon Springs covering an area ~2,000–3,000 km<sup>2</sup> in size in August and early September. In early October, the bloom extended up to 100 kilometers offshore between Tarpon Springs and Naples with maximal areal coverage >11,000 km<sup>2</sup>. By late 2006 and early 2007, the bloom had receded to the south and according to reports by Walsh et al. (2009) and Wolny et al. (2015), was eventually transported through the Florida Strait by the Florida Current and deposited on Florida's east coast.

## 2.5 Discussion and Summary

Various *K. brevis* remote sensing detection techniques have been proposed and used in the past two decades (Tester et al. 1998; Stumpf et al. 2003; Cannizzaro et al. 2004; Tomlinson et al. 2004; Hu et al. 2005; Cannizzaro et al. 2008, 2009; Amin et al. 2009; Tomlinson et al. 2009; Carvalho et al. 2010; Hu et al. 2011, 2015; Soto et al. 2015). In this case study, several of these techniques were combined and used to demonstrate how satellite ocean colour data can be used to detect and trace a *K. brevis* bloom on the WFS. *K. brevis* blooms are not visible in satellite imagery until they reach near-surface concentrations of  $\sim 5 \times 10^4$  cells  $l^{-1}$  (Tester et al. 1998). This means that bloom initiation cannot be detected. Instead, only blooms that have formed surface expressions and intensified may be detected. Most remote sensing *K. brevis* detection techniques have been reported to have a success rate around 70–80% (Soto et al. 2015). However, it is recommended to visually inspect algorithm results and validate with *in situ* data to compensate for issues such as cloud cover or other environmental factors that can cause the algorithms to fail.

Differentiating and quantifying various phytoplankton functional types (PFTs) through ocean colour remote sensing is still an active research area (IOCCG 2014). *Karenia* species represent one type of HAB and other types of HABs exist in different regions of the world. The case study here demonstrates the usefulness of multi-band ocean colour data in detecting and tracking such HABs. With more spectral bands available on future ocean colour satellite sensors, such abilities can only be enhanced.



## Chapter 3

# Case Studies: Remote Sensing of Cyanobacteria Blooms

**Stefan Simis, Mariano Bresciani, Hongtao Duan, Claudia Giardino, Chuanmin Hu, Tiit Kutser, Ronghua Ma, Erica Matta and Mark Matthews**

---

### 3.1 Introduction

Cyanobacteria blooms are a familiar sight in freshwater and brackish water bodies near centres of human activity, posing health and economic threats. A trend of increasing dominance of cyanobacteria in response to climate change can be shown in lakes (Elliott 2011). Consequently, water management authorities need targeted monitoring and mitigation efforts, for which traditional methods to quantify biomass in cell numbers provide insufficient frequency and spatial coverage. Remote sensing and *in situ* automated optical monitoring methods therefore increasingly receive attention. Case studies in this chapter illustrate the feasibility of current remote sensing techniques to map and distinguish cyanobacteria blooms, covering a wide geographical range and various trophic states in freshwater and coastal environments.

#### 3.1.1 Terminology, taxonomy, and functional diversity

Cyanobacteria are a diverse group of photosynthetic prokaryotes. They occupy a more primitive branch in the tree of life than the eukaryotic algae, a fact recognized in the 1970s when the term 'blue-green algae' was abandoned (see Sapp 2005; Govindjee and Shevela 2011). As a compromise in the otherwise confusing and unpractical naming conventions, the term phytoplankton is now widely accepted as the collective functional group of photosynthetic algae and cyanobacteria. Nevertheless, the term (harmful) algal bloom is still freely used in the remote sensing community to describe proliferations of phytoplankton dominated by either algae or cyanobacteria, possibly because the dominant phytoplankton group is rarely determined from remote platforms. It is nevertheless good to bear in mind that deeply rooted evolutionary and ecophysiological differences between cyanobacteria and algae warrant consideration when formulating phytoplankton optical models or interpreting remotely sensed signals.

Cyanobacteria are the most common bloom-forming phytoplankton group in freshwater bodies, and blooms may additionally form in rivers, estuaries, and coastal seas (Anderson et al. 2002). The most common bloom-forming (planktonic) cyanobacteria are globally represented by relatively few species from the genera *Aphanizomenon*, *Cylindrospermopsis*, *Dolichosper-*

*mum* (including planktonic former *Anabaena*), *Microcystis*, *Nodularia*, and *Planktothrix*. The role of (pico)cyanobacteria in primary production in the world oceans is not to be underestimated, but reports of bloom-forming cyanobacteria in the oceans are limited to filamentous *Trichodesmium*, not covered in this chapter.

The success of cyanobacteria in disturbed environments can be explained by a set of mechanisms often represented in the most notorious bloom-formers. These mechanisms are: regulation of buoyancy and pigmentation (discussed below), acclimation of pigment production (Tandeau de Marsac and Houmard 1988) and rapid acclimation of light utilization (Papageorgiou et al. 2007; Govindjee and Shevela 2011; Kaňa et al. 2012), elemental nitrogen fixation, colony formation either to aid light harvesting (Tamulonis et al. 2011) or to reduce grazing (Lampert 1987; Chan et al. 2004), poor food quality for higher trophic levels (Lampert 1987) and finally, though subject to debate, allelopathic effects of secondary metabolites including those toxic to animals (Babica et al. 2006).

Toxicity is the foremost reason to call for early warning of cyanobacteria blooms and dedicated monitoring, assessment, and remediation strategies in water bodies world-wide. Effects of cyanobacterial toxins on humans range from skin and respiratory irritation to liver and kidney damage; excessive exposure has resulted in death (WHO 1999). Public awareness of the risks of exposure is probably the most efficient preventive strategy for humans, although recently even living near water bodies where toxin-producing cyanobacteria proliferate was suggested as a risk factor for degenerative disease such as amyotrophic lateral sclerosis (Torbick et al. 2014). Meanwhile, livestock, (planktivorous) waterfowl, and pets are particularly vulnerable to toxins accumulated in surface scums, benthic mats, or in filter feeders (Codd et al. 1999, 2005).

High-biomass cyanobacterial blooms that can be linked to severe eutrophication are considered harmful for diverse reasons. New toxins and links to disease are still being regularly identified (WHO 1999), while blooms that are not toxic can still cause malodour or skin irritation, reducing the recreational and economic value of affected water bodies. Further, as with most algal blooms, cascading ecosystem-destabilizing effects can result from bacteria-mediated oxidation of collapsing blooms, in the worst case leading to mortality of fish and benthic fauna.

Two aspects of cyanobacterial growth and bloom formation influence our ability to detect and quantify cyanobacterial biomass using remote sensing, more than any other of the adaptive mechanisms found in cyanobacteria. These are the relatively unique optical signatures of cyanobacteria, which allow deterministic detection, and biomass accumulation through buoyancy regulation. These properties are discussed in more detail, below.

### 3.1.2 Pigmentation

The most important deterministic optical characteristic of cyanobacteria is the important role of phycobilipigments in their photochemistry. Phycobilipigments (main forms phycoerythrin, phycocyanin, and allophycocyanin) are consistently produced in all cyanobacteria except Prochlorophytes. These pigments are the dominant source of photosynthetic light harvesting

in cyanobacteria. Rhodophytes and cryptophytes (including endosymbionts) may also carry phycobilipigment so the presence of the pigment is not the sole indicator of cyanobacteria.

Phycobilipigment light absorption peaks in the yellow-green part of the visible light spectrum (Figure 3.1) where chlorophyll, xanthophyll, and carotenoid pigments have weaker absorption. The distinct absorption of phycocyanin is visible from remote sensors and has been studied since the 1990s from airborne imagery (Dekker et al. 1991; Jupp et al. 1994; Dekker 1993), and in bio-optical experiments (Gons et al. 1992; Hunter et al. 2008). In recent years, a number of empirical and semi-analytical algorithm development studies have emerged, ranging from the use of two (Schalles and Yacobi 2000; Hunter et al. 2009) to three or more wavebands (Simis et al. 2005; Simis et al. 2007; Hunter et al. 2010; Le et al. 2011; Sun et al. 2013; Mishra et al. 2013) and hyperspectral data (Kutser 2004). Kutser et al. 2006 demonstrate, through bio-optical modelling, that very few sensors can distinguish the diagnostic absorption profile of cyanobacteria. Nevertheless, cyanobacteria blooms may still be mapped and even quantified using purely empirical relationships between the limited band sets of Landsat TM (Vincent et al. 2004; Sun et al. 2015) or the Ocean Color Monitor on Oceansat-1 (Dash et al. 2011). Sensor requirements are discussed in more detail by Kutser (2009), but it is worth noting here that when the Medium Resolution Imaging Spectrometer (MERIS) on ENVISAT (2002-2012) became the first spaceborne sensor with global coverage to provide a channel tuned to phycocyanin, this prompted a marked increase in efforts to make cyanobacterial bloom monitoring from space possible. Several independent algorithm validation efforts have since demonstrated good retrieval results when cyanobacteria are sufficiently abundant, although accurate quantification in mixed phytoplankton assemblages often remains challenging (Ruiz-Verdú et al. 2008; Randolph et al. 2008; Li et al. 2010b; Wheeler et al. 2012).

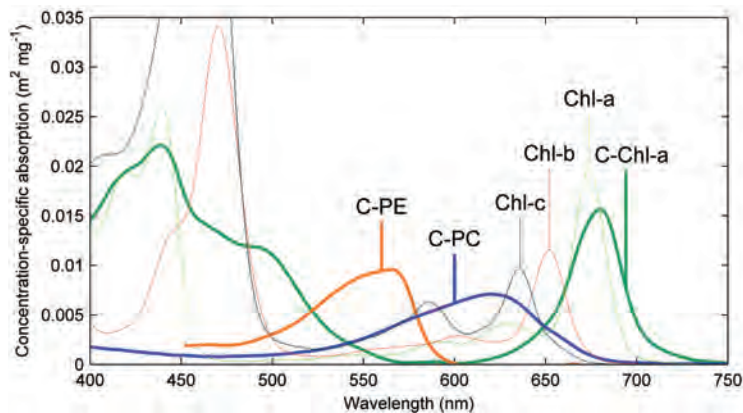


**Figure 3.1** Concentration-specific absorption of dominant cyanobacterial pigment groups (thick curves, Simis and Kauko 2012) and major algal pigments (thin curves, Bidigare et al. 1990). C-PC = phycocyanin including absorption by allophycocyanin, C-PE = phycoerythrin, C-Chl-a = chlorophyll-a including absorption by carotenoid and xanthophyll pigment, Chl-a,b,c = chlorophylls a, b, and c determined from algae.

Phycobilipigments are soluble in water, unlike other plant pigments. Chemotaxonomic methods for pigments extracted in organic solvents are therefore not useful to quantify

phycobilipigments. Alternative extraction methods (e.g., Sarada et al. 1999) have proven laborious and difficult to standardize. Consequently, the quantification of phycobilipigments is often based on *in vivo* optical properties such as fluorescence rather than on the analysis of extracted pigments. Today, a lack of concurrent observations of the optical properties and extracted phycobilipigment in bloom situations still hampers pigment-based algorithm development for remote sensing of cyanobacteria blooms.

The production of the accessory pigments depends both on species and environment (light intensity, light quality, and nutrient availability). This natural variability should be kept in mind when using remote sensing algorithms that target accessory pigments to quantify cyanobacterial biomass. The fraction of cyanobacteria in the phytoplankton assemblage will also determine the validity of algorithms based on accessory pigments, due to the overlap in absorption spectra of these diagnostic pigments with other (algal) pigments in the community (Figure 3.1).

### 3.1.3 Buoyancy

Risk of harmful or nuisance cell concentrations increases dramatically when cells accumulate near the water surface. Mechanisms of buoyancy regulation include formation and collapse of gas vesicles and changes in cell density. Even neutrally-buoyant species may show a circadian migration if nutrient and light conditions are inversely stratified and wind-mixing is weak (Walsby 1994; Visser et al. 2005). Vertical mixing velocity and depth of the mixed layer play a crucial role in whether buoyancy-regulating species accumulate at the water surface (Wynne et al. 2010).

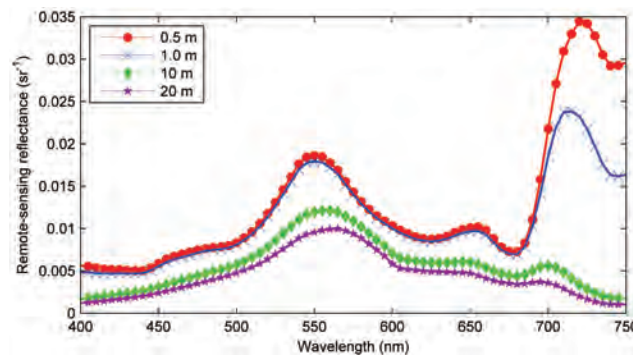


**Figure 3.2** Simulated remote-sensing reflectance of a bloom with the optical properties of *Microcystis* with a fixed areal biomass ( $200 \text{ mg m}^{-2}$ ) mixed in a layer up to 0.5 to 20 m depth. Near-surface backscattering increases with shallower mixing depth, which is particularly visible in the near infra-red. The spectra were simulated using Hydrolight using fixed inherent optical properties for non-phytoplankton components ( $1.8 \text{ g m}^{-3}$  tripton, absorption at  $440 \text{ nm} = 0.05 \text{ m}^{-1}$ ; coloured dissolved organic matter absorption at  $440 \text{ nm} = 1 \text{ m}^{-1}$ , default water absorption), and sun at zenith with the default atmospheric parameters. Credit: M. Matthews and L. Robertson (University of Cape Town, SA).

Near-surface accumulation increases areal light absorption and scattering by particles. With increasing near-surface light scattering, near infra-red (NIR) reflectance increases as the intensity of back-scattered light becomes larger than the strong light absorption by water

itself, up to the point where it resembles the spectral albedo of land vegetation. This effect is simulated in Figure 3.2 for a fixed biomass of *Microcystis* cells mixed over different depths from the surface, a problem previously also addressed for various depth distributions by Kutser (2004). The strong NIR reflectance of surfacing blooms is relatively easy to identify from satellite imagery using red and NIR bands (Hu et al. 2010), even without fully correcting for atmospheric effects on the remotely sensed signal (Matthews et al. 2012). It is therefore possible to use remote sensing techniques to map the risk of accumulated cyanobacterial toxins by focusing exclusively on (near) surface blooms.

Atmospheric correction of the water leaving radiance is strongly affected by increased reflectance in the NIR region. Misclassification of water pixels as land can be observed (Matthews et al. 2010), and a general reduction of the accuracy of atmospherically-corrected reflectance is common (see Baltic Sea case study, Section 3.5). This problem is evident even when buoyant blooms are only present at sub-pixel scales. Additional sources of information such as weather-based mixing models, may be used to predict the possibility of surfacing blooms of buoyant cells. Increased near-surface heat trapping in dense (near) surface layers can also reveal blooms in maps of sea surface temperature (Kahru et al. 1993).

The effects of near-surface accumulation on cell physiology are commonly ignored in remote sensing studies. Species of cyanobacteria have been shown to rapidly acclimate to fluctuating light intensities by redistributing antenna pigments between photosystems ('state changes'), effectively reducing their photosynthetic absorption-cross section (e.g., Papageorgiou et al. 2007; Govindjee and Shevela 2011; Kaña et al. 2012). Under prevailing intense light exposure, production of photoprotective rather than photosynthetic pigment is favoured. *In situ* observations of changes in the optical properties of cyanobacteria are lacking, probably due to the difficulties in sampling surface blooms without disturbing them. We may, however, expect that surface accumulations observed during calm days require different absorption terms for cyanobacteria compared to well-mixed conditions.

**Table 3.1** Characteristics of the cyanobacterial taxa dominant in the case studies.

Genus/species	Cases	Toxins <sup>†</sup>	Buoyancy	Nitrogen fixing	Morphology
<i>Cylindrospermopsis raciborskii</i>	Trasimeno	++	+	+	Colonial trichomes
<i>Planktothrix agardhii</i>	Trasimeno	++	+	-	Single filaments
<i>Microcystis aeruginosa</i>	Taihu, Hartbeespoort	+	+	-	Colonies, cells
<i>Dolichospermum</i> spp.	Baltic (minor)	++	+	+	Colonial trichomes
<i>Aphanizomenon flos-aquae</i>	Baltic	‡	+	+	Colonial trichomes
<i>Nodularia spumigena</i>	Baltic	+	+	+	Colonial filaments

<sup>†</sup>Double markers indicate multiple toxins on record.

<sup>‡</sup>Toxicity in *A. flos-aquae* is common in lakes but not in the Baltic Sea for which a case study is included.

The case studies presented in this chapter include studies on lakes and the brackish Baltic Sea. The densest blooms occur in eutrophic lakes where the optical signatures of cyanobacteria can dominate the water-leaving radiance. The use of state-of-the-art sensors, long time series from remote sensors, and optical proxies of biomass in oligotrophic to hyper-eutrophic waters

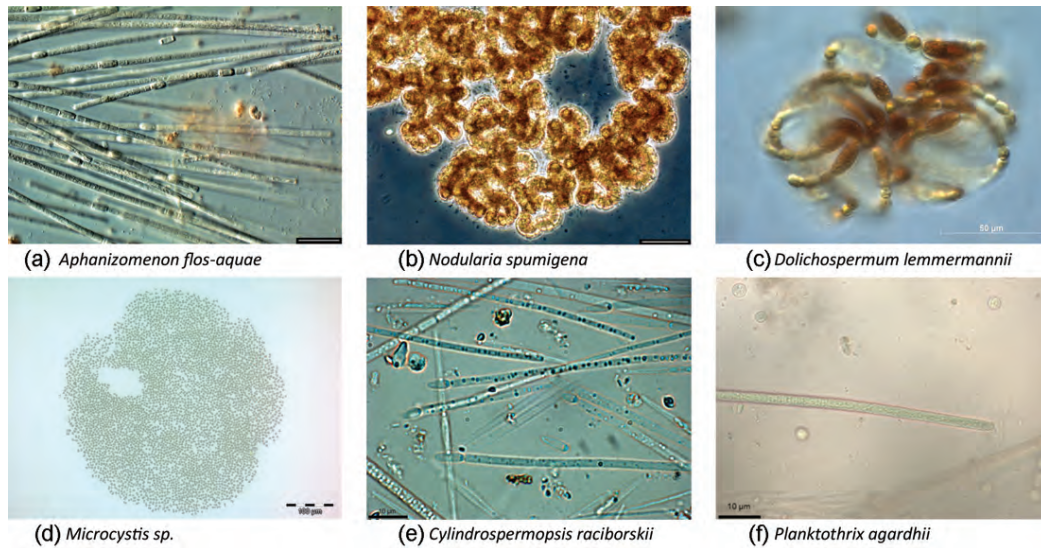


**Figure 3.3** Microscope images of common bloom-forming cyanobacteria. (a) *Aphanizomenon flos-aquae* (scale bar 30  $\mu\text{m}$ ), (b) *Nodularia spumigena* (scale bar 30  $\mu\text{m}$ ), (c) *Dolichospermum lemmermannii* (scale bar 50  $\mu\text{m}$ ), (d) *Microcystis* sp. (scale bar 100  $\mu\text{m}$ ), (e) *Cylindrospermopsis raciborskii* (scale bar 10  $\mu\text{m}$ ), (f) *Planktothrix agardhii* (scale bar 10  $\mu\text{m}$ ). Photo credits: (a-c) Seija Hällfors, (d) Mark Matthews, (e-f) Martina Austoni.

are demonstrated. Cyanobacteria blooms in the marine sphere are used to further demonstrate the effects of spatial and temporal resolution on the retrieval of patchy blooms and time series, and to highlight the advantages of assimilated *in situ* and remotely sensed data to monitor blooms in the sea environment. Figure 3.3 and Table 3.1 give an overview of the cyanobacteria taxa which dominated the bloom events presented in the case studies.

## 3.2 Case 1: Bloom Distribution in Lake Trasimeno, Italy using Multi-Sensor Data\*

### 3.2.1 Objective

This case study demonstrates how tuned optical models can be applied to data acquired by different spaceborne sensors to reveal the spatial distribution of cyanobacteria blooms in lakes. We compare images of Lake Trasimeno (Italy) taken on the same day with MERIS (pixel size 300 m) and CHRIS-PROBA (pixel size 18 m). MERIS was operational on ESA's Envisat satellite for more than 10 years and is still used for retrospective analysis and algorithm development, until the OLCI sensor on Sentinel-3, with similar spectral and radiometric characteristics, is operational. CHRIS, on the PROBA platform, is a hyperspectral instrument and provides a limited number of daily scenes.

\* Authors: Claudia Giardino, Mariano Bresciani and Erica Matta (CNR-IREA, Italy)

### 3.2.2 Study area

Lake Trasimeno, the fourth largest (124 km<sup>2</sup>) lake in central Italy (43°06'N; 12°07'E), is a closed, unstratified, and shallow lake (average depth 4.5 m, maximum depth 6 m), and was declared a protected area for its exceptional natural value (Directive CEE 1979). Tourism, agriculture and livestock breeding are the most important activities in the Trasimeno area. The annual load of organic carbon (500t), nitrogen (550t) and phosphorus (30t), negatively affects water quality (Cingolani et al. 2005): cyanobacteria blooms are present, sediments negatively impacted, the fish community altered and common reeds are in recession (Natali 1993; Cecchetti and Lazzerini 2007; Cingolani et al. 2007).

*Cylindrospermopsis raciborskii* and *Planktothrix agardhii* dominate the phytoplankton in late summer with cell densities reaching  $2\text{-}3 \times 10^7$  and  $2\text{-}5 \times 10^6 \text{ l}^{-1}$ , respectively (Cingolani et al. 2007; Lucentini and Ottaviani 2011). *Mycrocystis aeruginosa* is also common. Blooms occur in the water column and at the surface, but scum is rarely observed. Field data of August 2011 confirm elevated cyanobacteria biomass, mainly in the lake centre, with chlorophyll concentration values around  $40 \text{ mg m}^{-3}$ . During the bloom, on 19 August 2011, MERIS and CHRIS-PROBA data were acquired near-simultaneously.

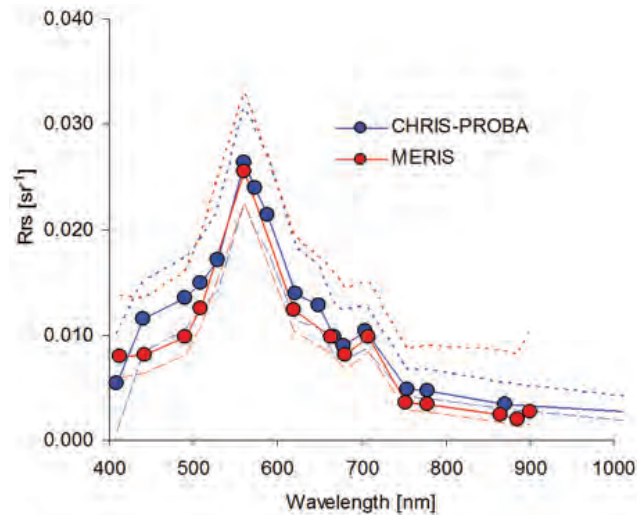


**Figure 3.4** MERIS FR and CHRIS-PROBA comparison of remote-sensing reflectance ( $R_{rs}$ ) averaged over the central area of Lake Trasimeno on 19 August 2011. Dotted lines show minimum and maximum values. Reflectance depressions caused by cyanobacteria pigments are visible in the orange-red range.

### 3.2.3 Image processing

MERIS full resolution (FR) and CHRIS-PROBA images acquired on 19 August 2011 were processed using BEAM tools (Fomferra and Brockmann 2006) to normalise radiometric noise at satellite level (smile correction for MERIS and noise reduction for CHRIS-PROBA). The top-of-atmosphere radiance was corrected for atmospheric effects using the 6S code (Vermote

et al. 1997; Kotchenova et al. 2006). The 6S-derived reflectances obtained from MERIS and CHRIS-PROBA were comparable both in magnitude and shape (Figure 3.4), confirming the accuracy of the absolute radiometric properties of both sensors over the central area of the lake. The spectral shapes of the reflectance, with reflectance minima near pigment absorption peaks in the blue and red regions, and the peak at 709 nm indicates a strong influence by phytoplankton on the signal. The depression of the reflectance signal in the 620 nm band suggests the presence of cyanobacteria-specific pigments. Water reflectances were then transformed into Chlorophyll-a (Chl-a) concentrations with the optimization technique BOMBER (Giardino et al. 2012). BOMBER hosts a three-component bio-optical model that was parameterised with optical coefficients suitable for Lake Trasimeno.

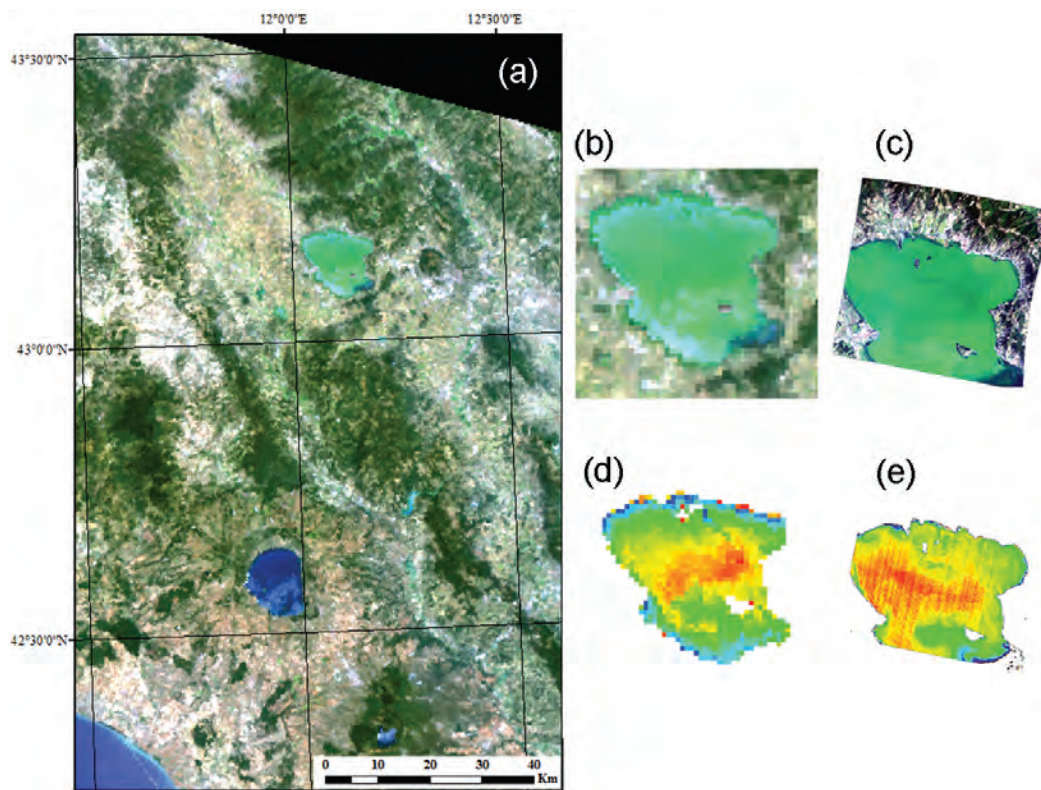


**Figure 3.5** Lake Trasimeno images acquired on 19 August 2011. (a) Pseudo true colour MERIS image of Lake Trasimeno (north) and Lake Bolsena (south). The image clearly shows the different appearance of these lakes. (b) MERIS (R:G:B = 620:560:442 nm) and (c) CHRIS-PROBA (R:G:B = 620:560:441 nm) images of Lake Trasimeno at the same scale; both images show the green hue of Lake Trasimeno waters affected by phytoplankton bloom. Chlorophyll-a concentration from (d) MERIS, and (e) CHRIS-PROBA images (colour scale 0-50  $\text{mg m}^{-3}$  from blue to red).

### 3.2.4 Results

The intense green appearance of Lake Trasimeno observed in pseudo-true colour images (Figure 3.5, visible in the north) contrasts sharply with the clear waters of Lake Bolsena (south-west),

a deep oligotrophic volcanic crater lake. Both MERIS (Figure 3.5b) and CHRIS (Figure 3.5c) coverage of Lake Trasimeno also highlight a contrast within the lake: cyanobacterial blooms cause the intense green hues, while submerged macrophyte beds in the southeast corner regulate water transparency, resulting in clear waters. Wind resuspension of sediments on 19 August 2011, with average wind speed  $8 \text{ m s}^{-1}$  and peak wind of  $15 \text{ m s}^{-1}$ , resulted in variable patterns of brightly scattering waters along the eastern lake shore. Maps of Chl-a concentration obtained with BOMBER (Figure 3.5d-e) show generally good correspondence, although the higher resolution of the CHRIS-PROBA image reveals many finer structures. The two images do not correspond well along the northern shore and in particular in the southeast corner of the lake. This is probably due to the adjacency effects that can alter the signal originated from the water column due to the multiple-reflection of radiation from the surrounding lands (Guanter et al. 2010). The adjacency effect also depends on pixel size and hence it causes different patterns in the two images.

### 3.2.5 Discussion

This study was presented to show that different satellite sensors can be used to map Chl-a concentration in lakes where well-calibrated and validated physics-based approaches are available for the study area. The approach used in this study was based on 6S and BOMBER: the first code was used to convert MERIS and CHRIS-PROBA radiances into water reflectance. BOMBER, in turn, was parameterised with the optical properties of Lake Trasimeno, and used to derive Chl-a concentration, which, for this study area, can be assumed to delineate cyanobacteria biomass. The results show that current sensors can be used to produce realistic and reproducible reflectance spectra. The Chl-a concentration patterns assessed from space reveal that even in medium sized lakes the horizontal variability warrants the use of remote sensing to complement point sampling.

## 3.3 Case 2: Lake Taihu, China Time Series Reveals Trends and Causes of Blooms<sup>†</sup>

### 3.3.1 Objective

Long-term studies of phytoplankton blooms in lakes and estuaries are extremely rare in remote sensing literature, due to the inherent problems in atmospheric correction and bio-optical inversion in waters where sediments and other non-living constituents can play dominant optical roles. This case study demonstrates that satellite sensors, even those not optimized for lake water quality remote sensing, can be used to derive meaningful descriptions and long-term patterns of extreme cyanobacterial blooms.

The work presented in this case study was supported by the Knowledge Innovation Program of the Chinese Academy of Sciences (KZCX2-EW-QN308 and KZCX2-YW-QN311), the National

---

<sup>†</sup>Authors: Chuanmin Hu<sup>1</sup>, Hongtao Duan<sup>2</sup>, Ronghua Ma<sup>2</sup> (<sup>1</sup>University of South Florida, USA; <sup>2</sup>Nanjing Institute of Geography and Limnology, Chinese Academy of Sciences)

Natural Science Foundation of China (41171271 and 41171273), and the U.S. NASA Ocean Biology and Biogeochemistry program and Water and Energy Cycle program.

### 3.3.2 Study area

Lake Taihu, the third largest freshwater lake in China with a surface area of 2,338 km<sup>2</sup> and average water depth of 1.9 m, is one of the most severely polluted freshwater reservoirs in China (Figure 3.6). In May 2007, a massive bloom of *Microcystis aeruginosa* disrupted water supply to Wuxi city leaving over 1 million people without drinking water for a week. The extreme bloom event placed Lake Taihu in the spotlight (Guo 2007; Yang et al. 2008; Qin et al. 2010) and inspired increased focus on studies and management of the eutrophication problems that affect water quality in the lake.

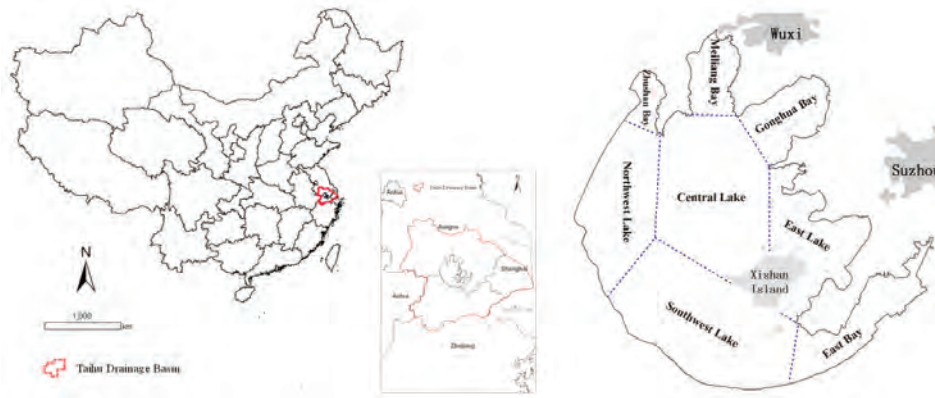


**Figure 3.6** Location of Lake Taihu in China. The cities of Wuxi and Suzhou are located to the Northeast and East of the lake, respectively. The lake is divided into segments based on morphology and hydrodynamics. Figure adapted from Duan et al. (2009). Need a higher resolution figure??

### 3.3.3 Image processing

MODIS 250-m resolution and Landsat TM/ETM 30-m resolution images are used. MODIS Level-0 (raw digital counts) data from both Terra and Aqua satellites were obtained from the U.S. NASA Goddard Flight Space Center (GSFC). Landsat data include nearly all cloud-free images over Lake Taihu since 1987, and were provided by the United States Geological Survey (USGS) and China Remote-Sensing Satellite Ground Station (Duan et al. 2009; Hu et al. 2010). Due to the 16-day revisit time, Landsat images were used to identify when blooms initially occurred up until the year 2000. From the year 2001 onwards, MODIS Level-0 data were converted to calibrated radiance data using the software package SeaDAS (version 5.1). Gaseous absorption and Rayleigh scattering were corrected using software provided by the MODIS Rapid Response Team, based on the radiative transfer calculations from 6S (Vermote et al. 1997). The resulting Rayleigh-corrected reflectance data,  $R_{rc}(\lambda)$  where  $\lambda$  is the central wavelength of the bands,

were geo-referenced to a cylindrical equidistance (rectangular) projection (errors less than 0.5 pixel). Landsat data were processed in a similar fashion to the MODIS scenes.

When the water surface is calm under low wind, buoyant cyanobacteria cells form floating mats (scums) at the surface. Under these circumstances the Floating Algae Index (FAI, Hu 2009) is sensitive to the presence of buoyant cyanobacteria in the lake. FAI is defined as (Hu 2009; Hu et al. 2010):

$$FAI = R_{rc}(\lambda_1) - R'_{rc}(\lambda_1) \quad (3.1)$$

$$R'_{rc}(\lambda_1) = R_{rc}(\lambda_2) + (R_{rc}(\lambda_3) - R_{rc}(\lambda_2)) \times (\lambda_1 - \lambda_2) / (\lambda_3 - \lambda_2)$$

For MODIS, the wavebands used to generate the FAI were  $\lambda_1 = 859$  (841–876) nm,  $\lambda_2 = 645$  (620–670) nm, and  $\lambda_3 = 1240$  (1230–1250) nm. With Landsat, the used bands were  $\lambda_1 = 825$  (750–900) nm,  $\lambda_2 = 660$  (630–690) nm, and  $\lambda_3 = 1650$  (1550–1750) nm. The FAI detects the red-edge of reflectance of surface vegetation (in this case, cyanobacteria bloom mats). Basically, FAI quantifies the surface reflectance in the NIR normalized against a baseline formed linearly between the red and short-wave infrared (SWIR) wavebands. FAI values  $> -0.004$  were empirically established to delineate blooms (Hu et al. 2010).

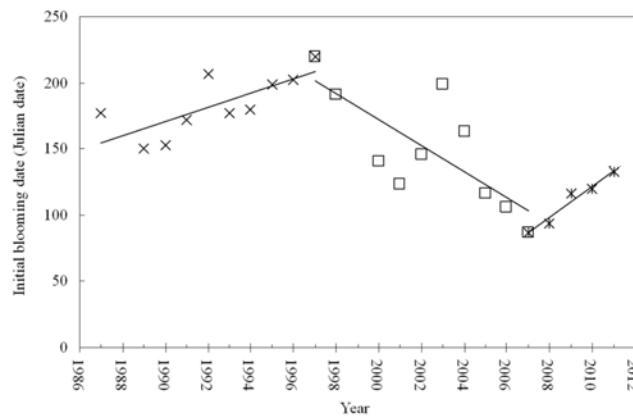


**Figure 3.7** Initial outburst date for lake Taihu blooms through the time-period 1987–2011. Regression lines for specific periods: 1987–1997:  $y = 5.35x - 10473$  ( $R^2 = 0.56$ ); 1997–2007:  $y = -9.84x + 19844$  ( $R^2 = 0.57$ ); 2007–2011:  $y = 11.8x - 23596$  ( $R^2 = 0.96$ ). Figure adapted from Duan et al. (2014).

### 3.3.4 Image analysis

Several lake segments (Gong Bay and East Lake, see Figure 3.6) have seasonal water plants (Ma et al. 2008) which may appear as blooms but should be interpreted as mixed plants and phytoplankton. The seasonal cycle of East Bay is almost purely from water plants. Results labelled to represent the whole lake should be interpreted as Lake Taihu excluding East Bay.

Temporal dynamics of the bloom are described using two indicators: the initial blooming date and bloom duration. The initial blooming date is the first date of each year when blooms could be discerned by visual inspection of the Landsat and MODIS FAI and Red-Green-Blue

imagery. Blooms occurred every year in the observed period, although the years 1988 and 1999 had to be excluded due to lack of sufficient imagery. Three distinct trends in the initial bloom date were observed (Figure 3.7); from 1987 to 1997, the blooms appeared with an increasing delay of 5.35 days per year. From 1997 to 2007, blooms started increasingly earlier by 9.83 days per year. Since 2007, blooms have again started to appear later with a delay of 11.8 days per year.

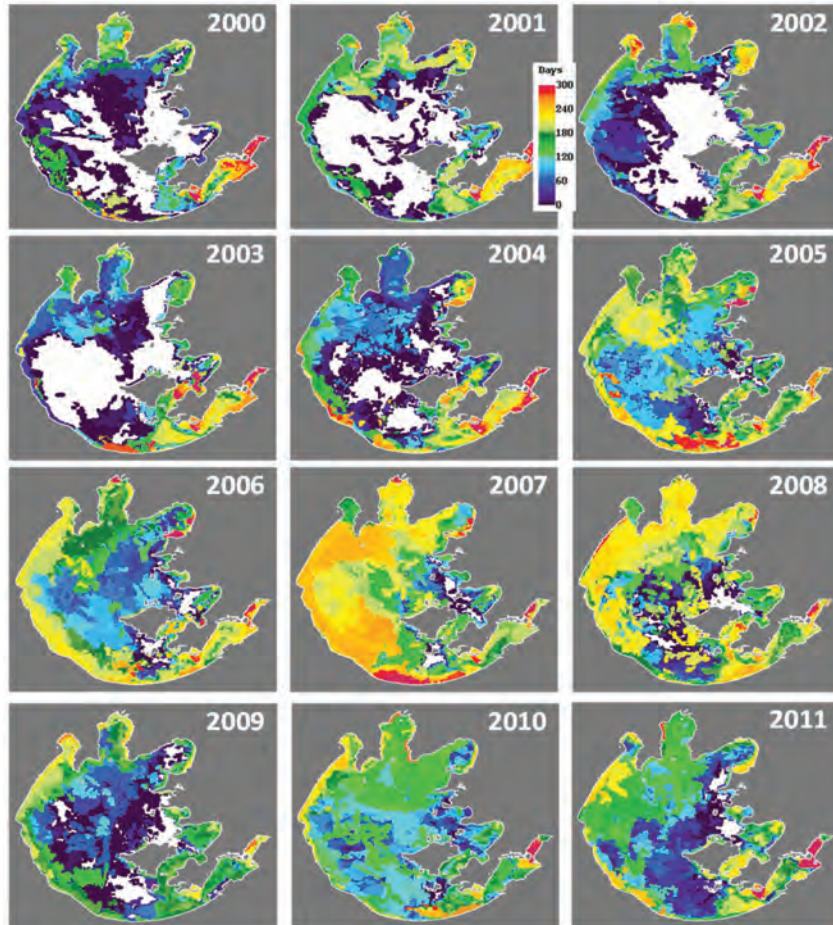


**Figure 3.8** Duration of cyanobacteria blooms, defined as the period between the first and last day with FAI > -0.004 in MODIS imagery. White areas showed no bloom during the entire year. Figure adapted from Hu et al. (2010).

Bloom duration is defined as the period between first and last appearance in MODIS FAI imagery. More than one bloom may occur in any period. The bloom duration is mapped for the years 2000–2011 in Figure 3.8. The period 2006–2011 showed longer bloom duration in most of the lake compared to the years prior, despite later starts to the bloom (Figure 3.7). The trend actually began in 2005, with 2007 the worst bloom year. More than half the lake surface had blooms lasting for > 7 months during 2007. Earlier and longer blooms in the period 2007–2011 are apparent for NW Lake, SW Lake, Central Lake, and the whole lake. Bloom

coverage never exceeded 25% of the lake area between 2000 and 2003, and exceeded 25% of the lake area only twice during 2004 when the entire lake was considered. This suggests that the lake was relatively healthy between 2000 and 2004.

### 3.3.4.1 Spatial patterns

Besides time-series analysis, the archive of bloom imagery can also be used for spatial analyses, such as where blooms initiate and how they expand. Blooms were first observed in Meiliang Bay and Gonghu Bay in June, 1987. Throughout the past two decades, the initial bloom location was Meiliang Bay (14 times) and Zhushan Bay (9 times) — on four of these occasions, blooms occurred simultaneously in both locations. Since 2000, blooms have also started to spread from western and southern bays, which may indicate changes in the hydrodynamic regime or nutrient delivery to the lake. The blooms show a sprawling trend, covering an increasing area from year to year. The bloom area has increased from 4.8 km<sup>2</sup> in July 1991 to 216.4 km<sup>2</sup> in 2000, and the extreme situation in 2007 when blooms covered >1,000 km<sup>2</sup>.

For most lake areas (NW Lake, SW Lake, Central Lake) as well as when considering the entire lake, 2005 marks a transition year from relatively rare bloom occurrence to highly frequent blooms (high FAI in >25% of the area), particularly during summer months.

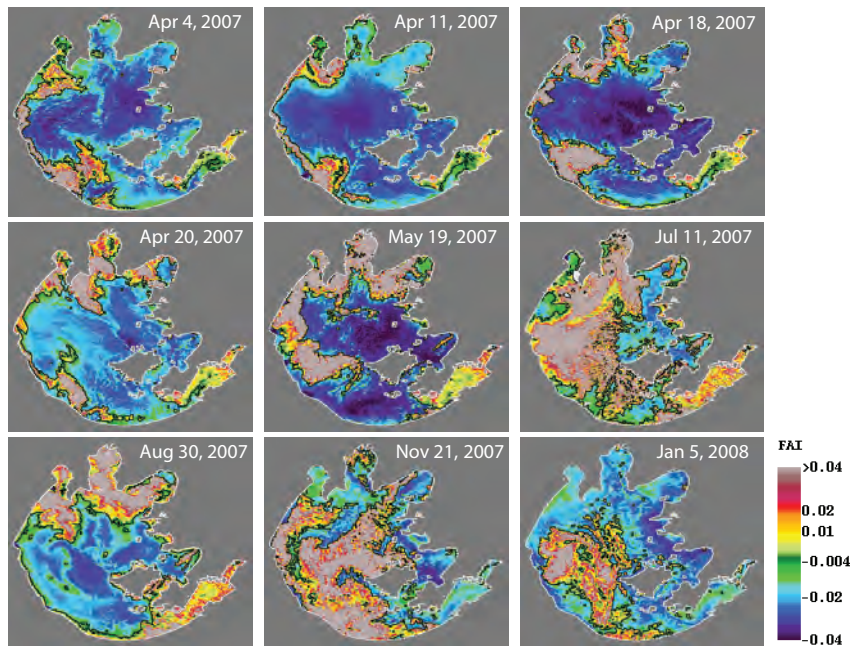


**Figure 3.9** Initiation and evolution of the 2007 cyanobacteria bloom in Lake Taihu. Figure adapted from Hu et al. (2010).

The 2007 bloom event in Lake Taihu, and particularly Meiliang Bay, was reported to start in late April (Yang et al. 2008) and by 25 April extensive blooms were found in Meiliang Bay (Kong et al. 2007). The MODIS FAI image series of 2007 (Figure 3.9) reveals that an extensive bloom was already established on 4 April 2007 in NW Lake and SW Lake, three weeks earlier than

reported as the onset of the bloom. By 18 April the bloom was already extensive in Meiliang Bay, again a week earlier than reported. Between 20 April and 30 August, the bloom covered almost the entire Meiliang Bay. On 11 July and 21 November, more than half of the entire lake was covered by the intense bloom, which remained until at least 5 January 2008, making it the longest bloom event since MODIS data became available (2000) and possibly the longest bloom event in history. In June 2007, at least 6000 tons of organic material was harvested from the bloom in an attempt to reduce the bloom (Guo 2007). The remotely sensed imagery suggests, however, that the impact of this effort on bloom size was limited.

### 3.3.5 Factors forcing blooms

- ❖ **Temperature:** Cell recruitment in Lake Taihu has been shown to be tightly coupled to temperature both in the laboratory and in the field (Cao et al. 2008). The initial blooming date calculated from MODIS imagery was significantly correlated to the minimum water temperature during the preceding winter (November–January,  $p = 0.048$ ). The winter of 2007 was one of the warmest winters in the last 25 years particularly in the period January–March (0.36, 2.78, and 1.98°C above average in January, February, and March, respectively). The elevated water temperatures may have supported the extreme bloom of that year. If minimum winter temperature is indeed a driving force behind recruitment and bloom formation, current trends of increasing minimum temperature (at a rate of 0.0539°C yr<sup>-1</sup>) suggest further bloom expansion in years to come.
- ❖ **Nutrients:** Nutrient loading resulting from human activities contributes to the blooms in Lake Taihu. During the period 1991–1996, the annual average total nitrogen (TN) increased from 1.18 mg l<sup>-1</sup> to 3.62 mg l<sup>-1</sup>, total phosphorus (TP) increased from 0.10 mg l<sup>-1</sup> to 0.18 mg l<sup>-1</sup>. By 2006, TN and TP were 200% and 150% higher than in 1996 (Kong et al. 2007). Nutrient analysis at Taihu field station showed that inputs of TN and TP from the catchment area increased by 3 and 5%, respectively, between 2002 and 2003 (Kong et al. 2007). The spatial patterns displayed by the blooms support the hypothesis that nutrient availability drives the blooming. The southward expansion of the blooms reflects the higher nutrient loading northwest of Lake Taihu. For example, TP loading from the northwest catchments accounted for 53–55% of the entire area in the period 2002–2003, and TN loading from this area accounted for 65–72% in 2002–2003. The southward delivery of nutrients explains the frequent occurrences of blooms in the north, and increasing detection of blooms in the center and south.
- ❖ **Wind:** Despite the shallow average depth of Lake Taihu, wind mixing can have a large effect on the appearance of floating cyanobacteria mats. During days with consecutive MODIS imagery in September 2005 and November 2007, bloom size was observed to be as large as >770 km<sup>2</sup> for wind speed < 2 m s<sup>-1</sup> but reduced to <140 km<sup>2</sup> for wind speed > 3 m s<sup>-1</sup>. It is unlikely that an extensive bloom could disappear in one day and a new bloom initiate immediately thereafter. Therefore, the observed oscillation in bloom size over consecutive days must be due to changes in physical conditions (primarily wind forcing), and not due

to changes in the total biomass.

- ❖ Economic prosperity: The combined pressures of land use (sewage, livestock, drainage, soil nutrients and loss of fertilizers from agricultural lands (see Lai et al. 2006) on the lake ecosystem can be associated with human population and economic development. Human population and the gross domestic product (GDP) per capita are used here to explore the correlation of anthropogenic activities with phytoplankton blooms. Including these factors, as well as winter temperature, in a multivariate regression shows that GDP and GDP per capita are the best predictors of bloom occurrence: GDP was the dominant factor for initial blooming date ( $R^2 = 0.988$ ), while GDP per capita has the strongest relation with bloom duration ( $R^2 = 0.747$ ). These findings imply that economic activities outweigh the environmental effect of the preceding winter temperature despite the fact that temperature does explain the variability of the bloom initiation dates.

GDP in the Taihu Basin increased from 847.66 to 2,662.23 Billion Yuan (RMB) from 1998 to 2007. GDP per capita increased from  $2.06 \times 10^4$  to  $6.16 \times 10^4$  Yuan (RMB). Correspondingly, the number of months of detected algal blooms increased from two in 1998 to ten in 2007; the initial blooming date advanced more than 100 days. Significant correlations were found between the annual duration, initial blooming date and total GDP and GDP per capita in the adjacent area for the time period of 1998–2007. Human activity is projected to further grow in this area in the next decades.

### 3.3.6 Discussion

The Taihu case shows that a reflectance band index such as FAI can delineate cyanobacterial bloom mats at the water surface due to the associated dominant NIR optical feature. This approach is valid even without the use of rigorous atmospheric correction and bio-optical inversion algorithms. Unlike algorithms which target the absorption feature of phycocyanin around 620 nm in mixed conditions, and available from a limited number of satellite sensors, FAI uses a NIR band to quantify surface mats of buoyant cyanobacteria. The surface mats show spectral characteristics similar to surface vegetation. At the time of writing, both MODIS-Terra (2000 to present) and MODIS-Aqua (2002 to present) are functional, and the recently launched Landsat 8 (February 2013 to present) is expected to continue the Landsat series to provide Earth science data. Thus, the time-series analysis can be continued to assess bloom conditions in the coming years. Even if both MODIS instruments stop functioning (both were designed to have a 5-year mission life), the Visible Infrared Imager Radiometer Suite (VIIRS) instrument on Suomi NPP (National Polar-orbiting Partnership) satellite (October 2011 to present) is expected to provide continuity of the bloom observations. VIIRS is equipped with several imaging and ocean colour bands in the red, NIR, and SWIR that are suitable to derive the FAI, as with MODIS. Alternatively, the recent Landsat-8 OLI sensor with 30-m spatial resolution has suitable red, NIR, and SWIR bands and improved signal-to-noise ratios compared to its predecessors (Hu et al. 2012; Pahlevan et al. 2014). The uninterrupted observations from these environmental satellites will provide seamless data records to assure data continuity to assess the long-term bloom status in Lake Taihu and similar water bodies under heavy pressure.

The results obtained from satellite-based observations are not only useful in understanding the potential causes of the blooms and their long-term trends, but also useful to aid decision-making. For example, the statistics of the spatial and temporal bloom patterns can help management agencies in implementing nutrient release and reduction plans. The timely information from the near real-time satellite images can help local groups to determine where to harvest scums to improve water quality. Currently, at the Nanjing Institute of Geography and Limnology (China), the MODIS and Landsat-based observations are being integrated with other information (wind, field observations, temperature) to establish a bloom monitoring system, with the ultimate goal of predicting bloom occurrence and helping water quality management. Continuous satellite observations will play an essential role in such a system.

### **3.4 Case 3: Detecting Trophic Status, Cyanobacteria Dominance, and Surface Scums in Lakes<sup>‡</sup>**

#### **3.4.1 Introduction**

This case study illustrates retrieval of quantitative bloom biomass over a wide trophic range. Issues with image quality over severe blooms and near land masses are tackled by using bottom-of-atmosphere radiance rather than signals corrected for the full atmosphere. Biomass can be quantified using a series of empirical algorithms that use the shape of the red to near infra-red radiance spectrum. The choice of algorithm is based on a decision tree that separates clear and turbid waters from those where surface blooms or vegetation are present.

Trophic status remains a crucial variable in water management, and its detection from satellite provides a unique opportunity, especially in the developing world where information on water quality is often difficult to obtain. The identification of high biomass cyanobacterial blooms and their changes in space and time is another major priority for water and public health management. Despite the high impact and great opportunity presented by Earth observation from space, there has been an absence of simple, reliable information products for trophic status and cyanobacteria detection in inland and eutrophic waters. The development of algorithms targeted at filling this information gap has now become a priority for scientists and space agencies. This case study demonstrates how the Maximum Peak Height (MPH) algorithm (Matthews et al. 2012) can be used to provide trophic status, surface scum and floating vegetation (macrophyte) detection in a variety of South African and global inland waters. It also demonstrates a pixel flagging process aimed at identifying high-biomass ( $\text{Chl-a} > 20 \text{ mg m}^{-3}$ ) cyanobacterial blooms using the Full Resolution (FR) data archived from Envisat MERIS.

#### **3.4.2 The MPH algorithm**

Detection of Chl-a concentration and other water constituents commonly follows interpretation of water-leaving reflectances, which are obtained after atmospheric correction of top-of-

---

<sup>‡</sup> Author: Mark Matthews (CyanoLakes (Pty) Ltd, South Africa

atmosphere (TOA) radiances. However, atmospheric correction is challenging and error-prone over optically-complex water types which contain high and uncoupled concentrations of various constituents (Guanter et al. 2010). While atmospheric effects caused by aerosols (dust, particles, and smoke) are highly variable and stochastic, Rayleigh or molecular scattering can be corrected for relatively easily. The Bottom-of-Rayleigh (BRR) processor in the Envisat BEAM software was used to produce the Rayleigh-corrected TOA imagery used with the MPH algorithm. The band ratio type algorithm used by MPH subsequently normalises remaining aerosol effects.

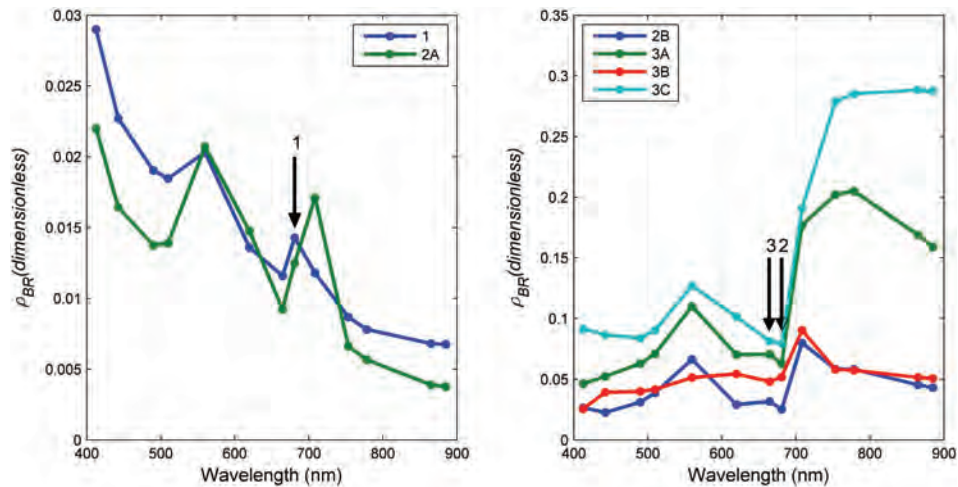


**Figure 3.10** BRR spectra showing reflectance features applicable to each trophic class/water type: (1) mixed oligo-mesotrophic waters with eukaryotic phytoplankton possessing a Chl-a fluorescence signal at 681 nm (arrow 1) (2) high biomass eutrophic/hypertrophic waters with (2A) algae and (2B) cyanobacteria, and cyanobacteria with surface scum (3A), extremely high biomass blooms of algae (3B), and floating vegetation (3C). The arrows 2 and 3 indicate the reflectance features used to identify waters as cyanobacteria dominant (only present in spectra 2B and 3A).

The MPH algorithm utilises the signal derived from phytoplankton pigments, fluorescence, and backscattering in the red/NIR bands of MERIS (for a full description see Matthews et al. 2012). These features may be detected using the Rayleigh corrected TOA signal (e.g., Giardino et al. 2005). The algorithm uses a baseline-subtraction procedure (see Gower et al. 1999) to derive the height of the peak of the MERIS bands between 664 and 885 nm. The three peaks are centred on phytoplankton Chl-a fluorescence (681 nm), the particulate scattering and water absorption induced peak (709 nm), and the red edge vegetation band (754 nm). Three cases are targeted by this technique (see Figure 3.10):

1. mixed oligo-mesotrophic waters with eukaryotic phytoplankton (algae),
2. high biomass eutrophic/hypertrophic waters with either algae or cyanobacteria,
3. extremely high biomass blooms of algae or cyanobacteria with surface scum or floating vegetation.

In each trophic case, MPH exploits a different signal source. In the first case, the Chl-a fluorescence signal at 681 nm is correlated to biomass and provides information on trophic

state at low-medium biomass with Chl-a  $< 20 \text{ mg m}^{-3}$  (e.g., Giardino et al. 2005). This signal becomes masked by particulate absorption and scattering as biomass increases. The second case utilises the backscattering/absorption induced peak around 709 nm, which is highly correlated with algae and cyanobacterial biomass at higher trophic states (Chl-a  $> 20 \text{ mg m}^{-3}$ ) (e.g., Gitelson 1992). The final case utilises the vegetation red-edge which becomes apparent in surface scum conditions (Chl-a  $> \text{approx. } 300 \text{ mg m}^{-3}$ ) and is characteristic of floating vegetation with minimal water absorption (Figure 3.2, Kutser 2009). The MPH variable is designed to seamlessly shift between these cases which occur in inland waters, providing an operational algorithm for effective trophic status determination through estimates of Chl-a concentration.

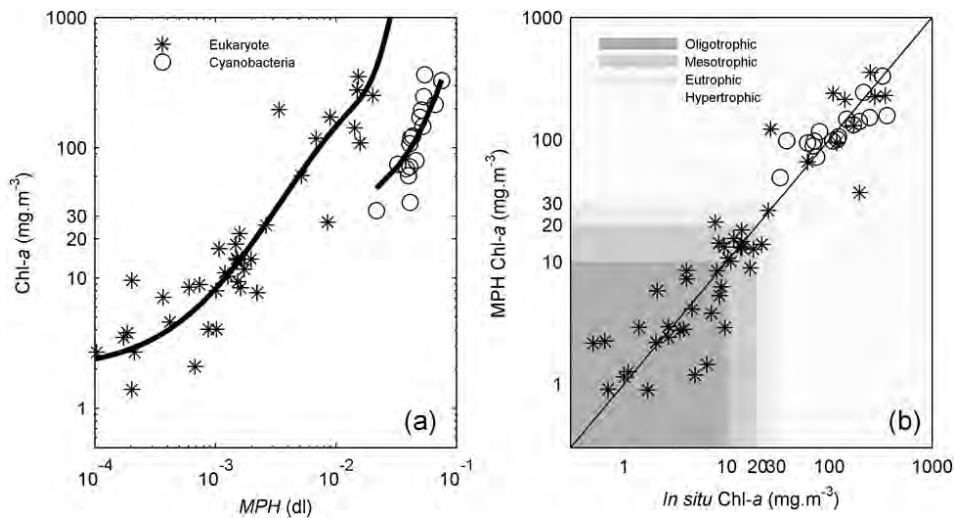


**Figure 3.11** a) Empirical algorithms derived from the MPH variable using data from eutrophic eukaryote dinoflagellate/diatom dominant waters and hypertrophic cyanobacteria (*Microcystis*) dominated waters. (b) Algorithm performances over several trophic classes.

The detection of waters dominated by high biomass blooms of cyanobacteria uses reflectance features produced by their unique pigmentation. These are an apparent absence of Chl-a fluorescence causing a trough near 681 nm, and a small peak at 664 nm caused by sparse pigment absorption (potentially enhanced by phycobilipigment fluorescence) and the absorption of phycocyanin at 620 nm. These reflectance features are used together to flag pixels as cyanobacteria dominant water (see Figure 3.11).

### 3.4.3 Detection of eukaryote and cyanobacteria dominated waters

The MPH variable (the height of the peak in the red/NIR) is proportional to backscattering from phytoplankton as long as phytoplankton is the dominant optically-active constituent. The concentration of Chl-a is strongly linearly correlated to phytoplankton backscattering on a species-specific basis (Whitmire et al. 2010). If the backscattering to biomass ratio between species or bloom types is sufficiently large, distinct relationships between the MPH variable and Chl-a concentration can be defined and used for diagnostic bloom detection. The MPH

algorithm was calibrated to two data sets: one from eutrophic eukaryote dinoflagellate/diatom dominated waters, and one from hypertrophic waters dominated by *Microcystis* (Figure 3.11). MPH in the *Microcystis*-dominated waters was almost an order of magnitude higher than the eukaryotic blooms, likely owing to small size and the presence of gas vacuoles (Matthews and Bernard 2013). This result supports the use of MPH to identify high-backscattering cyanobacteria species such as *Microcystis*.

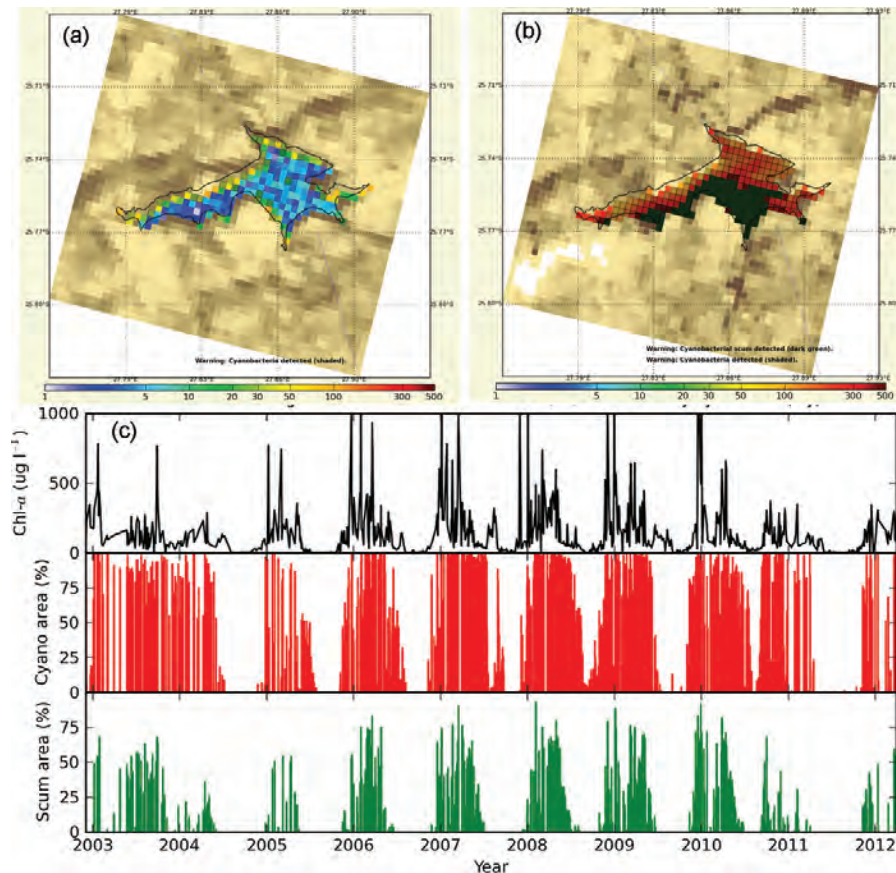


**Figure 3.12** Chl-a concentration maps derived from from MERIS FR imagery of Hartbeespoort Lake during (A) clear (oligotrophic) and (B) hypertrophic phases. Cyanobacteria dominant pixels are shaded and surface scum is dark green. (C) A 10-year time series of Chl-a concentration, cyanobacteria coverage, and surface scum coverage of the lake, based on the full MERIS FR archive.

Application of the MPH algorithm in Hartbeespoort Lake shows the detection over time of trophic status, cyanobacteria, and surface scum accumulations (Figure 3.12). The lake is dominated by spring outbreaks of *Microcystis* which persist well into autumn and only occasionally disappear in winter as the water cools. The mean Chl-a concentration regularly reaches  $500 \text{ mg m}^{-3}$  in summer and spring, and may be as high as  $1,000 \text{ mg m}^{-3}$  (the limit assigned to the algorithm). The bloom phenology (initiation and persistence) is strongly seasonal. Cyanobacteria are dominant over the majority of the lake surface area for most of the year, with only a temporary respite during winter months, with the exception of a

prolonged clear phase observed during the winter and spring of 2005 and 2011. This clear phase may be a result of mitigation measures to reduce eutrophication in the reservoir, or from interannual variations in weather. Surface scum (defined by Chl-a > 500 mg m<sup>-3</sup>) are frequent during spring and summer months and cover large areas of the lake.

## 3.5 Case 4: Summer Blooms in the Baltic Sea<sup>§</sup>

### 3.5.1 Objective

This case study demonstrates the use of remote sensors to follow the seasonal development of the typical summer bloom of filamentous cyanobacteria in the Baltic Sea. Bloom biomass is in the order of 4–10 mg Chl-a m<sup>-3</sup> under well-mixed conditions. Diagnostic pigment absorption features are therefore not quantifiable from remotely sensed imagery. Under calm weather, however, buoyant species can accumulate near the water surface. This phenomenon enhances the distinct optical signatures of cyanobacterial pigment absorption, but simultaneously degrades the performance of atmospheric correction procedures. A highly patchy distribution of the bloom introduces significant sub-pixel variation, increasing the uncertainty in the quality of quantitative remote sensing products. These uncertainties stress the need for careful interpretation of image quality and illustrate the added value of data assimilation with *in situ* observations.

### 3.5.2 Study area

The Baltic Sea is a eutrophic coastal sea with limited water exchange with the North Sea, high nutrient input, and summer stratification supporting cyanobacteria-dominated phytoplankton populations when temperatures increase and inorganic nitrogen-phosphorous ratios decrease. Summer blooms commonly include the filamentous *Aphanizomenon flos-aqua*, *Nodularia spumigena*, and *Dolichospermum* spp. and occur naturally (Niemi 1973; Leppänen et al. 1995; Bianchi et al. 2000).

The peak period of cyanobacteria growth is around mid-July, although *A. flos-aqua* is found in low densities in all seasons. The rate of bloom development depends on nutrients available after the spring bloom (up to 50 mg Chl-a m<sup>-3</sup>) and on water temperature. Summer cyanobacterial bloom biomass is typically in the range 4–10 mg Chl-a m<sup>-3</sup>. Under calm conditions, the filamentous species rise to the surface and locally accumulate higher biomass. Water samples taken from ships tend to disturb near-surface stratified layers, so measured concentration ranges do not typically represent such situations.

### 3.5.3 Image analysis: Delineating blooms

Phytoplankton are the dominant source of light scattering in the open Baltic Sea during bloom periods and away from river plumes and shallow areas. Deriving maps of phytoplankton

<sup>§</sup>Authors: Stefan Simis<sup>1,2</sup>, Tiit Kutser<sup>3</sup>, Claudia Giardino<sup>4</sup>, Mariano Bresciani<sup>4</sup> (<sup>1</sup>Plymouth Marine Laboratory, UK; <sup>2</sup>Finnish Environment Institute SYKE, Finland; <sup>3</sup>University of Tartu, Estonia; <sup>4</sup>CNR-IREA, Italy)

biomass in the open sea can therefore be as straightforward as extracting the dominant optical signal from satellite imagery. The absorption of light by phytoplankton is, in contrast, strongly masked by coloured dissolved organic matter. Traditional algorithms to retrieve Chl-a biomass therefore show poor performance in this sea and require at least region-specific tuning.

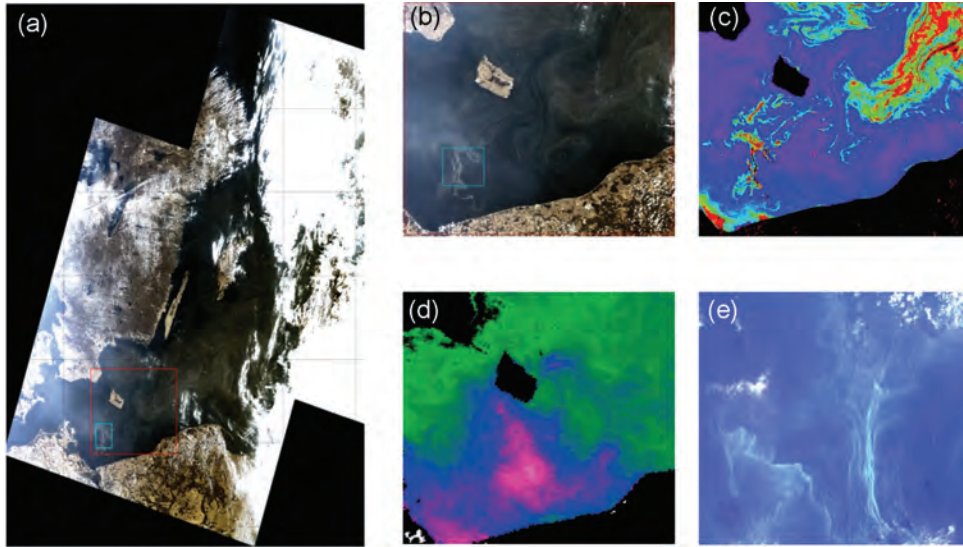


**Figure 3.13** Comparison of remotely sensed products indicating a cyanobacterial bloom (partially at the sea surface) in the Baltic Sea on 14 July 2010 (except for Landsat recorded on 10 July 2010). (a) MERIS RGB mosaic with frames indicating position of sub-scenes (MERIS and MODIS in red, Landsat in cyan). (b) RGB MERIS sub-scene of bloom area in southern Baltic. (c) Chl-a concentration derived from the WeW-FUB processor (Chl-a colour scale (purple to red) 1–80  $\text{mg m}^{-3}$ ). (d) MODIS SST (green to magenta: SST 20–26°C). (e) LANDSAT-5 RGB acquired on 10 July 2010.

To illustrate how the summer blooms can be delineated using a range of sensors and methods, several techniques are compared for the same bloom event in July 2010 around the Bornholm island in the southern Baltic (Figure 3.13). The included products are pseudo-true colour from MERIS FR, Chl-a concentration produced from the same image using the WeW-FUB processor in the BEAM toolbox, sea surface temperature (SST) from MODIS on the same date, and a LANDSAT RGB image from the same week. The MERIS RGB scene (Figure 3.13a,b) outlines the extent of the bloom, with a patchy distribution which suggests the influence of currents and mixing on its horizontal distribution. The Chl-a product (Figure 3.13c) reveals an additional near-coast bloom in the southwest corner of the selected sub-scene, which is also visible as warmer water in the SST image. Phytoplankton blooms contribute to heat, trapping in the surface layer, and regions where SST exceeds that of the surrounding area (Figure 3.13d) may indicate layers of phytoplankton that are less easily recognized from a targeted chlorophyll product (Figure 3.13c). This behaviour can be explained by the production of photoprotective rather than Chl-a pigment in light saturated environments (near the water surface), or by elevated light scattering of less pigmented material. Weak correspondence between visible light products and SST can be explained by physiological differences between bloom populations, but differences in the vertical distribution between bloom sites cannot be

ruled out either, without the use of mixing models or *in situ* measurements. It is nevertheless evident that each of the demonstrated products has value in delineating the presence of bloom phenomena.

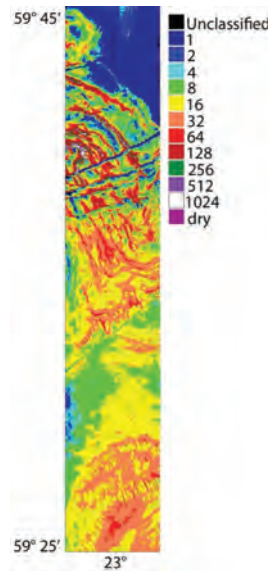


**Figure 3.14** Chl-a (colour scale in  $\text{mg m}^{-3}$ , 'dry' indicates surface scum) in a cyanobacteria bloom in the Gulf of Finland, Baltic Sea on 14 July 2002. The map is produced from a Hyperion image with 30 m spatial resolution (Kutser 2004). Disturbed near-surface accumulations in the wake of ships are visible as low concentrations in four east-west oriented bands across the top half of the scene.

### 3.5.4 Spatial resolution

Spatial and temporal undersampling of phytoplankton biomass is problematic in environmental baseline monitoring, particularly in a system like the Baltic Sea where short-lived and patchy blooms occur frequently (Rantajarvi et al. 1998; Kutser 2004). A 30-m resolution Hyperion image from 14 July 2002, processed to depict Chl-a concentration (Figure 3.14, after Kutser 2004) illustrates the heterogeneous distribution of such blooms. High biomass estimates over a large part of the scene suggest that surface accumulations are present, enhancing the optical signature of the cyanobacteria rather than being representative of mixed column concentration, as explained in Figure 3.2. The image also illustrates how such surface blooms are disturbed in the wake of ships: estimated pigment concentrations are several orders of magnitude lower than in the areas surrounding the ship wake.

Because of the uncertainty in concentration estimates associated with stratified blooms, hydrodynamic modelling, multiple-sensor approaches (combining SST, surface roughness, and optical remote sensing), as well as data assimilation with *in situ* platforms, are necessary to assess the severity of buoyant cyanobacteria blooms.

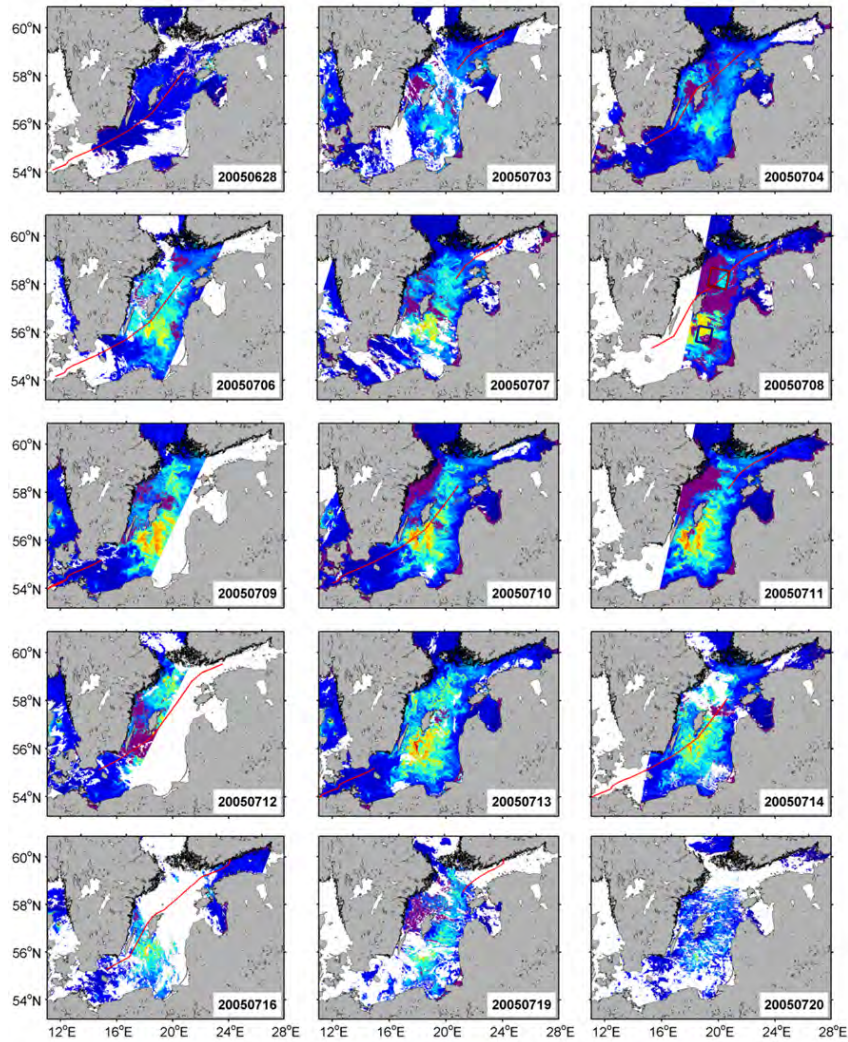


**Figure 3.15** Cyanobacteria bloom development in the Baltic Sea in the summer of 2005. MERIS RR imagery are shown as the band product [(5/7) - 12], used to highlight particulate backscatter with associated Chl-a absorption. Suspected surface accumulations are masked purple based on the condition [band 13 > band 4], which indicates water absorption in the NIR is masked by light scattering near the surface. Atmospheric correction failed for these pixels (Figure 3.16). The route of ship-of-opportunity M/S Finnpartner during the 24-h period around the overpass is overlaid in red.

### 3.5.5 Time series and matching *in situ* observations

The last bloom example from the Baltic Sea concerns an extensive surface bloom which occurred in July 2005. The year was generally warm and July was calm and clear, offering a large number of satellite images and excellent conditions for development and occasional surfacing of cyanobacteria blooms. Research cruises in the Gulf of Finland (between longitudes 21–27°E) in the period 4–29 July recorded an average ( $\pm$  standard deviation) Secchi disk depth of  $3.8 \pm 0.5$  m, and surface (1–3 m depth samples) Chl-a concentrations of  $5.7 \pm 1.4$  mg m<sup>-3</sup>.

Wind speeds rarely exceeded  $10 \text{ m s}^{-1}$ . Water temperatures at 5 m depth measured along the ferry transect Helsinki - Travemunde (Finland - Germany) ranged from 18–25°C in July. The filamentous *A. flos-aquae*, *N. spumigena*, and *Dolichospermum* spp. (formerly planktonic *Anabaena* spp.) were abundant in water samples taken along the ferry route (Seppälä et al. 2007).

Time series of reduced-resolution (1200 m) MERIS imagery from July 2005 presented in Figure 3.15 show the development of the bloom. The band ratio product of MERIS bands 5 and 7, offset by band 12 (center wavelengths at 560, 665, and 779 nm, respectively) mainly targets turbidity and pigmented particles, and offers a high dynamic range in this water type. Bands 13 and 4 (865 and 510 nm) are compared to detect strong reflectance in the near infra-red spectrum, which indicates that absorption by water molecules is masked by strong particle scattering near the water surface, e.g., by buoyant filaments. The default MERIS L2B image processing (MEGS 8.0) did not result in valid reflectance spectra in these areas, masked purple in the processed scenes.

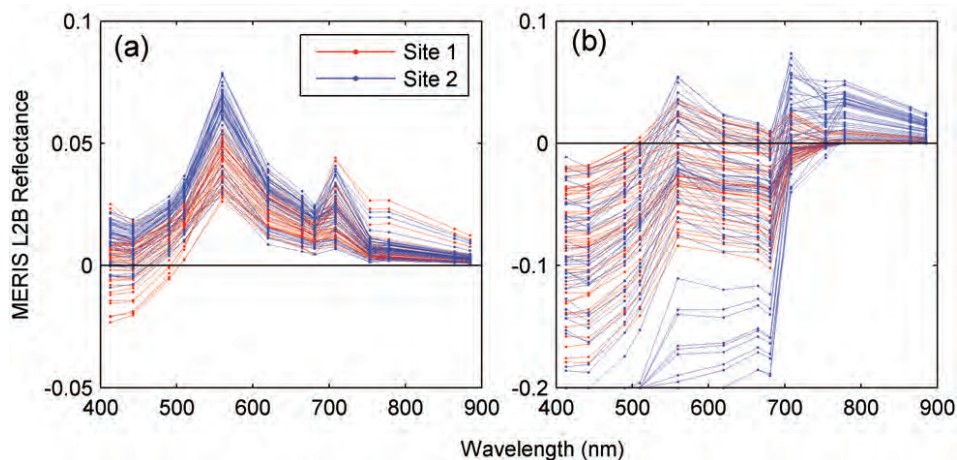


**Figure 3.16** Reflectance spectra extracted from two sites in the MERIS RR scene on 8 July 2005 with suspected (a) mixed bloom and (b) surface bloom.

To illustrate that default atmospheric correction typically fails over surface bloom areas, reflectance spectra are extracted from two sites recorded on 8 July 2005 (marked with boxes in the corresponding scene in Figure 3.15, numbered 20050708). Both sites contain adjacent areas of suspected surface accumulations and deeper mixing. A random selection of 50 reflectance spectra from the mixed and surface bloom areas is shown for each site in Figure 3.16. Spectra corresponding to well-mixed water (Figure 3.16a) are of variable magnitude but consistent shape. In contrast, the suspected surface bloom site (Figure 3.16b) shows the characteristic shape of surfacing blooms with high NIR reflectance, similar to the simulated spectra in Figure 3.2. Negative values result from a limitation of the standard atmospheric correction method to yield high NIR reflectance, causing the whole spectrum to be shifted to lower values while the shape of the spectrum remains realistic. Algorithms that are not sensitive to absolute reflectance values (such as baseline subtraction algorithms) will therefore not be strongly

affected.

*In situ* observations from ferries equipped with thermosalinograph, chlorophyll and phycocyanin fluorometers, and turbidimeter were available for a large number of scenes included in the time series of Figure 3.15. A markedly good correspondence is observed between the along-transect pixel values shown in Figure 3.15 and the turbidity measurements (Figure 3.17). For this comparison, both products were normalized to their geometric mean and standard deviation. This normalizes the variable correspondence throughout the study period between turbidity measured at 5 m by the ferrybox and the reflectance product which is more sensitive to near-surface accumulations. Whenever the ferry traversed a suspected surface bloom, the area is marked in green on the horizontal axes of Figure 3.17 panels. As may be expected from the poor quality of reflectance spectra for surface blooms, correspondence of the *in situ* and remotely sensed data sources is poorest in these areas.

### 3.5.6 Discussion

The Baltic Sea case illustrates that blooms of cyanobacteria in coastal water pose several additional challenges to remote sensing. Vertical mixing cannot be assumed and individual remote sensing scenes should then be interpreted with caution. Time series, particularly when overlapping with sporadic *in situ* observations, are more straightforward to interpret. Uncertainty in the vertical distribution of the cyanobacteria biomass may also lead to different bloom products derived with algorithms targeting different band sets, or using sea surface temperature. The coherence between these different approaches may well be the best indicator of the mixing and physiological state of the bloom biomass. Mixing models, *in situ* observations, and remote sensing techniques should be brought together to provide synoptic phytoplankton monitoring in heterogeneous systems with limited optical sensing possibilities, such as the Baltic Sea.

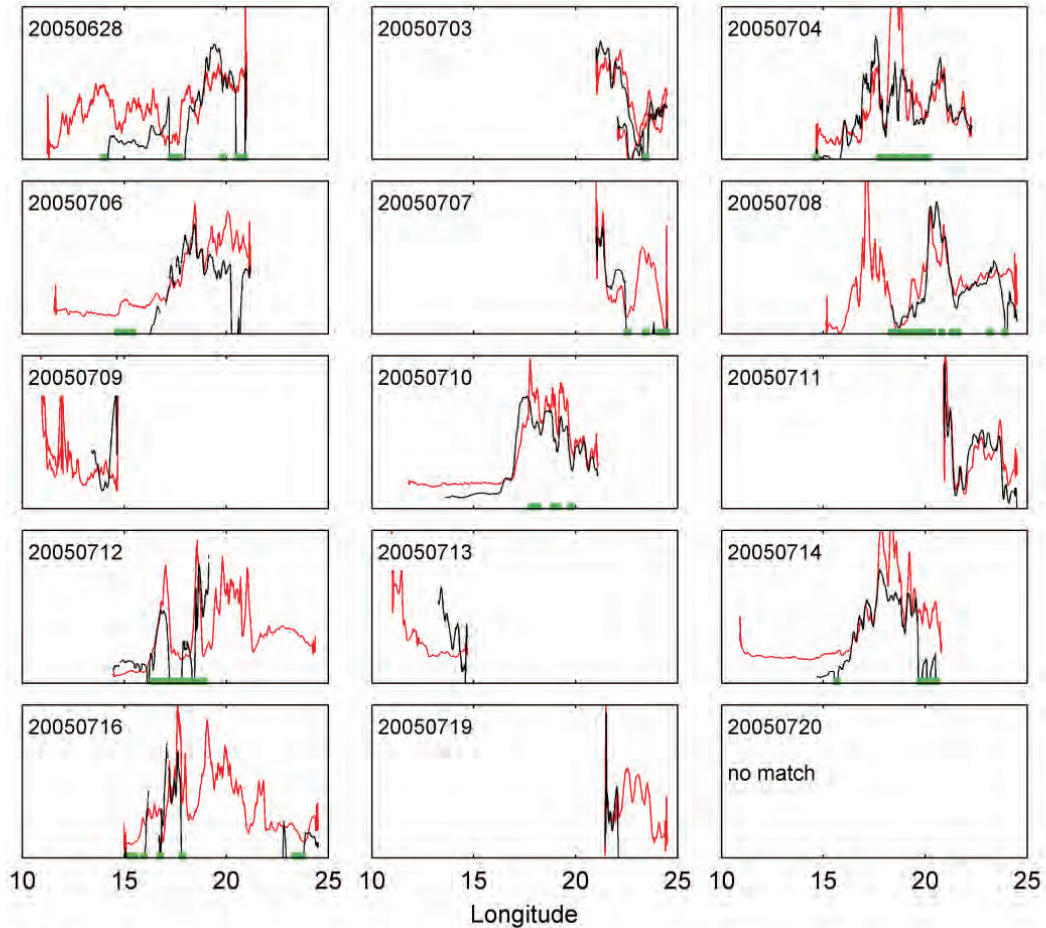


**Figure 3.17** Turbidity measured in the flow-through system of M/S Finnpartner (red) and matching pixel profiles (black) along the ferry transects, corresponding to the time series in the previous figure. Both signal sources were standardized before plotting. Sections of transects where surface accumulations were evident are marked green along the horizontal axis, and invalid reflectance in one or more bands used in the band ratio product resulted in most cases (but not, for example, on 8 July 2005). Fronts and finer structures are generally in agreement between the platforms, suggesting that *in situ* data can be extrapolated with the aid of remote sensors at least on a scene-by-scene basis. Sections of transects where the correlation between *in situ* and imagery data correlate poorly may be caused by stratification of the surface waters or strong currents displacing the bloom.

## Acronyms and Abbreviations

---

BRR	Bottom-of-Rayleigh
C	Carbon
CDOM	Coloured Dissolved Organic Matter
CHL	Chlorophyll-a concentration
Chl-a	Chlorophyll-a
CHRIS	Compact High Resolution Imaging Spectrometer (ESA)
DIN	Dissolved Inorganic Nitrogen
DIP	Dissolved Inorganic Phosphorus
ERGB	Enhanced-RGB
ESA	European Space Agency
FAI	Floating Algae Index
FR	Full Resolution
FWC-FWRI	Florida Fish and Wildlife Conservation Commission's Fish and Wildlife Research Institute
GDP	Gross Domestic Product
GoM	Gulf of Mexico
GSFC	Goddard Space Flight Center
HAB	Harmful Algal Bloom
JGOFS	Joint Global Ocean Flux Study
MPH	Maximum Peak Height
MERIS	Medium Resolution Imaging Spectrometer (ESA)
MODIS	Moderate Resolution Imaging Spectroradiometer
N	Nitrogen
NASA	National Aeronautics and Space Administration
nFLH	Normalized Fluorescence Line Height
NIR	Near Infra-red
NOAA	National Oceanic and Atmospheric Administration
NPP	National Polar-orbiting Partnership
NSP	Neurotoxic Shellfish Poisoning
P	Phosphorus
PFT	Phytoplankton Functional Types
QAA	Quasi-Analytical Algorithm
RBD	Red Band Difference
RCA	Red tide Chlorophyll Algorithm
RGB	Red, Green, Blue
RMB	Renminbi (Chinese Currency)

ROS	Reactive Oxygen Species
SeaDAS	SeaWiFS Data Analysis System
SeaWiFS	Sea-viewing Wide Field-of-view Sensor
Si	Silica
SST	Sea Surface Temperature
SWIR	Short Wave Infra-red
TN	Total Nitrogen
TOA	Top-of-Atmosphere
TP	Total Phosphorus
USGS	United States Geological Survey
VIIRS	Visible Infrared Imager Radiometer Suite
WFS	West Florida Shelf

---

## Bibliography

---

- Adolf, J., T. Bachvaroff, and A. Place (2008). Can cryptophytes trigger toxic *Karlodinium veneficum* blooms in eutrophic estuaries? *Harmful Algae* 81: 19–128.
- Adolf, J., T. Bachvaroff, and A. Place (2009). Environmental modulation of karlotoxin levels in strains of the cosmopolitan dinoflagellate, *Karlodinium veneficum*. *J. Phycol.* 45: 176–192.
- Ahn, Y.-H. and P. Shannmugam (2006). Detecting the red tide algal blooms from satellite ocean color observations in optically complex Northeastern-Asia coastal waters. *Remote Sens. Environ.* 103: 419–437.
- Aké-Castillo, J., Y. Okolokov, K. González-González, and H. Pérez-España (2012). *Karenia* sp. “Mexican hat” first bloom in México. *Harmful Algae News* 41: 16–17.
- Alcock, F. (2007). *An Assessment of Florida red tide: causes, consequences and management strategies*. 1190. Tech. rep. MOTE Marine Laboratory, Sarasota, Florida.
- Amin, R., B. Penta, and S. deRada (2015). Occurrence and spatial extent of HABs on the West Florida Shelf 2002 – present. *IEEE Geosc. Remote Sens. Lett.* 12:10, 2080–2084. DOI: [10.1109/LGRS.2015.2448453](https://doi.org/10.1109/LGRS.2015.2448453).
- Amin, R., J. Zhou, A. Gilerson, B. Gross, F. Moshary, and S. Ahmed (2009). Novel optical techniques for detecting and classifying toxic dinoflagellate *Karenia brevis* blooms using satellite imagery. *Opt. Express* 17:11, 9126–9144.
- Anderson, D. M., P. M. Glibert, and J. M. Burkholder (2002). Harmful algal blooms and eutrophication: nutrient sources, composition, and consequences. *Estuaries* 25:4, 704–726.
- Al-Azri, A., S. Piontkovski, K. A. Al-Hashmi, J. Goes, H. D. R. Gomes, and P. Glibert (2014). Mesoscale and nutrient conditions associated with the massive 2008 *Cochlodinium polykrikoides* bloom in the Sea of Oman/Arabian Gulf. 37: 325–338. *Estuar. Coast.*
- Babica, P., L. Blaha, and B. Marsalek (2006). Exploring the natural role of microcystins - A review of effects on photoautotrophic organisms. *J. Phycol.* 42:1, 9–20.
- Backer, L. and D. McGillicuddy (2006). Harmful algal blooms: At the interface between coastal oceanography and human health. *Oceanography* 19: 94–106.
- Baden, D. and T. Mende (1979). Amino acid utilization by *Gymnodinium breve*. *Phytochemistry* 18:2, 247–251.
- (1982). Toxicity of two toxins from the Florida red tide marine dinoflagellate, *Ptychodiscus brevis*. *Toxicon* 20:2, 457–461.
- Berg, G. M., M. Balode, I. Purina, S. Bekere, C. Béchemin, and S. Maestrini (2003). Plankton community composition in relation to availability an uptake of oxidized and reduced nitrogen. *Aquat. Microb. Ecol.* 30: 263–274.
- Berman, T. (1997). Dissolved organic nitrogen utilization by an *Aphanizomenon* bloom in Lake Kinneret. *J. Plank. Res.* 19: 577–586.
- Berman, T. and D. Bronk (2003). Dissolved organic nitrogen: a dynamic participant in aquatic ecosystems. *Aquat. Microb. Ecol.* 31: 279–305.
- Bianchi, T. S., E. Engelhaupt, P. Westman, T. Andren, C. Rolff, and R. Elmgren (2000). Cyanobacterial blooms in the Baltic Sea: Natural or human-induced? *Limnol. Oceanogr.* 45:3, 716–726.
- Bidigare, R. R., M. E. Ondrusek, J. H. Morrow, and D. A. Kiefer (1990). In-vivo absorption properties of algal pigments. *SPIE Proc. Ocean Optics X* 1302: 290–302.
- Bjørnland, T. F., T. Haxo, and S. Liaaen-Jensen (2003). Carotenoids of the Florida red tide dinoflagellate *Karenia brevis*. *Biochem. System. Ecol.* 31: 1147–1162.
- Bossart, G., D. Baden, R. Ewing, B. Roberts, and S. Wright (1998). Brevetoxicosis in manatees (*Trichechus manatus latirostris*) from the 1996 epizootic: gross, histologic, and immunohistochemical features. *Toxicol. Pathol.* 26:2, 276–282.
- Botes, L., S. Sym, and C. Pitcher (2003). *Karenia cristata* sp. nov. and *Karenia bicuneiformis* sp. nov. (Gymnodinales, Dinophyceae): two new *Karenia* species of the South African coast. *Phycologia* 42:6, 563–571.
- Boyd, P. and S. Doney (2003). The impact of climate change and feedback processes on the ocean carbon cycle. In: *Ocean Biogeochemistry — The Role of the Ocean Carbon Cycle in Global Change*. Ed. by M. Fasham. Springer-Verlag, 157–193.

- Brand, L., L. Campbell, and E. Bresnan (2012). *Karenia*: the biology and ecology of a toxic genus. *Harmful Algae* 14: 156–178.
- Bronk, D., M. Sanderson, M. Mulholland, C. Heil, and J. O'Neil (2004). Organic and inorganic nitrogen uptake kinetics in field populations dominated by *Karenia brevis*. In: *Harmful Algae 2002*. Ed. by K. Steidinger, J. Landsberg, C. Tomas, and G. Vargo. Florida Fish, Wildlife Conservation Commission, Florida Institute of Oceanography, and Intergovernmental Oceanographic Commission of UNESCO, 80–82.
- Burkholder, J., P. Glibert, and H. Skelton (2008). Mixotrophy, a major mode of nutrition for harmful algal species in eutrophic waters. *Harmful Algae* 8: 77–93.
- Cannizzaro, J., K. Carder, F. Chen, C. Heil, and G. Vargo (2008). A novel technique for detection of the toxic dinoflagellate, *Karenia brevis*, in the Gulf of Mexico from remotely sensed ocean color data. *Cont. Shelf Res.* 28:1, 137–158.
- Cannizzaro, J., K. Carder, F. Chen, J. Walsh, Z. Lee, and C. Heil (2004). A novel optical classification technique for detection of red tides in the Gulf of Mexico: application to the 2001–2002 bloom event. In: *Harmful Algae 2002*. Ed. by K. Steidinger, J. Landsberg, C. Tomas, and G. Vargo. Florida Fish, Wildlife Conservation Commission, Florida Institute of Oceanography, and Intergovernmental Oceanographic Commission of UNESCO., 282–284.
- Cannizzaro, J., C. Hu, D. English, K. Carder, C. Heil, and F. Müller-Karger (2009). Detection of *Karenia brevis* blooms on the west Florida shelf using in situ backscattering and fluorescence data. *Harmful Algae* 8:6, 898–909.
- Cannizzaro, J. et al. (2013). On the accuracy of SeaWiFS ocean color data products on the West Florida Shelf. *J. Coastal Res.* 29:6, 1257–1272.
- Cannon, J. (1990). Development and dispersal of red tides in the Port River, South Australia. In: *Toxic Marine Phytoplankton*. Ed. by E. Granéli, B. Sundstrom, L. Edler, and D. Anderson. Elsevier, 110–115.
- Cao, H., Y. Tao, F. Kong, and Z. Yang (2008). Relationship between temperature and cyanobacterial recruitment from sediments in laboratory and field studies. *J. Freshwater Ecol.* 23: 405–412.
- Carvalho, G., P. Minnett, L. Fleming, V. Banzon, and W. Baringer (2010). Satellite remote sensing of harmful algal blooms: a new multi-algorithm method for detecting the Florida Red Tide (*Karenia brevis*). *Harmful Algae* 9:5, 440–448.
- Cecchetti, A. and G. Lazzerini (2007). *La vegetazione idrofitica del Lago Trasimeno*. Campagna di monitoraggio 2007. Parco del Lago Trasimeno, Regione Umbria.
- CEE, D. (1979). *Council Directive on the conservation of wild birds, 1979/409/CEE, Directive, Vol. 103*. Tech. rep. Official Journal of the European Union, Legislation.
- Chan, F., M. L. Pace, R. W. Howarth, and R. M. Marino (2004). Bloom formation in heterocystic nitrogen-fixing cyanobacteria: The dependence on colony size and zooplankton grazing. *Limnol. Oceanogr.* 49:6, 2171–2178.
- Chang, F. (1999). *Gymnodinium brevisulcatum* sp. nov. (Gymnodiniales, Dinophyceae), a new species isolated from the 1998 summer toxic bloom in Wellington Harbour, New Zealand. *Phycologia* 38:5, 337–384.
- Chang, F. and K. Ryan (2004). *Karenia concordia* sp. nov. (Gymnodiniales, Dinophyceae), a new nonthecate dinoflagellate isolated from the New Zealand northeast coast during the 2002 harmful algal bloom events. *Phycologia* 43:5, 552–562.
- Cingolani, L., R. Padula, M. D. Brizio, and E. Ciccarelli (2007). Eutrofizzazione del Lago Trasimeno: il problema delle fioriture algali. In: *14th Conf. Igiene Industriale, Corvara, Italy*.
- Codd, G. A., S. G. Bell, K. Kaya, C. J. Ward, K. A. Beattie, and J. S. Metcalf (1999). Cyanobacterial toxins, exposure routes and human health. *Eur. J. Phycol.* 34:4, 405–415.
- Codd, G. A., J. Lindsay, F. M. Young, L. F. Morrison, and J. S. Metcalf (2005). Harmful cyanobacteria. From mass mortalities to management measures. In: *Harmful Cyanobacteria*. Ed. by H. Huisman J., C. P. Matthijs, and P. M. Visser. Dordrecht: Springer, 1–23.
- Cortés-Altamirano, R., D. Hernández-Becerril, and R. Luna-Soria (1995). Mareas rojas en México, una revision. *Rev. Latinoam. Microbiol.* 37: 343–352.
- Craig, S., S. Lohrenz, Z. Lee, K. Mahoney, G. Kirkpatrick, O. Schofield, and R. Steward (2006). Use of hyperspectral remote sensing reflectance for detection and assessment of the harmful alga, *Karenia brevis*. *Appl. Opt.* 45:21, 5414–5425.
- Dash, P., N. D. Walker, D. R. Mishra, C. Hu, J. L. Pinckney, and E. J. D'Sa (2011). Estimation of cyanobacterial pigments in a freshwater lake using OCM satellite data. *Remote Sens. Environ.* 115:12, 3409–3423.
- Dason, J., I. Huertas, and B. Colman (2004). Source of inorganic carbon for photosynthesis in two marine dinoflagellates. *J. Phycol.* 40: 285–292.

- Davidson, K., P. Miller, T. Wilding, J. Shutler, E. Bresnan, K. Kennington, and S. Swan (2009). A large and prolonged bloom of *Karenia mikimotoi* in Scottish waters in 2006. *Harmful Algae* 8: 349-361.
- Davis, C. (1948). *Gymnodinium brevis* sp. nov., a cause of discolored water and animal mortality in the Gulf of Mexico. *Bot. Gaz.* 109:3, 358-360.
- De Salas, M., C. Bolch, and G. Hallengraeff (2004). *Karenia umbrella* sp. nov. (Gymnodiniales, Dinophyceae), a new potentially ichthyotoxic dinoflagellate species from Tasmania, Australia. *Phycologia* 43:2, 166-175.
- Dekker, A. G., T. J. Malthus, and E. Seyhan (1991). Quantitative modeling of inland water-quality for high-resolution MSS systems. *IEEE Trans. Geosci. Remote Sens.* 29: 89-95.
- Dekker, A. (1993). Detection of optical water quality parameters for eutrophic waters by high resolution remote sensing. Phd Thesis. Vrije Universiteit Amsterdam.
- Dickey, R. et al. (1999). Monitoring for brevetoxins during a *Gymnodinium breve* red tide: comparison of sodium channel specific cytotoxicity assay and mouse bioassay for determination of neurotoxic shellfish in shellfish extracts. *Nat. Toxins* 7: 157-165.
- Dierssen, H., R. Kudela, J. Ryan, and R. Zimmerman (2006). Red and black tides: Quantitative analysis of water-leaving radiance and perceived color for phytoplankton, colored dissolved organic matter, and suspended sediments. *Limnol. Oceanogr.* 51:6, 2646-2659.
- Dragovich, A. and J. Kelly (1966). *Distribution and occurrence of Gymnodinium breve on the west coast of Florida, 1964-1965*. U.S. Dep. Int. Bureau of Commercial Fishing, U.S. Fisheries and Wildlife Sciences Washington. Dragovich1966.
- Duan, H., R. Ma, Y. Zhang, and S. A. Loiselle (2014). Are algal blooms occurring later in Lake Taihu? Climate local effects outcompete mitigation prevention. *J. Plankton Res.* 36:3, 866-871.
- Duan, H. et al. (2009). Two-decade reconstruction of algal blooms in China's Lake Taihu. *Environ. Sci. Technol.* 43:10, 3522-3528.
- Dumont, E., J. Harrison, C. Kroeze, E. Bakker, and S. Seitzinger (2005). Global distribution and sources of dissolved inorganic nitrogen export to the coastal zone: results from a spatially explicit, global model. *Global Biogeochem. Cy.* 19: GB4S02.
- Dürr, H., G. Laruelle, C. V. Kempen, C. Slomp, M. Meybeck, and H. Middelkoop (2011). Worldwide typology of nearshore coastal systems: Defining the estuarine filter of river inputs to the ocean. *Estuar. Coast* 34: 441-458.
- Elliott, J. (2011). Is the future blue-green? A review of the current model predictions of how climate change could affect pelagic freshwater cyanobacteria. *Water Res.* 46:5, 1364-1367.
- Elser, J. et al. (2009). Shifts in lake N:P stoichiometry and nutrient limitation driven by atmospheric nitrogen deposition. *Science* 326: 835-837.
- Evens, T., G. Kirkpatrick, D. Millie, D. Chapman, and O. Schofield (2001). Photophysiological responses of the toxic red-tide dinoflagellate *Gymnodinium breve* (Dinophyceae) under natural sunlight. *J. Plankton Res.* 23:11, 1177-1194.
- Faust, M. and R. Gulledge (2002). Identifying harmful marine dinoflagellates. *Contrib. U. S. Natl. Herb.* 42: 1-144.
- Feki, W. et al. (2013). What are the potential drivers of blooms of the toxic dinoflagellate *Karenia selliformis*? A 10-year study in the Gulf of Gabes, Tunisia, southwestern Mediterranean Sea. *Harmful Algae* 23: 8-18.
- Finucane, J. (1964). *Distribution and seasonal occurrence on Gymnodinium breve on the west coast of Florida, 1954-57*. U.S. Dept. of the Interior, Bureau of Commercial Fisheries, Washington.
- Fleming, L., B. Kirkpatrick, L. Backer, J. Bean, A. Wanner, D. Dalpra, and R. Tamer (2005). Initial evaluation of the effects of aerosolized Florida red tide toxins (brevetoxins) in persons with asthma. *Environ. Health Perspect.* 113:5, 650-657.
- Fleming, L. et al. (2007). Aerosolized red-tide toxins (brevetoxins) and asthma. *Chest* 131:1, 187-194.
- Fleming, L. et al. (2009). Exposure and effect assessment of aerosolized red tide toxins (brevetoxins) and asthma. *Environ. Health Perspect.* 117: 7.
- Fleming, L. et al. (2011). Review of Florida red tide and human health effects. *Harmful Algae* 10:2, 224-233.
- Flewelling, L. et al. (2005). Brevetoxicosis: red tides and marine mammal mortalities. *Nature* 435:7043, 755-756.
- Flynn, K. J. et al. (2013). Misuse of the phytoplankton-zooplankton dichotomy: the need to assign organisms as mixotrophs within plankton functional types. *J. Plankt. Res.* 35: 3-11.
- Flynn, K., J. Franco, P. Fernández, B. Reguera, M. Zepata, G. Wood, and K. Flynn (1994). Changes in toxin content, biomass and pigments of the dinoflagellate *Alexandrium minutum* during nitrogen refeeding and growth into nitrogen and phosphorus stress. *Mar. Ecol. Prog. Ser.* 111: 99-109.
- Fomferra, N. and C. Brockmann (2006). *The BEAM project web page*. Brockmann Consult.

- Franks, P. and D. Anderson (1992). Alongshore transport of a toxic phytoplankton bloom in a buoyancy current: *Alexandrium tamarense* in the Gulf of Maine. *Mar. Biol.* 112: 153-164.
- Fu, X., A. Tatters, and D. Hutchins (2012). Global change and the future of harmful algal blooms in the ocean. *Mar. Ecol. Prog. Ser.* 470: 207-233.
- Galloway, J., E. Cowling, S. Seitzinger, and R. Socolow (2002). Reactive nitrogen: too much of a good thing? *Ambio* 31: 60-63.
- GEOHAB (2001). *Global Ecology and Oceanography of Harmful Algal Blooms Programme, Science Plan*. Ed. by P. Glibert and G. Pitcher. SCOR, IOC, Baltimore, and Paris.
- (2010). *Global Ecology and Oceanography of Harmful Algal Blooms in Asia: A Regional Comparative Programme*. Ed. by K. Furuya, P. Glibert, M. Zhou, and R. Raine. IOC, SCOR, Paris, and Newark, Delaware.
- Geraci, J. (1989). *Clinical investigation of the 1987-1988 mass mortality of bottlenose dolphins along the US Central and South Atlantic Coast. Report to the National Marine Fisheries Service and US Navy*.
- Giardino, C., G. Candiani, and E. Zilioli (2005). Detecting Chlorophyll-a in Lake Garda Using TOA MERIS Radiances. *Photogramm. Eng. Rem. S.* 71:9, 1045-1051.
- Giardino, C., G. Candiani, M. Bresciani, Z. Lee, S. Gagliano, and M. Pepe (2012). BOMBER: A tool for estimating water quality and bottom properties from remote sensing images. *Comput. Geosci.* 45: 313-318.
- Gitelson, A. (1992). The peak near 700 nm on radiance spectra of algae and water - Relationships of its magnitude and position with Chlorophyll concentration. *Int. J. Remote Sens.* 13:17, 3367-3373.
- Glibert, P. M., T. Kana, and K. Brown (2013). From limitation to excess: consequences of substrate excess and stoichiometry for phytoplankton physiology, trophodynamics and biogeochemistry, and implications for modeling. *J. Marine Syst.* 125: 14-28.
- Glibert, P. (in press). Margalef revisited: A new phytoplankton mandala incorporating twelve dimensions including nutritional physiology. *J. Plankton Res.*
- Glibert, P., D. Anderson, P. Gentien, E. Granéli, and K. Sellner (2005). The global, complex phenomena of harmful algal blooms. *Oceanography* 18:2, 136-147.
- Glibert, P. and J. Burkholder (2006). The complex relationships between increasing fertilization of the earth, coastal eutrophication and proliferation of harmful algal blooms. In: *Ecology of Harmful Algae*. Ed. by E. Granéli and J. Turner. Springer, 341-354.
- (2011). Eutrophication and HABs: Strategies for nutrient uptake and growth outside the Redfield comfort zone. *Chinese J. Oceanol. Limnol.* 29: 724-738.
- Glibert, P., J. Burkholder, and T. Kana (2012). Recent advances in understanding of relationships between nutrient availability, forms and stoichiometry and the biogeographical distribution, ecophysiology, and food web effects of pelagic and benthic *Prorocentrum* spp. *Harmful Algae* 14: 231-259.
- Glibert, P., J. Burkholder, T. Kana, J. Alexander, C. Schiller, and H. Skelton (2009). Grazing by *Karenia brevis* on *Synechococcus* enhances their growth rate and may help to sustain blooms. *Aquat. Microb. Ecol.* 55: 17-30.
- Glibert, P., D. Fullerton, J. Burkholder, J. Cornwell, and T. Kana (2011). Ecological stoichiometry, biogeochemical cycling, invasive species and aquatic food webs: San Francisco Estuary and comparative systems. *Rev. Fish. Sci.* 19: 358-417.
- Glibert, P., J. Harrison, C. Heil, and S. Seitzinger (2006). Escalating worldwide use of urea - a global change contributing to coastal eutrophication. *Biogeochem.* 77: 441-463.
- Glibert, P., C. Heil, D. Hollander, M. Revilla, A. Hoare, J. Alexander, and S. Murasko (2004). Evidence for dissolved organic nitrogen and phosphorus uptake during a cyanobacterial bloom in Florida Bay. *Mar. Ecol. Prog. Ser.* 280: 73-83.
- Glibert, P., D. Hinkle, B. Sturgis, and R. Jesien (2014a). Eutrophication of a Maryland/Virginia coastal lagoon: A tipping point, ecosystem changes, and potential causes. *Estuar. Coast* 37: S128-S146. DOI: [10.1007/s12237-013-9630-3](https://doi.org/10.1007/s12237-013-9630-3).
- Glibert, P. and C. Legrand (2006). The diverse nutrient strategies of HABs: Focus on osmotrophy. In: *Ecology of Harmful Algae*. Ed. by E. Granéli and J. Turner. Springer, 163-176.
- Glibert, P., E. Mayorga, and S. Seitzinger (2008). *Prorocentrum minimum* tracks anthropogenic nitrogen and phosphorus inputs on a global basis: application of spatially explicit nutrient export models. *Harmful Algae* 8: 33-38.
- Glibert, P. et al. (2001). Harmful algal blooms in the Chesapeake and Coastal Bays of Maryland, USA: Comparisons of 1997, 1998, and 1999 events. *Estuaries* 24: 875-883.

- Glibert, P. et al. (2002). A fish kill of massive proportion in Kuwait Bay, Arabian Gulf, 2001: the roles of bacterial disease, harmful algae, and eutrophication. *Harmful Algae* 1: 215–231.
- Glibert, P. et al. (2014b). Vulnerability of coastal ecosystems to changes in harmful algal bloom distribution in response to climate change: projections based on model analysis. *Glob. Change Biol.* 20: 3845–3858. DOI: [10.1111/gcb.12662](https://doi.org/10.1111/gcb.12662).
- Glibert, P. et al. (2015). Pluses and minuses of ammonium and nitrate uptake and assimilation by phytoplankton and implications for productivity and community composition, with emphasis on nitrogen-enriched conditions. *Limnol. Oceanogr.* DOI: [10.1002/lno.10203](https://doi.org/10.1002/lno.10203).
- Goes, J. and H. D. R. Gomes (in press). An ecosystem in transition: the emergence of mixotrophy in the Arabian Sea. In: *Aquatic Microbial Ecology and Biogeochemistry: A Dual Perspective*. Ed. by P. M. Glibert and T. Kana. Springer.
- Goes, J., P. Thoppil, H. Gomes, and J. Fasullo (2005). Warming of the Eurasian landmass is making the Arabian Sea more productive. *Science* 308: 545–547.
- Gomes, H., J. Goes, S. Matondkar, E. J. Buskey, S. Basu, S. Parab, and P. Thoppil (2014). Massive outbreaks of *Noctiluca scintillans* blooms in the Arabian Sea due to spread of hypoxia. *Nat. Comm.* 5:4862. DOI: [10.1038/ncomms5862](https://doi.org/10.1038/ncomms5862).
- Gomes, H., J. Goes, P. Matondkar, S. Parab, A. Al-Azri, and P. Thoppil (2008). Blooms of *Noctiluca miliaris* in the Arabian Sea - an *in situ* and satellite study. *Deep-Sea Res.* 55:11, 751–765.
- Gons, H. J., J. Kromkamp, M. Rijkeboer, and O. Schofield (1992). Characterization of the light-field in laboratory scale enclosures of eutrophic lake water (Lake Loosdrecht, the Netherlands). *Hydrobiologia* 238: 99–109.
- Govindjee and D. Shevela (2011). Adventures with cyanobacteria: a personal perspective. *Front. Plant Sci.* 2: 28. DOI: [10.3389/fpls.2011.00028](https://doi.org/10.3389/fpls.2011.00028).
- Gower, J. F. R., R. Doerffer, and G. A. Borstad (1999). Interpretation of the 685 nm peak in water-leaving radiance spectra in terms of fluorescence, absorption and scattering, and its observation by MERIS. *Int. J. Remote Sens.* 20:9, 1771–1786.
- Granéli, E., L. Edler, D. Gedziorowska, and U. Nyman (1985). Influence of humic and fulvic acids on *Prorocentrum minimum* (Pav.) J. Schiller. In: *Toxic Dinoflagellates*. Ed. by D. Anderson, A. White, and D. Baden. Elsevier, 201–206.
- Granéli, E. and K. Flynn (2006). Chemical and physical factors influencing toxin content. In: *Ecology of Harmful Algae*. Ed. by E. Granéli and J. Turner. Springer, 229–241.
- Guanter, L. et al. (2010). Atmospheric correction of ENVISAT/MERIS data over inland waters: Validation for European lakes. *Remote Sens. Environ.* 114:3, 467–480.
- Guo, L. (2007). Doing battle with the green monster of Taihu Lake. *Science* 317:5842, 1166–1166.
- Hails, A., C. Boyes, A. Boyes, R. Currier, K. Henderson, A. Kotlewski, and G. Kirkpatrick (2009). The Optical Phytoplankton Discriminator. In: *OCEANS 2009. MTS/IEEE Biloxi - Marine Technology for Our Future: Global and Local Challenges*.
- Hallegraeff, G. and J. Maclean (1989). Biology, epidemiology and management of *Pyrodinium* red tides. In: *ICLARM Conf. Proc. 21*. Fisheries Dept., Brunei Darussalam and International Center for Living Aquatic Resources Management, Manila, Phillipines.
- Harrison, J., N. Caraco, and S. Seitzinger (2005a). Global patterns and sources of dissolved organic matter export to the coastal zone: results from a spatially explicit, global model. *Global Biogeochem. Cy.* 19: GB4S04.
- Harrison, J., S. Seitzinger, N. Caraco, A. Bouwman, A. Beusen, and C. Vörösmarty (2005b). Dissolved inorganic phosphorous export to the coastal zone: results from a new, spatially explicit, global model (NEWS-SRP). *Global Biogeochem. Cy.* 19: GB4S03.
- Harrison, P. et al. (2011). Geographical distribution of red and green *Noctiluca scintillans*. *Chinese J. Oceanol. Limnol.* 29: 807–831.
- Haywood, A., K. Steidinger, E. Truby, P. Bergquist, P. Bergquist, J. Adamson, and L. Mackenzie (2004). Comparative morphology and molecular phylogenetic analysis of three new species of the genus *Karenia* (Dinophyceae) from New Zealand. *J. Phycol.* 40: 165–179.
- Hecky, P. P. K. (1988). Nutrient limitation of phytoplankton in freshwater and marine environments: A review of recent evidence on the effects of enrichment. *Limnol. Oceanogr.* 33: 796–822.
- Heil, C., P. Glibert, and C. Fan (2005). *Prorocentrum minimum* (Pavillard) Schiller — A review of a harmful algal bloom species of growing worldwide importance. *Harmful Algae* 4: 449–470.

- Heil, C., P. Glibert, M. Al-Sarawi, M. Faraj, M. Behbehani, and M. Husain (2001). First record of a fish-killing *Gymnodinium* sp. bloom in Kuwait Bay, Arabian Sea: chronology and potential causes. *Mar. Ecol. Prog. Ser.* 214: 15-23.
- Heil, C., M. Revilla, P. Glibert, and S. Murasko (2007). Nutrient quality drives phytoplankton community composition on the West Florida Shelf. *Limnol. Oceanogr.* 52: 1067-1078.
- Heisler, J., P. Glibert, J. Burkholder, D. Anderson, W. Cochlan, W. Dennison, and C. Gobler (2008). Eutrophication and harmful algal blooms: A scientific consensus. *Harmful Algae* 8: 3-13.
- Hillebrand, H., G. Steinert, M. Boersma, A. Malzahn, C. Meunier, C. Plum, and R. Ptacnik (2013). Goldman revisited: Faster-growing phytoplankton has lower N:P and lower stoichiometric flexibility. *Limnol. Oceanogr.* 58: 2076-2088.
- Hoagland, P. and S. Scatasta (2006). The economic effects of harmful algal blooms. In: *Ecology of Harmful Algae*. Ed. by E. Granéli and J. Turner. Vol. 189. Ecological Studies Series. Springer-Verlag Heidelberg, 391-401. DOI: [10.1007/978-3-540-32210-8\\_30](https://doi.org/10.1007/978-3-540-32210-8_30).
- Hodgkiss (2001). The N:P ratio revisited. In: *Prevention and Management of Harmful Algal Blooms in the South China Sea*. Ed. by K. C. Ho and Z. D. Wang. School of Science and Technology, The Open University of Hong Kong, China.
- Hodgkiss, I. and K. Ho (1997). Are changes in N:P ratios in coastal waters the key to increased red tide blooms? *Hydrobiol.* 352: 141-147.
- Howarth, R. (2008). Coastal nitrogen pollution: A review of sources and trends globally and regionally. *Harmful Algae* 8: 14-20.
- Howarth, R., A. Sharpley, and D. Walker (2002). Sources of nutrient pollution to coastal waters in the United States: Implications for achieving coastal water quality goals. *Estuaries* 25: 656-676.
- Hu, C. (2009). A novel ocean color index to detect floating algae in the global oceans. *Remote Sens. Environ.* 113: 2118-2129.
- Hu, C., B. Barnes, L. Qi, and A. Corcoran (2015). A harmful algal bloom of *Karenia brevis* in the northeastern Gulf of Mexico as revealed by MODIS and VIIRS: A comparison. *Sensors* 15: 2873-2887. DOI: [10.3390/s150202873](https://doi.org/10.3390/s150202873).
- Hu, C., J. Cannizzaro, K. Carder, Z. Lee, F. Muller-Karger, and I. Soto (2011). Red tide detection in the eastern Gulf of Mexico using MODIS imagery. In: *Handbook of satellite remote sensing image interpretation: applications for marine living resources conservation and management*. Ed. by J. Morales, V. Stuart, T. Platt, and S. Sathyendranath. EU PRESPO and IOCCG, Dartmouth, Canada.
- Hu, C., Z. Lee, R. Ma, K. Yu, D. Li, and S. Shang (2010). Moderate Resolution Imaging Spectroradiometer (MODIS) observations of cyanobacteria blooms in Taihu Lake, China. *J. Geophys. Res.* 115: C04002.
- Hu, C., F. Muller-Karger, and P. Swarzenski (2006). Hurricanes, submarine groundwater discharge, and Florida's red tides. *Geophys. Res. Lett.* 33:11, L11601.
- Hu, C., F. Muller-Karger, C. Taylor, K. Carder, C. Kelble, E. Johns, and C. Heil (2005). Red tide detection and tracing using MODIS fluorescence data: a regional example in SW Florida coastal waters. *Remote Sens. Environ.* 97:3, 311-321.
- Hu, C., L. Feng, Z. Lee, C. O. Davis, A. Mannino, C. R. McClain, and B. A. Franz (2012). Dynamic range and sensitivity requirements of satellite ocean color sensors: Learning from the past. *Appl. Optics* 51:25, 6045-6062.
- Hunter, P. D., A. N. Tyler, L. Carvalho, G. A. Codd, and S. C. Maberly (2010). Hyperspectral remote sensing of cyanobacterial pigments as indicators for cell populations and toxins in eutrophic lakes. *Remote Sens. Environ.* 114:11, 2705-2718.
- Hunter, P. D., A. N. Tyler, D. J. Gilvear, and N. J. Willby (2009). Using remote sensing to aid the assessment of human health risks from blooms of potentially toxic cyanobacteria. *Environ. Sci. Technol.* 43:7, 2627-2633.
- Hunter, P. D., A. N. Tyler, M. Présing, A. W. Kovács, and T. Preston (2008). Spectral discrimination of phytoplankton colour groups: The effect of suspended particulate matter and sensor spectral resolution. *Remote Sens. Environ.* 112:4, 1527-1544.
- Ingle, R. and D. Martin (1971). Prediction of the Florida red tide by means of the iron index. *Environ. Lett.* 1:1, 69-74.
- IOCCG (2014). *Phytoplankton Functional Types from Space*. Ed. by S. Sathyendranath. Vol. No. 15. Reports of the International Ocean Colour Coordinating Group. Dartmouth, Canada: IOCCG.
- Irigoin, X., K. Flynn, and R. Harris (2005). Phytoplankton blooms: A 'loophole' in microzooplankton grazing impact? *J. Plankton Res.* 27: 313-321.
- Jeong, H., Y. Yoo, J. Kim, K. Seong, N. Kang, and T. Kim (2010). Growth, feeding and ecological roles of the mixotrophic and heterotrophic dinoflagellates in marine planktonic food webs. *Ocean. Sci. J.* 45: 65-91.

- Jeong, H. et al. (2005). Feeding by the phototrophic red-tide dinoflagellates: five species newly revealed and six species previously known to be mixotrophic. *Aquat. Microb. Ecol.* 40: 133-155.
- Johansson, N. and E. Granéli (1999a). Cell density, chemical composition and toxicity of *Chrysochromulina polylepis* (Haptophyta) in relation to different N:P supply ratios. *Mar. Biol.* 135: 209-217.
- (1999b). Influence of different nutrient conditions on cell density, chemical composition and toxicity of *Prymnesium parvum* (Haptophyta) in semi-continuous cultures. *J. Exp. Mar. Biol. Ecol.* 239: 243-258.
- Johnsen, G., M. Moline, L. Pettersson, J. Pinckney, D. Pozdnyakov, E. Egeland, and O. Schofield (2011). Optical monitoring of phytoplankton bloom pigment signatures. In: *Phytoplankton Pigments: Characterization, Chemotaxonomy and Applications in Oceanography*. Ed. by S. Roy, C. Llewellyn, E. Egeland, and G. Johnsen. Cambridge University Press.
- Johnson, P. et al. (2010). Linking environmental nutrient enrichment and disease emergence in humans and wildlife. *Ecol. Appl.* 20: 16-29.
- Jupp, D. L. B., J. T. O. Kirk, and G. P. Harris (1994). Detection, identification and mapping of cyanobacteria - Using remote-sensing to measure the optical-quality of turbid inland waters. *Aust. J. Mar. Fresh. Res.* 45:5, 801-828.
- Kahru, M., J. Leppanen, and O. Rud (1993). Cyanobacterial blooms cause heating of the sea surface. *Mar. Ecol. Prog. Ser.* 101: 1-7.
- Kamykowski, D. and H. Yamazaki (1997). A study of metabolism-influence orientation in the diel vertical migration of marine dinoflagellates. *Limnol. Oceanogr.* 42: 1189-1202.
- Kaňa, R., E. Kotabová, O. Komárek, B. Šedivá, G. C. Papageorgiou, Govindjee, and O. Prášil (2012). The slow S to M fluorescence rise in cyanobacteria is due to a state 2 to state 1 transition. *Biochimica et Biophysica Acta (BBA) - Bioenergetics* 1817:8, 1237-1247.
- Kana, T., P. Glibert, R. Goericke, and N. Welschmeyer (1988). Zeaxanthin and  $\beta$ -carotene in *Synechococcus* WH7803 respond differently to irradiance. *Limnol. Oceanogr.* 33: 1623-1627.
- Kirkpatrick, B. et al. (2004). Literature review of Florida red tide: implications for human health effects. *Harmful Algae* 3:2, 99-115.
- Kirkpatrick, B. et al. (2010). Inland transport of aerosolized Florida red tide toxins. *Harmful Algae* 9:2, 186-189.
- Kirkpatrick, B. et al. (2011). Aerosolized red tide toxins (brevetoxins) and asthma: continued health effects after 1 hour beach exposure. *Harmful Algae* 10:2, 138-143.
- Kirkpatrick, G., D. Millie, M. Moline, and O. Schofield (2000). Optical discrimination of a phytoplankton species in natural mixed populations. *Limnol. Oceanogr.* 45:2, 467-471.
- Klausmeier, C., E. Litchman, T. Daufresne, and S. Levin (2004). Optimal nitrogen-to-phosphorus stoichiometry of phytoplankton. *Nature* 429: 171-174.
- Kong, F., W. Hu, X. Gu, G. Yang, C. Fan, and K. Chen (2007). On the cause of cyanophyta bloom and pollution in water intake area and emergency measures in Meiliang Bay, Lake Taihu in 2007. *J. Lake Sci.* 19: 357-358.
- Kotchenova, S. Y., E. F. Vermote, R. Matarrese, and F. J. Klemm Jr (2006). Validation of a vector version of the 6S radiative transfer code for atmospheric correction of satellite data. Part I: Path radiance. *Appl. Opt.* 45: 6762-6774.
- Kurekin, A., P. Miller, and H. V. der Woerd (2014). Satellite discrimination of *Karenia mikimotoi* and *Phaeocystis* harmful algal blooms in European coastal waters: Merged classification of ocean colour data. *Harmful Algae* 31: 163-176.
- Kutser, T. (2004). Quantitative detection of chlorophyll in cyanobacterial blooms by satellite remote sensing. *Limnol. Oceanogr.* 49:6, 2179-2189.
- (2009). Passive optical remote sensing of cyanobacteria and other intense phytoplankton blooms in coastal and inland waters. *Int. J. Remote Sens.* 30:17, 4401-4425.
- Kutser, T., L. Metsamaa, N. Strombeck, and E. Vahtmae (2006). Monitoring cyanobacterial blooms by satellite remote sensing. *Estuar. Coast. Shelf Sci.* 67:1-2, 303-312.
- Lackey, J. (1956). Known geographic range of *Gymnodinium breve* Davis. *Q. J. Fl. Acad. Sci.* 17: 71.
- Lai, G., G. Yu, and F. Gui (2006). Preliminary study on assessment of nutrient transport in the Taihu Basin based on SWAT modeling. *Science in China Series D* 49:1, 135-145.
- Lampert, W. (1987). Laboratory studies on zooplankton-cyanobacteria interactions. *N.Z. J. Mar. Freshwater Res.* 21:3, 483-490.
- Landsberg, J. (2002). The effects of harmful algal blooms on aquatic organisms. *Rev. in Fish. Sci.* 10: 1-113.
- Landsberg, J., L. Flewelling, and J. Naar (2009). *Karenia brevis* red tides, brevetoxins in the food web, and impacts on natural resources: Decadal advancements. *Harmful Algae* 8:4, 598-607.

- LaRoche, J., R. Nuzzi, K. Waters, K. Wyman, P. G. Falkowski, and D. Wallace (1997). Brown tide blooms in Long Island's coastal waters linked to variability in groundwater flow. *Glob. Change Biol.* 3: 397-410.
- Le, C., Y. Li, Y. Zha, Q. Wang, H. Zhang, and B. Yin (2011). Remote sensing of phycocyanin pigment in highly turbid inland waters in Lake Taihu, China. *Int. J. Remote Sens.* 32:23, 8253-8269.
- Lee, Z., K. Carder, and R. Arnone (2002). Deriving inherent optical properties from water color: a multiband quasi-analytical algorithm for optically deep waters. *Appl. Opt.* 41:27, 5755-5772.
- Lenes, J. et al. (2001). Iron fertilization and the *Trichodesmium* response on the West Florida Shelf. *Limnol. Oceanogr.* 46: 1261-1277.
- Leppänen, J.-M., E. Rantajärvi, S. Hällfors, M. Kruskopf, and V. Laine (1995). Unattended monitoring of potentially toxic phytoplankton species in the Baltic Sea in 1993. *J. Plank. Res.* 17:4, 891-902.
- Letelier, R. and M. Abbott (1996). An analysis of chlorophyll fluorescence algorithms for the moderate resolution imaging spectrometer (MODIS). *Remote Sens. Environ.* 58:2, 215-223.
- Li, J., P. M. Glibert, and Y. Gao (2015). Temporal and spatial changes in Chesapeake Bay water quality and relationships to *Prorocentrum minimum*, *Karlodinium veneficum*, and CyanoHAB events, 1991-2008. *Harmful Algae* 42: 1-14.
- Li, J., P. Glibert, P.M., and M. Zhou (2010a). Temporal and spatial variability in nitrogen uptake kinetics during harmful dinoflagellate blooms in the East China Sea. *Harmful Algae* 9: 531-539.
- Li, J., P. Glibert, M. Zhou, S. Lu, and D. Lu. (2009). Relationships between nitrogen and phosphorus forms and ratios and the development of dinoflagellate blooms in the East China Sea. *Mar. Ecol. Prog. Ser.* 383: 11-26.
- Li, L., R. Sengpiel, D. Pascual, L. Tedesco, J. Wilson, and E. Soyeux (2010b). Using hyperspectral remote sensing to estimate chlorophyll-a and phycocyanin in a mesotrophic reservoir. *Int. J. Remote Sens.* 31:15, 4147-4162.
- Lomas, M. W. and P. M. Glibert (1999). Temperature regulation of NO<sub>3</sub> uptake: A novel hypothesis about NO<sub>3</sub> uptake and cool-water diatoms. *Limnol. Oceanogr.* 44: 556-572.
- Lou, X., W. Huang, X. Mao, A. Shi, H. Zhang, and P. Chen (2006). Satellite observation of a red tide in the East China Sea during 2005. *Proc. SPIE: Remote Sensing of the Marine Environment* 6404: DOI: [10.1117/12.693856](https://doi.org/10.1117/12.693856).
- Lu, D. and J. Gobel (2001). Five red tide species in genus *Prorocentrum* including the description of *Prorocentrum donghaiense* Lu sp. nov. from the East China Sea, China. *Chinese J. Oceanol. Limnol.* 19: 337-344.
- Lucentini, L. and M. Ottaviani (2011). *Cianobatteri in acque destinate a consumo umano. Linee guida per la gestione del rischio*. Tech. rep. Istituto Superiore di Sanità.
- Ma, R., H. Duan, X. Gu, and S. Zhang (2008). Detecting aquatic vegetation changes in Taihu Lake, China using multi-temporal satellite imagery. *Sensors* 8: 3988-4005.
- Magaña, H., C. Contreras, and T. Villareal (2003). A historical assessment of *Karenia brevis* in the western Gulf of Mexico. *Harmful Algae* 2:3, 163-171.
- Maier Brown, A. et al. (2006). Effect of salinity on the distribution, growth, and toxicity of *Karenia* spp. *Harmful Algae* 5:2, 199-212.
- Margalef, R. (1978). Life-forms of phytoplankton as survival alternatives in an unstable environment. *Oceanol. Acta.* 1: 493-509.
- Martin, D., M. Doig, and R. Pierce (1971). *Distribution of naturally occurring chelators (humic acids) and selected trace metals in some west coast Florida streams, 1968-1969*. Prof. Paper Series 12, Florida. Department of Natural Resources.
- Matthews, M. W. and S. Bernard (2013). Using a two-layered sphere model to investigate the impact of gas vacuoles on the inherent optical properties of *Microcystis aeruginosa*. *Biogeosciences* 10:1, 8139-8157.
- Matthews, M. W., S. Bernard, and K. Winter (2010). Remote sensing of cyanobacteria-dominant algal blooms and water quality parameters in Zeekoevlei, a small hypertrophic lake, using MERIS. *Remote Sens. Environ.* 114:9, 2070-2087.
- Matthews, M. W., S. Bernard, and L. Robertson (2012). An algorithm for detecting trophic status (chlorophyll-a), cyanobacterial-dominance, surface scums and floating vegetation in inland and coastal waters. *Remote Sens. Environ.* 124: 637-652.
- McLeod, D., G. Hallegraeff, G. Hosie, and A. Richardson (2012). Climate-driven range expansion of the red-tide dinoflagellate *Noctiluca scintillans* into the Southern Ocean. *J. Plankton Res.* 34: 332-337.
- Merino-Virgilio, F. d. C., J. Herrera-Silveira, Y. Okolodkov, and K. Steidinger (2012). *Karenia* blooms in Gulf of Mexico. *Harmful Algae News* 46: 8.
- Mier, J., T. Suárez, V. Georgana, H. Mayor-Nucamendi, and J. Brito-López (2006). Florecimientos algales en Tabasco. *Salud en Tabasco* 12:1, 414-422.

- Miller, P., J. Shutler, G. Moore, and S. Groom (2006). SeaWiFS discrimination of harmful algal bloom evolution. *Int. J. Remote Sens.* 27: 2287-2301.
- Millie, D. F., G. J. Kirkpatrick, and B. T. Vinyard (1995). Relating photosynthetic pigments and *in vivo* optical density spectra to irradiance for the Florida red-tide dinoflagellate *Gymnodinium breve*. *Mar. Ecol. Prog. Series* 120: 65-75.
- Millie, D., O. Schofield, G. Kirkpatrick, G. Johnsen, P. Tester, and B. Vinyard (1997). Detection of harmful algal blooms using photopigments and absorption signatures: a case study of the Florida red tide dinoflagellate, *Gymnodinium breve*. *Limnol. Oceanogr.* 42:5, 1240-1251.
- Mishra, S., D. R. Mishra, Z. Lee, and C. S. Tucker (2013). Quantifying cyanobacterial phycocyanin concentration in turbid productive waters: A quasi-analytical approach. *Remote Sens. Environ.* 133: 141-151.
- Mitra, A. and K. Flynn (2006). Promotion of harmful algal blooms by zooplankton predatory activity. *Biol. Lett.* 2: 194-197.
- Moestrup, Ø. (1994). Economic aspects: 'blooms', nuisance species and toxins. In: *The Haptophyte Algae*. Ed. by J. Green and B. Leadbeater. Clarendon Press, 265-285.
- Moore, C. (2006). *Fear of red tides remains*. Saint Petersburg Times.
- Morel, A. (1988). Optical modeling of the upper ocean in relation to its biogenous matter content (Case I waters). *J. Geophys. Res.* 93:C9, 10749-10768.
- Mulholland, M., P. Bernhardt, C. Heil, D. Bronk, A. Deborah, and J. O'Neil (2006). Nitrogen fixation and release of fixed nitrogen by *Trichodesmium* spp. in the Gulf of Mexico. *Limnol. Oceanogr.* 51:4, 1762-1776.
- Mulholland, M., C. Heil, D. Bronk, J. O'Neil, and P. Bernhardt (2004). Does nitrogen regeneration from the N<sub>2</sub> fixing cyanobacteria *Trichodesmium* spp. fuel *Karenia brevis* blooms in the Gulf of Mexico? In: *Harmful Algae 2002*. Ed. by K. Steidinger, J. Landsberg, C. Tomas, and G. Vargo. Florida Fish, Wildlife Conservation Commission, Florida Institute of Oceanography, and Intergovernmental Oceanographic Commission of UNESCO, 47-49.
- Natali, M. (1993). *The fish fauna of the Trasimeno Lake*. Tech. rep. Provincia di Perugia.
- Niemi, Å. (1973). *Ecology of phytoplankton in the Tvärminne area, SW coast of Finland I. Dynamics of hydrography, nutrients, chlorophyll a and phytoplankton*. Societas pro fauna et flora Fennica.
- Ning, X., C. Lin, Q. Hao, C. Liu, F. Le, and J. Shi (2009). Long term changes in the ecosystem in the Northern South China Sea during 1976-2004. *Biogeosciences* 6: 2227-2243.
- Odum, H., J. Lackey, J. Hynes, and N. Marshall (1955). Some red tide characteristics during 1952-1954. *Bull. Mar. Sci.* 5:4, 247-258.
- Okaichi, T. (2004). Red tide phenomena. In: *Red Tides*. Ed. by T. Okaichi. TERRAPUB, Kluwer, 7-60.
- Olenina, I. et al. (2010). Assessing impacts of invasive phytoplankton: The Baltic Sea case. *Mar. Pollut. Bull.* 60: 1691-1700.
- O'Reilly, J. et al. (2000). Ocean color chlorophyll-a algorithms for SeaWiFS, OC2 and OC4. In: *SeaWiFS Postlaunch Calibration and Validation Analyses*. Ed. by S. Hooker and E. Firestone. Vol. 11. Part 3. SeaWiFS Postlaunch Technical Report Series 4. NASA Goddard Space Flight Center, Greenbelt, Maryland, 9-23.
- O'Shea, T., G. Rathbun, R. Bonde, C. Buergelt, and D. Odell (1991). An epizootic of Florida manatees associated with a dinoflagellate bloom. *Mar. Mammal Sci.* 7:2, 165-179.
- Paerl, H. W. (1988). Nuisance phytoplankton blooms in coastal, estuarine, and inland waters. *Limnol. Oceanogr.* 33: 823-847.
- (2009). Controlling eutrophication along the freshwater-marine continuum: dual nutrient (N and P) reductions are essential. *Estuar. Coast.* 32: 593-601.
- Pahlevan, N., Z. Lee, J. Wei, C. B. Schaaf, J. R. Schott, and A. Berk (2014). On-orbit radiometric characterization of OLI (Landsat-8) for applications in aquatic remote sensing. *Remote Sens. Environ.* 154: 272-284.
- Papageorgiou, G. C., M. Tsimilli-Michael, and K. Stamatakis (2007). The fast and slow kinetics of chlorophyll-a fluorescence induction in plants, algae and cyanobacteria: a viewpoint. *Photosynth. Res.* 94:2-3, 275-290.
- Pederson, B. A., G. J. Kirkpatrick, A. J. Haywood, B. A. Berg, and C. J. Higham (2004). Differentiating two Florida harmful algal bloom species using HPLC pigment characterization. In: *Harmful Algae 2002*. Ed. by K. Steidinger, J. Landsberg, C. Tomas, and G. Vargo. Florida Fish, Wildlife Conservation Commission, Florida Institute of Oceanography, and Intergovernmental Oceanographic Commission of UNESCO, 449-451.
- Proctor, N., S. Chan, and A. Trevor (1975). Production of saxitoxin by cultures of *Gonyaulax catenella*. *Toxicon* 13: 1-9.
- Qin, B., G. Zhu, G. Gao, Y. Zhang, W. Li, H. W. Paerl, and W. W. Carmichael (2010). A drinking water crisis in Lake Taihu, China: linkage to climatic variability and lake management. *Environ. Manage.* 45:1, 105-112.

- Randolph, K., J. Wilson, L. Tedesco, L. Li, D. L. Pascual, and E. Soyeux (2008). Hyperspectral remote sensing of cyanobacteria in turbid productive water using optically active pigments, chlorophyll-a and phycocyanin. *Remote Sens. Environ.* 112:11, 4009–4019.
- Rantajarvi, E., R. Olsonen, S. Hällfors, J. Leppänen, and M. Raateoja (1998). Effect of sampling frequency on detection of natural variability in phytoplankton: unattended high-frequency measurements on board ferries in the Baltic Sea. *ICES J. Mar. Sci.* 55: 697–704.
- Redfield, A. (1934). On the proportions of organic derivations in sea water and their relation to the composition of plankton. In: *James Johnstone Memorial Volume*. Ed. by R. Daniel. University Press of Liverpool, 177–192.
- Reñé, A., J. Camp, and E. Garcés (2015). Diversity and phylogeny of Gymnodiniales (Dinophyceae) from the NW Mediterranean Sea revealed by a morphological and molecular approach. *Protist* 166: 234–263.
- Reynolds, C. (1999). Non-determinism to probability, or N:P in the community ecology of phytoplankton. *Arch. Hydrobiol.* 146: 23–35.
- Rhodes, L., A. Haywood, J. Adamson, K. Ponikla, and C. Scholin (2004). DNA probes for the rapid detection of *Karenia* species in New Zealand's coastal waters. In: *Harmful Algae 2002*. Ed. by K. Steidinger, J. Landsberg, C. Tomas, and G. Vargo. Florida Fish, Wildlife Conservation Commission, Florida Institute of Oceanography, and Intergovernmental Oceanographic Commission of UNESCO, 273–275.
- Richardson, T., J. Pinckney, E. Walker, and D. Marshalonis (2006). Photopigment radiolabelling as a tool for determining *in situ* growth rates of the toxic dinoflagellate *Karenia brevis* (Dinophyceae). *Eur. J. Phycol.* 41:4, 415–423.
- Ruiz-Verdú, A., S. G. H. H. Simis, S. dSimis, H. J. Gons, and R. Peña-Martínez (2008). An evaluation of algorithms for the remote sensing of cyanobacterial biomass. *Remote Sens. Environ.* 112:11, 3996–4008.
- Sapp, J. (2005). The prokaryote-eukaryote dichotomy: meanings and mythology. *Microbiol. Mol. Biol. Rev.* 69:2, 292–305.
- Sarada, R., M. G. Pillai, and G. A. Ravishankar (1999). Phycocyanin from *Spirulina* sp: influence of processing of biomass on phycocyanin yield, analysis of efficacy of extraction methods and stability studies on phycocyanin. *Process Biochem.* 34:8, 795–801.
- Satake, M., Y. Tanaka, Y. Ishikura, Y. Oshima, H. Naoki, and T. Yasumoto (2005). Gymnocin-B with the largest contiguous polyether rings from the red tide dinoflagellate, *Karenia* (formally *Gymnodinium*) *mikimotoi*. *Tetrahedron Lett.* 46: 3537–3540.
- Schalles, J. F. and Y. Z. Yacobi (2000). Remote detection and seasonal patterns of phycocyanin, carotenoid and chlorophyll pigments in eutrophic waters. *Arch. Hydrobiol.* 55: Special Issue: Advances in Limnology, 153–168.
- Schindler, D. W. et al. (2008). Eutrophication of lakes cannot be controlled by reducing nitrogen input: Results of a 37-year whole-ecosystem experiment. *Proc. Nat. Acad. Sci. U.S.A.* 105: 11254–11258.
- Schofield, O., J. Kerfoot, K. Mahoney, M. Moline, M. Oliver, S. Lohrenz, and G. Kirkpatrick (2006). Vertical migration of the toxic dinoflagellate *Karenia brevis* and the impact on ocean optical properties. *J. Geophys. Res.* 111:C6, C06009.
- Seitzinger, S., J. Harrison, E. Dumont, A. Beusen, and A. Bouwman (2005). Sources and delivery of carbon, nitrogen and phosphorous to the coastal zone: An overview of global nutrient export from watersheds (NEWS) models and their application. *Global Biogeochem. Cy.* 19: GB4S09.
- Seppälä, J., P. Ylöstalo, S. Kaitala, S. Hällfors, M. Raateoja, and P. Maunula (2007). Ship-of-opportunity based phycocyanin fluorescence monitoring of the filamentous cyanobacteria bloom dynamics in the Baltic Sea. *Estuar. Coast. Shelf Sci.* 73:3-4, 489–500.
- Shanley, E. and G. Vargo (1993). Cellular composition, growth, photosynthesis, and respiration rates of *Gymnodinium brevis* under varying light levels. In: *Toxic phytoplankton blooms in the Sea*. Ed. by T. Smayda and Y. Shimizu. Elsevier, Amsterdam, 831–836.
- Shen, Z.-L. and Q. Liu (2009). Nutrients in the Changjiang River. *Environ. Monit. Assess.* 153: 27–44.
- Shimizu, Y., N. Watanabe, and G. Wrensford (1995). Biosynthesis of brevetoxins and heterotrophic metabolism in *Gymnodinium breve*. In: *Harmful Algal Blooms*. Ed. by P. Lassus, G. Arzul, E. Erard, P. Gentien, and C. Marcaillour. Lavoisier Paris, 351–357.
- Shimizu, Y. and G. Wrensford (1993). Peculiarities in the biosynthesis of brevetoxins and metabolism of *Gymnodinium breve*. In: *Toxic phytoplankton blooms in the Sea*. Ed. by T. Smayda and Y. Shimizu. Elsevier, Amsterdam, 919–923.
- Shutler, J., P. Miller, S. Groom, and J. Aiken (2005). *Automatic near-real time mapping of MERIS data in support of CASIX and as input to a phytoplankton classifier*. Proc. of the ESA MERIS (A)ATSR Workshop 2005.

- Sierra-Beltran, A., R. Cortes-Altamirano, and M. Cortes-Lara (2005). Occurrences of *Prorocentrum minimum* (Pavillard) in Mexico. *Harmful Algae* 4: 507–518.
- Simis, S. and H. Kauko (2012). *In vivo* mass-specific absorption spectra of phycobilipigments through selective bleaching. *Limnol. Oceanogr.: Methods* 10: 214–226.
- Simis, S., S. Peters, and H. J. Gons (2005). Remote sensing of the cyanobacterial pigment phycocyanin in turbid inland water. *Limnol. Oceanogr.* 50:1, 237–245.
- Simis, S. G. H., A. Ruiz-Verdú, J. A. Domínguez-Gómez, R. Peña-Martínez, S. W. M. Peters, and H. J. Gons (2007). Influence of phytoplankton pigment composition on remote sensing of cyanobacterial biomass. *Remote Sens. Environ.* 106:4, 414–427.
- Sinclair, G., D. Kamykowski, and P. Glibert (2009). Growth, uptake, and assimilation of ammonium, nitrate, and urea, by three strains of *Karenia brevis* grown under low light. *Harmful Algae* 8:5, 770–780.
- Singer, L. (1998). Inhaled Florida red tide toxins induce bronchoconstriction (BC) and airway hyperresponsiveness (AHR) in sheep. *Am. J. Resp. Crit. Care* 157:3, A158.
- Siswanto, E., J. Ishizaka, S. Tripathy, and K. Miymura (2013). Detection of harmful algal blooms of *Karenia mikimotoi* using MODIS measurements: a case study of Seto-Inland Sea, Japan. *Remote Sens. Environ.* 129: 185–196.
- Smayda, T. (1990). Novel and nuisance phytoplankton blooms in the sea: Evidence for a global epidemic. In: *Toxic Marine Phytoplankton*. Ed. by E. Granéli, B. Sundstrom, L. Edler, and D. M. Anderson. Elsevier, 29–40.
- Smayda, T. and C. Reynolds (2001). Community assembly in marine phytoplankton: application of recent models to harmful dinoflagellate blooms. *J. Plankton Res.* 23: 447–461.
- Smil, V. (2001). *Enriching the Earth: Fritz Haber, Carl Bosch, and the Transformation of World Food*. The MIT Press, Cambridge, United Kingdom.
- Soto, I. (2013). Harmful Algal Blooms of the West Florida Shelf and Campeche Bank: Visualization and Quantification using Remote Sensing Methods. PhD thesis. University of South Florida.
- Soto, I., J. Cannizzaro, F. Muller-Karger, C. Hu, J. Wolny, and D. Goldgof (2015). Evaluation and optimization of remote sensing techniques for detection of *Karenia brevis* blooms on the West Florida Shelf. *Remote Sens. Environ.* 170C: 239–254. DOI: [10.1016/j.rse.2015.09.026](https://doi.org/10.1016/j.rse.2015.09.026).
- Soto, I. et al. (2012). Binational collaboration to study Gulf of Mexico's harmful algae. *EOS Trans AGU* 93:5, 1–2.
- Steidinger, K. (1975). Basic factors influencing red tides. In: *Proceedings of the 1st International Conference on Toxic Dinoflagellate Blooms*. Ed. by V. LoCicero. Massachusetts Science and Technology Foundation, Boston, 153–162.
- (1979). Quantitative ultrastructural variation between culture and field specimens of the dinoflagellate *Ptychodiscus brevis*. PhD thesis. University of South Florida.
- (2009). Historical perspective on *Karenia brevis* red tide research in the Gulf of Mexico. *Harmful Algae* 8:4, 549–561.
- Steidinger, K. and K. Haddad (1981). Biologic and hydrographic aspects of red tides. *BioScience* 31:11, 814–819.
- Steidinger, K., G. Vargo, P. Tester, and C. Tomas (1998). Bloom dynamics and physiology of *Gymnodinium breve*, with emphasis on the Gulf of Mexico. In: *Physiological Ecology of Harmful Algal Blooms*. Ed. by E. Anderson and G. Hallegraff. Springer, New York, 135–153.
- Steidinger, K., J. Wolny, and A. Haywood (2008). Identification of *Kareniaceae* (Dinophyceae) in the Gulf of Mexico. *Nova Hedwigia* 133: 269–284.
- Sterner, R. and J. Elser (2002). *Ecological stoichiometry: The biology of elements from molecules to the biosphere*. Princeton University Press.
- Stibor, H. and U. Sommer (2003). Mixotrophy of a photosynthetic flagellate viewed from an optimal foraging perspective. *Protist* 15: 91–98.
- Stoecker, D., U. U. Tillmann, and E. Granéli (2006). Phagotrophy in harmful algae. In: *Ecology of Harmful Algae*. Ed. by E. Granéli and J. Turner. Springer-Verlag, 177–187.
- Stumpf, R., R. Litaker, L. Lanerolle, and P. Tester (2008). Hydrodynamic accumulation of *Karenia* off the west coast of Florida. *Cont. Shelf Res.* 28:1, 189–213.
- Stumpf, R. et al. (2003). Monitoring *Karenia brevis* blooms in the Gulf of Mexico using satellite ocean color imagery and other data. *Harmful Algae* 2:3, 147–160.
- Sun, D., C. Hu, Z. Qiu, and K. Shi (2015). Estimating phycocyanin pigment concentration in productive inland waters using Landsat measurements: A case study in Lake Dianchi. *Opt. Express* 23:3, 3055–3074.
- Sun, D., Y. Li, Q. Wang, J. Gao, C. Le, C. Huang, and S. Gong (2013). Hyperspectral Remote Sensing of the Pigment C-Phycocyanin in Turbid Inland Waters, Based on Optical Classification. *IEEE T. Geosci. Remote Sens.* 51:7-1, 3871–3884.

- Sun, J., D. Hutchins, Y. Feng, E. Seubert, D. Caron, and F. Fu (2011). Effects of changing pCO<sub>2</sub> and phosphate availability on domoic acid production and physiology of the marine harmful bloom diatom *Pseudo-nitzschia multiseries*. *Limnol. Oceanogr.* 56: 829–840.
- Sutton, M., A. Bleeker, C. Howard, M. Bekunda, B. Grizzetti, W. de Vries, and H. van Grinsven (2013). *Our Nutrient World: The Challenge to Produce more Food and Energy with Less Pollution*. Global Overview of Nutrient Management. Centre for Ecology, Hydrology, Edinburgh on behalf of the Global Partnership on Nutrient Management, and the International Nitrogen Initiative.
- Tamulonis, C., M. Postma, and J. Kaandorp (2011). Modeling filamentous cyanobacteria reveals the advantages of long and fast trichomes for optimizing light exposure. *PLoS One* 6:7.
- Tandeau de Marsac, N. and J. Houmard (1988). Complementary chromatic adaptation: physiological conditions and action spectra. *Methods Enzymol.* 167: 318–328.
- Tang, T., J. Tai, and Y. Yang (2000). The flow pattern north of Taiwan and the migration of the Kuroshio. *Cont. Shelf Res.* 20: 349–371.
- Tatters, A., F. Fu, and D. Hutchins (2012). A CO<sub>2</sub> and silicate synergism determined the toxicity of the harmful blooms diatoms *Pseudo-nitzschia fraudulenta*. *PLoS ONE* 7: e32116.
- Tester, P. and R. Stumpf (1998). Phytoplankton blooms and remote sensing: what is the potential for early warning. *J. Shellfish Res.* 17:5, 1469–1471.
- Tester, P., R. Stumpf, and K. Steidinger (1998). Ocean color imagery: What is the minimum detection level for *Gymnodinium breve* blooms? In: *Harmful Algae*. Ed. by B. Reguera, J. Blanco, M. Fernandez, and T. Wyatt. Xunta de Galicia and Intergovernmental Oceanographic Commission of UNESCO.
- Tester, P., R. Stumpf, F. Vukovich, P. Fowler, and T. Jefferson (1991). An expatriate red tide bloom: transport, distribution, and persistence. *Limnol. Oceanogr.* 36:5, 1053–1061.
- Ti, C. . X. Y. (2013). Spatial and temporal variations of river nitrogen exports from major basins in China. *Environ. Sci. Pollut. Res.* 20: 6509–6520.
- Tomlinson, M., T. Wynne, and R. Stumpf (2009). An evaluation of remote sensing techniques for enhanced detection of the toxic dinoflagellate, *Karenia brevis*. *Rem. Sens. Environ.* 113:3, 598–609.
- Tomlinson, M. et al. (2004). Evaluation of the use of SeaWiFS imagery for detecting *Karenia brevis* harmful algal blooms in the eastern Gulf of Mexico. *Rem. Sens. Environ.* 91:3-4, 293–303.
- Torbick, N., S. Hession, E. Stommel, and T. Caller (2014). Mapping amyotrophic lateral sclerosis lake risk factors across northern New England. *Int. J. Health Geogr.* 13:1, 1.
- Van Dolah, F., G. Doucette, F. Gulland, T. Rowles, and G. Bossart (2003). Impacts of algal toxins on marine mammals. In: *Toxicology of Marine Mammals*. Ed. by J. Vos, M. Fournier, and T. O'Shea. Taylor and Francis, London, 247–270.
- Vargo, G. (2009). A brief summary of the physiology and ecology of *Karenia brevis* Davis (G. Hansen and Moestrup comb. nov.) red tides on the West Florida Shelf and of hypotheses posed for their initiation, growth, maintenance, and termination. *Harmful Algae* 8:4, 573–584.
- Vargo, G. and D. Howard-Shamblott (1990). Phosphorus requirements in *Ptychodiscus brevis*: Cell phosphorus, uptake and growth requirements. In: *Toxic Marine Phytoplankton*. Ed. by E. Graneli, B. Sundstrom, L. Edler, and D. Anderson. Elsevier, Amsterdam, 324–329.
- Vargo, G. and E. Shanley (1985). Alkaline phosphatase activity in the red-tide dinoflagellate, *Ptychodiscus brevis*. *Mar. Ecol.* 6:3, 251–264.
- Vargo, G. et al. (2008). Nutrient availability in support of *Karenia brevis* blooms on the central West Florida Shelf: What keeps *Karenia* blooming? *Cont. Shelf Res.* 28:1, 73–98.
- Vermote, E. F., D. Tanré, J. L. Deuzé, M. Herman, and J.-J. Morcette (1997). Second simulation of the satellite signal in the solar spectrum, 6S: An overview. *IEEE T. Geosci. Remote* 35:3, 675–686.
- Vincent, R. K., X. M. Qin, R. M. L. McKay, J. Miner, K. Czajkowski, J. Savino, and T. Bridgeman (2004). Phycocyanin detection from LANDSAT TM data for mapping cyanobacterial blooms in Lake Erie. *Remote Sens. Environ.* 89:3, 381–392.
- Visser, P. M., B. W. Ibelings, L. Mur, and A. E. Walsby (2005). The ecophysiology of the harmful cyanobacterium *Microcystis*. In: *Harmful cyanobacteria*. Ed. by J. Huisman, H. C. P. Matthijs, and P. M. Visser. Springer, 177–199.
- Walsby, A. (1994). Gas vesicles. *Microbiol. Rev.* 58:1, 94.
- Walsh, J. and K. Steidinger (2001). Saharan dust and Florida red tides: the cyanophyte connection. *J. Geophys. Res.* 106:C6, 11597–11612.

- Walsh, J. et al. (2006). Red tides in the Gulf of Mexico: Where, when and why? *J. Geophys. Res.* 111:C11003. DOI: [10.1029/2004JC002813](https://doi.org/10.1029/2004JC002813).
- Walsh, J. et al. (2009). Isotopic evidence for dead fish maintenance of Florida red tides, with implications for coastal fisheries over both source regions of the West Florida shelf and within downstream waters of the South Atlantic Bight. *Prog. Oceanogr.* 80: 51-73.
- Wang, B., L. Xie, and X. Sun (2011). Water quality and marginal seas off China in the last two decades. *Int. J. Oceanogr.* 731828.
- Wang, J. and J. Wu (2009). Occurrence and potential risks of harmful algal blooms in the East China Sea. *Sci. Total Environ.* 407: 4012-4021.
- Wang, S. F., D. Tang, F. He, Y. Fukuyo, and R. Azanza (2008). Occurrences of harmful algal blooms (HABs) associated with ocean environments in the South China Sea. *Hydrobiologia* 596: 79-93.
- Watkins, S., A. Reich, L. Fleming, and R. Hammond (2008). Neurotoxic shellfish poisoning. *Mar. Drugs* 6:3, 431-455.
- Wheeler, S. M., L. A. Morrissey, S. N. Levine, G. P. Livingston, and W. F. Vincent (2012). Mapping cyanobacterial blooms in Lake Champlain's Missisquoi Bay using QuickBird and MERIS satellite data. *J. Great Lakes Res.* 38: 68-75.
- Whitmire, A. L., W. S. Pegau, L. Karp-Boss, E. Boss, and T. J. Cowles (2010). Spectral backscattering properties of marine phytoplankton cultures. *Opt. Express* 18:14, 15073-15093.
- WHO (1999). *Toxic Cyanobacteria in Water: A Guide to their Public Health Consequences, Monitoring and Management*. Ed. by I. Chorus and J. Bartram. Geneva: World Health Organization.
- Wilson, W. (1966). *The suitability of sea-water for the survival and growth of Gymnodinium breve Davis and some effects of phosphorus and nitrogen on its growth*. Salt Water Fisheries Division, Florida Board of Conservation.
- Wilson, W., S. Ray, and D. Aldrich (1975). *Gymnodinium breve*: population growth and development of toxicity in cultures. In: *Proceedings of the First International Conference on Toxic Dinoflagellates*. Ed. by V. LoCicero. Massachusetts Science and Technical Foundation, Massachusetts., 127-141.
- Wolny, J., P. Scott, J. Tustison, and C. Brooks (2015). Monitoring the 2007 Florida east coast *Karenia brevis* (Dinophyceae) red tide and neurotoxic shellfish poisoning (NSP) event. *Algae* 30: 49-58.
- Wynne, T., R. Stumpf, M. Tomlinson, and J. Dyble (2010). Characterizing a cyanobacterial bloom in western Lake Erie using satellite imagery and meteorological data. *Limnol. Oceanogr.* 55:5, 2025-2036.
- Yang, M., J. Yu, Z. Li, Z. Guo, M. Burch, and T. Lin (2008). Lake Taihu not to blame for Wuxi's woes. *Science* 319: 158-158.
- Yang, Z., I. Hodgkiss, and G. Hansen (2001). *Karenia longicanalis* sp. nov. (Dinophyceae): a new bloom-forming species isolated from Hong Kong, May 1998. *Bot. Mar.* 44: 67-74.
- Yeung, P., V. Hung, and F. C. J. Wong (2005). Characterization of a *Karenia papilionacea*-like dinoflagellate from the South China Sea. *J. Mar. Biol. Assoc. U.K.* 85: 779-781.
- Zhou, M., Z. Shen, and R. Yu (2008). Responses of a coastal phytoplankton community to increased nutrient input from the Changjiang (Yangtze) River. *Cont. Shelf Res.* 28: 1483-1489.
- Zhou, M., T. Yan, and J. Zou (2003). Preliminary analysis of the characteristics of red tide areas in Chiangjiang River estuary and its adjacent sea. (in Chinese with English abstract). *Chinese J. Appl. Ecol.* 14: 1031-1038.